Floor-Supply Displacement Ventilation System

Final Report Submitted to
National Institute of Occupational Safety and Health

GRANT NUMBER: R01 OH004076
Project Period: 9/30/2001 – 9/29/2004

Qingyan (Yan) Chen, Ph.D.; Principal Investigator
Josephine Lau, Research Assistant
Nubokazu Kobayashi, Research Assistant
School of Mechanical Engineering
Purdue University
585 Purdue Mall
West Lafayette, IN 47907-2088
Phone: (765) 496-7562 FAX: (765) 496-7534
Email: yanchen@purdue.edu
http://widget.ecn.purdue.edu/~yanchen

December 29, 2004

TABLE OF CONTENTS

ABSTRACT

This report presents the research results on floor-supply displacement ventilation sponsored by the National Institute of Occupational Safety and Health under grant number R01 OH004076.

The research was to improve the design of the floor-supply displacement ventilation system for the removal of a high cooling load without draft risk. A displacement system provides fresh air directly to the occupied zone. However, the existing side-wall displacement ventilation systems have some problems. There are slow recirculations in the lower part of the room, which increase the risk of cross-contamination among occupants. Hence, the objective of this research was to improve upon the weaknesses of the current system and to develop a new design for the floor-supply displacement ventilation system by studying the effects of swirl diffusers and perforated panels.

The performance of the floor-supply ventilation system was evaluated by using a validated Computational Fluid Dynamics (CFD) program for indoor environment study. The parameters calculated and used to evaluate the indoor environment were the distributions of air temperature, air velocity, percentage of dissatisfied people due to draft (PD), predicted percentage dissatisfied people for thermal comfort (PPD), contaminant concentration, mean age of air, and ventilation effectiveness.

Generally, the impacts of a changed parameter are similar for offices and workshops. The parameters studied were cooling load, diffuser types, room size, supply airflow rate (also known as the air change rate), supply air temperature, number of diffusers, partition arrangement, occupant arrangement, furniture arrangement, location and number of exhausts, and location of diffusers.

The study found that the air change rate, supply air velocity, supply air temperature, and number of diffusers have a large impact on the air distributions; partition location and exhaust location have a moderate impact on the distributions; and diffuser location, occupant location, and furniture arrangement have little impact on the distributions. When the ventilation effectiveness of a space is higher, the indoor air quality is better and therefore, the risk of cross contamination would be reduced by the increased ventilation effectiveness.

The present investigation also compared the energy consumption of the displacement ventilation systems with that of mixing ventilation systems for an individual office and a large industrial workshop in five U.S. climate regions. The investigation accounted for the most important characteristics of a displacement ventilation system, such as air temperature stratification and high ventilation effectiveness. The results showed that the displacement ventilation system may use more fan and boiler energy but less chiller energy than the mixing ventilation system. The total energy used is slightly less with displacement ventilation, although the ventilation rate was increased in order to handle the high cooling loads found in U.S. buildings. Therefore, the displacement ventilation system can save some energy in cooling mode, but not in heating mode.

Therefore, the floor-supply ventilation system is a suitable ventilation system for use in offices and workshops in U.S. buildings for improvement of indoor working environment.

SIGNIFICANT FINDINGS

Displacement ventilation has received considerable attention recently since it improves indoor air quality. The system provides fresh air directly to the occupied zone and the airflow in the occupied zone is one-dimensionally upwards, so the air quality is better. Although U.S. buildings have large interiors and most offices in the U.S. are partitioned into cubicles, the general conclusions obtained in Europe and Japan are similar to those found in this study, which is for U.S. buildings.

This investigation conducted experimental measurements of thermal comfort and indoor air quality parameters in a full-scale environmental chamber, obtaining reliable data on the floor-supply ventilation system. With the reliable data, a computational-fluid-dynamics (CFD) program used in this research was validated. The CFD program can reasonably predict the distributions of air velocity and temperature for a simulated office and a simulated workshop with floor-supply displacement ventilation. However, it seemed more difficult to simulate the distribution of gaseous contaminant concentration with the SF_6 tracer-gas used in the experiment.

This study has successfully simulated a complex air supply device, such as a swirl diffuser, a perforated panel, and a perforated carpet. The experimental data, such as air velocity and flow direction, are crucial for a correct simulation by CFD.

The results from both the experimental measurements and CFD simulations demonstrate that an office and a workshop with floor-supply displacement ventilation can greatly improve indoor air quality in terms of the distributions of CO_2 concentration, the mean age of air, and ventilation effectiveness. However, the indoor spaces with floor-supply displacement ventilation could have a high risk of discomfort, because of the high temperature stratification between the ankle and head levels. The swirl diffuser can provide a better comfort level than perforated panels or carpets due to the mixing around the diffuser. Nevertheless, the draft risk is high in an area within 1 m around the diffuser.

The results also show that the risk of cross contamination in an indoor space with floor-supply displacement ventilation is much smaller than that with a traditional side-wall supply displacement ventilation.

This research used the CFD program as a tool to study the impacts of several parameters, such as the air change rate and supply air temperature, number of diffusers, furniture and occupant arrangement, and cooling loads, on the indoor environment, based on the thermal comfort and indoor air quality levels. The total supply air flow rate and number of diffusers affected most critically the thermal comfort and indoor air quality. In addition, the partition and exhaust location will also have significant impacts on indoor air quality.

The present investigation also studied the energy consumption of the displacement and mixing ventilation systems in an office and an industrial workshop for five U.S. climate regions. The investigation accounted for the most important characteristics of the displacement ventilation system, such as air temperature stratification and high ventilation effectiveness. The results show that a displacement ventilation system may use more fan and boiler energy but less chiller energy

than a mixing ventilation system. The total energy used is slightly less with displacement ventilation.

TRANSLATION OF FINDINGS

The research project has studied a floor-supply displacement ventilation system for large offices and workshops with a cooling load of up to 100 W/m^2 floor area. The system does not have cross recirculation in the lower part of the offices and workshops. Displacement ventilation can reduce the risk of cross-contamination in workplaces with an acceptable thermal comfort level. The investigation has studied the applications of the system in five different U.S. climate conditions. This ventilation system can be applicable to most U.S. buildings. It could also be used in other spaces, such as schools with allergic children, homeless shelters, patient waiting rooms, and hospital wards, in order to minimize the health risk of the workers there. When displacement ventilation systems are widely used in U.S. buildings, the indoor environment would be improved.

IMPACT

The floor-supply displacement ventilation is a ventilation system that can reduce the cross-contamination in our workspaces. In past years, health has become a major concern in American daily life. As a result, the federal government has increased its budget for health related research by 14% in the fiscal year of 1999. If the floor-supply system demonstrates to be effective in reducing infection, the health benefits are huge for the government, the industry, and the working American.

Since offices with partitions are very common non-industrial workspaces in the U.S., and workshops are common industrial workspaces, the application of the floor-supply systems has great potential. The floor-supply displacement ventilation system can bring new opportunities to the U.S. industry.

PUBLICATIONS

One journal paper has been published as the preliminary results for the research:

Kobayashi, N. and Chen, Q. 2003. "Floor-supply displacement ventilation in a small office," *Indoor and Built Environment*, 12(4), 281-292.

Two more journal papers are under preparation, and will be the major outcomes of the research.

1. INTRODUCTION

Indoor environment is important to a worker's health and welfare because more than half of the U.S. workforce is employed indoors and up to 90% of a typical worker's time is spent indoors. A worker's productivity is related to the indoor environment, such as the indoor air quality and thermal comfort. The economic cost in the United States (U.S.) due to a poor indoor environment would annually amount to tens of billions of dollars.

Displacement ventilation is a good ventilation system to improve the indoor air quality with an acceptable thermal comfort level. However, the widely used side-wall-supply displacement ventilation generates recirculations in the occupied zone of a large office or a workshop. These recirculations present the risk of cross contamination between the workers. The floor-supply displacement ventilation could be a solution to avoid the recirculations. On the other hand, the floor-supply system may not remove a high cooling load often found in most U.S. offices and workshops, because the cold air is directly supplied to the occupied zone and the floor can be too cold. In addition, U.S. buildings have large interiors and a lot of U.S. offices are large ones with cubicles. The spatial arrangement has a significant on the performance of a ventilation system. The design experience and guides from other countries may not be appropriate for U.S. buildings. It is necessary to study the systems under U.S. building and climate conditions.

1.1 Background of Displacement Ventilation

Most of the heating, ventilating and air-conditioning (HVAC) systems used in U.S. buildings are mixing ventilation. The design of the systems assumes that fresh air delivered from the HVAC systems will completely mix with the pollutants indoors to reduce the concentration level of the pollutants to an acceptable level. However, a complete mixing is difficult to achieve. The concentration level in some parts of an indoor space often exceeds the permitted level. In addition, the complete mixing could enhance cross contamination between occupants. The cross contamination can be serious in workshops and large offices, a common office type in the U.S.

In order to improve the indoor air quality, displacement ventilation has received considerable attention recently, because the system is supposed to provide fresh air directly to the occupied zone and the airflow in the occupied zone should be one-dimensionally upwards. The system was originally developed in Scandinavia. It has been increasingly popular in the past decade all over the world. The most common supply configuration is a horizontal discharge from a low side wall position. The heated objects, such as the occupants and equipment, will bring the contaminants to the upper zone through the thermal plumes generated by the heat. Return exhausts are located at or close to the ceiling through which the warm air with higher contaminant concentrations is removed, as shown in Figure 1.1.1. Unfortunately, the airflow from the displacement ventilation system is not one-dimensional in the occupied zone. As shown in Figure 1.1.1, there are slow cross recirculations in the lower part of the room. These recirculations present the risk of cross contamination between the workers. Therefore, it is necessary to develop a new ventilation system without the risk of cross contamination.

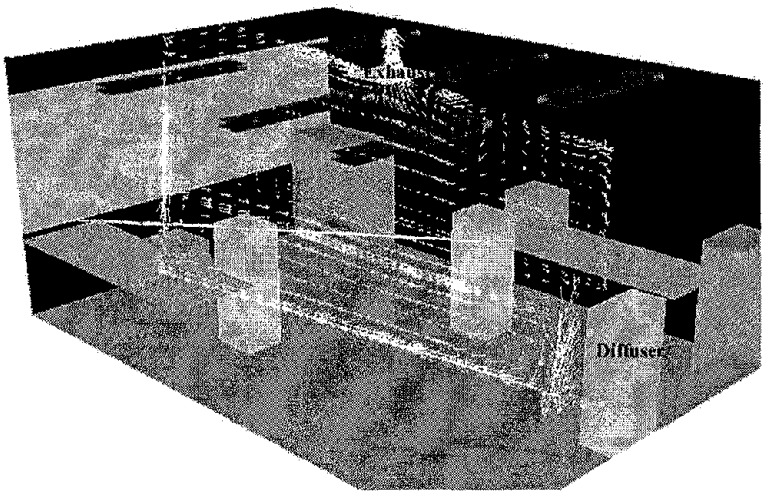

(a) Computed airflow pattern in an office with side-wall-supply displacement ventilation

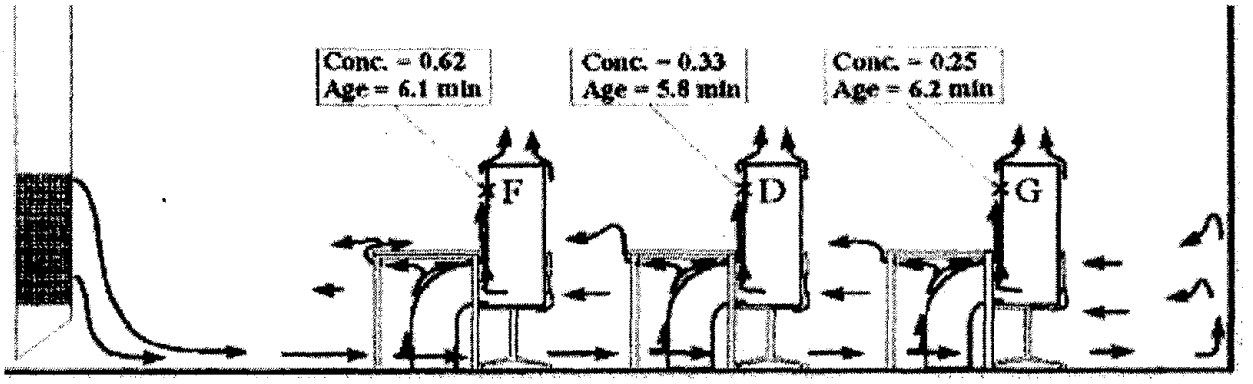

(b) Measured airflow pattern in a room with side-wall-supply displacement ventilation (Sandberg et al. 1998)

Figure 1.1.1 Typical air flow pattern in displacement ventilation

Floor-supply displacement ventilation (as shown in Figure 1.1.2) could be a solution to avoid the recirculation problem. As reviewed by Akimoto (1998), the Japanese have used the perforated floor-supply system with considerable success. The floor-supply displacement ventilation system is superior to the side-wall supply system because it can also be used directly for heating. Sodec and Craig (1990) found that floor-supply displacement ventilation systems can provide a better indoor air quality than mixing ventilation systems. The contaminant concentration level in the breathing area is 20-30% lower as shown in Figure 1.1.3(a). Matsunawa et al. (1995) compared the local air change index of a floor-supply system with that of a ceiling supply system by using the tracer–gas measuring technique. The local air change index indicates that the fresh air rate in the area is related to the local age of air. Therefore, the higher the index, the better the air quality. Figure 1.1.3(b) shows that the air quality provided by the under-floor system is much better.

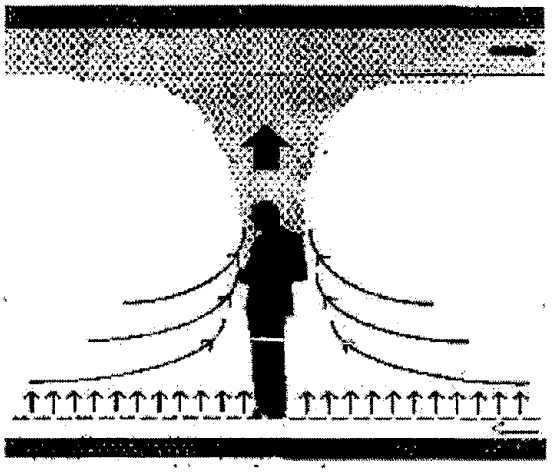

Figure 1.1.2 Perforated floor with an air permeable carpet.

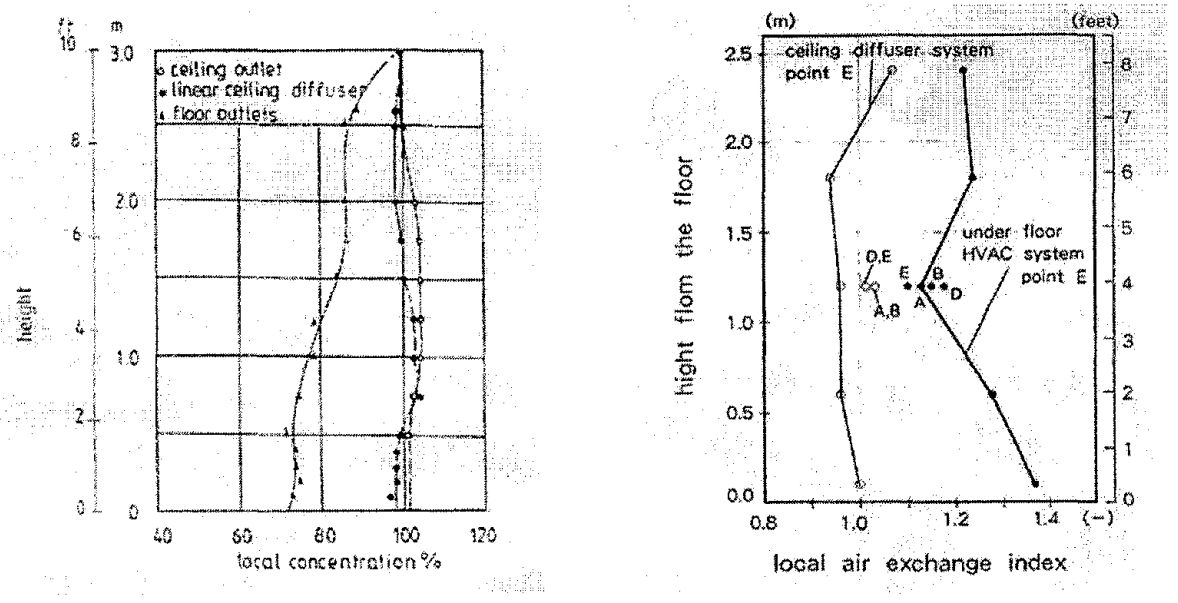

(a) (b)

Figure 1.1.3 Comparison of air quality in areas with floor-supply displacement ventilation systems and mixing ventilation systems.

Since the floor-supply displacement ventilation systems supply air from the floor level, there are concerns about the dust concentration level in such a space. Since dust tends to settle downwards, perhaps the dust might be suspended in the air. Matsunawa (1995) measured the dust concentration in an environmental chamber. His results (shown in Figure 1.1.4) indicate that the dust concentration with the use of the floor-supply system is lower than that of the ceiling-supply system. The floor-supply system can directly bring small dust particles to the exhaust while the ceiling-supply mixing system tends to re-circulate the dust particles in the space. On the other hand, large particles would stay firmly on the floor and their size is so large that it is not a risk to health.

Good air quality in the space with the floor-supply system is not only found in chamber measurements but also in field measurements. For example, Spoormaker (1990) found a very satisfactory air quality in a 50,000 m^2 office building with floor supply displacement ventilation.

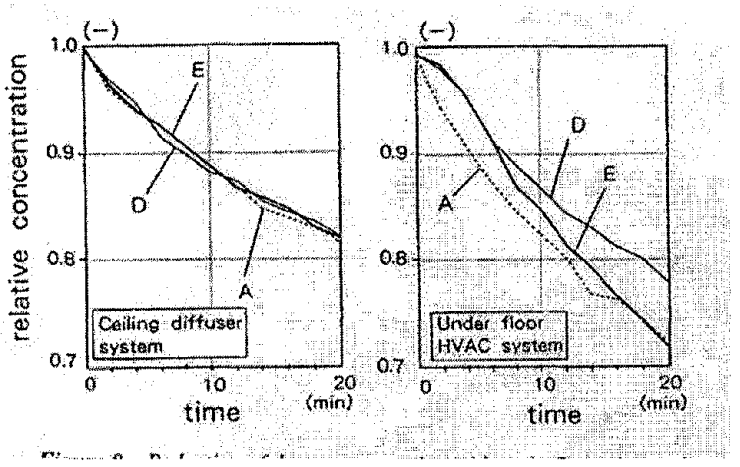

Figure 1.1.4 Dust concentration measured in an environmental chamber.

In addition to air quality, another serious concern on floor-displacement ventilation is the thermal comfort in such a space, because the conditioned air is supplied directly to the occupied zone. Tanigawa et al. (1993) found that the discomfort problem is more severe for cooling than heating. If a perforated floor is used as shown in Figure 1.1.2, the air velocity is very low in the space (Akimoto 1998). However, it is much more difficult to design floor-supply displacement ventilation with diffusers as shown in Figure 1.1.5. Matsunawa et al. (1995) measured the airflow distribution with floor diffusers that provide swirl-type airflow. When the cooling load is low, the air velocity around the diffuser is low because of the low airflow rate (as shown in Figure 1.1.6). However, the velocity near the diffuser is too high to be accepted when the cooling load is high (airflow rate is high). The diffuser needs a careful design.

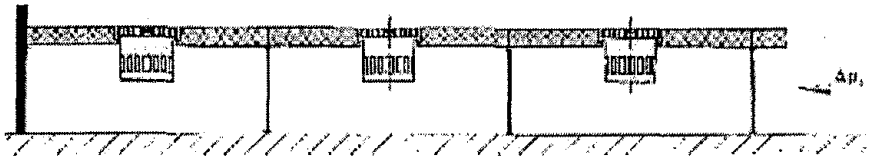

Figure 1.1.5 Floor-supply system with diffusers.

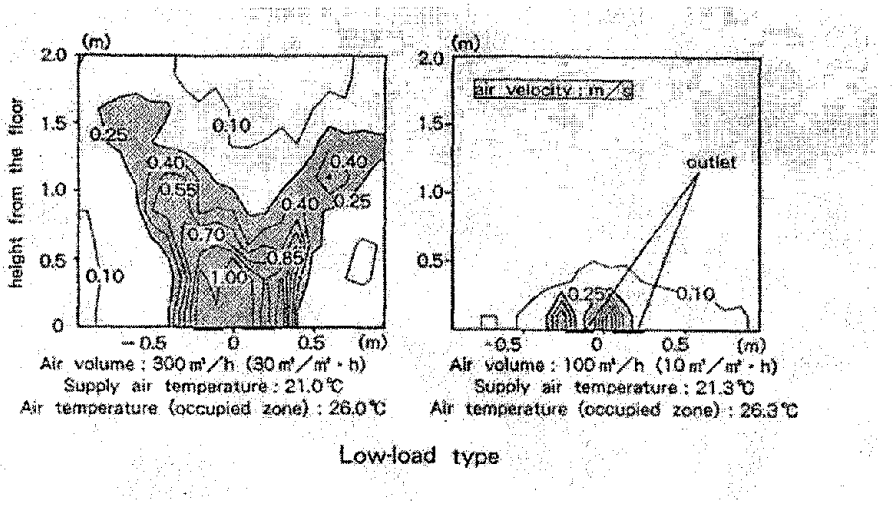

Figure 1.1.6 Measured air velocity with different loads in a space with floor-supply diffusers.

Temperature gradient is another criterion for thermal comfort. Figure 1.1.7 compares the vertical temperature profile for cooling measured in different experimental chambers and existing buildings with floor-supply systems (Sodec and Craig 1990, Spoormaker 1990, McCarry 1995, Matsunmawa et al. 1995, and Liu and Hiraoka 1997). The results show that the shapes of the temperature profiles are similar. Although the room air temperature is quite different, the temperature difference between the head and feet satisfies most of the ASHRAE thermal comfort standard. Tanabe et al. (1994) conducted detailed measurements of temperature on a thermal mannequin in an office station with floor-supply displacement ventilation. If a diffuser is used, local discomfort near the diffuser is occasionally found.

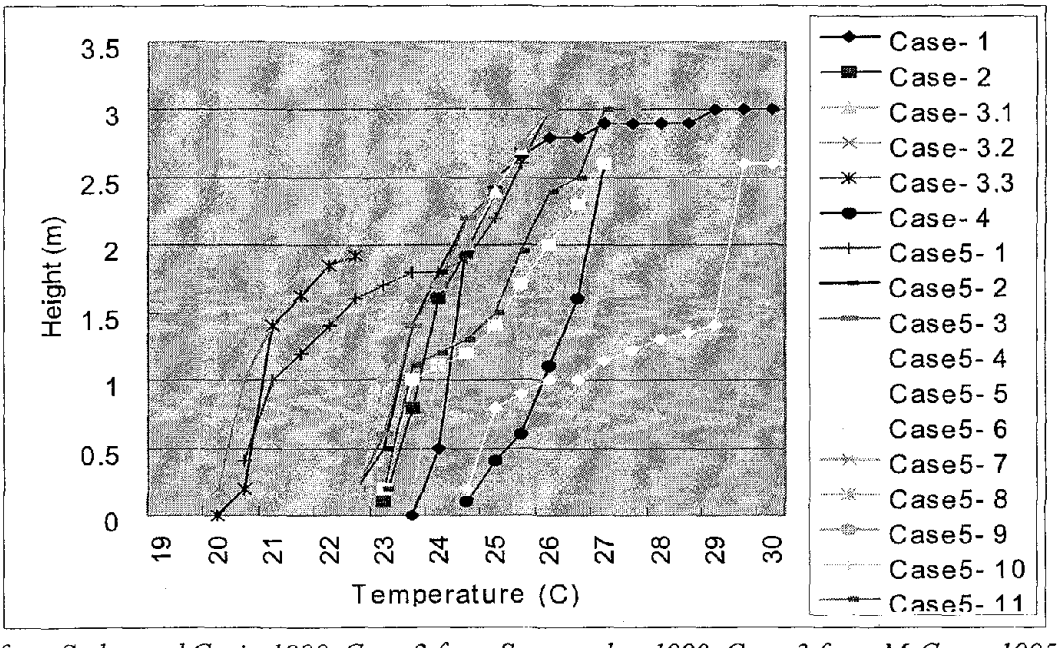

Case- 1 from Sodec and Craig 1990, Case-2 from Spoormaker 1990, Case-3 from McCarry 1995, Case-4 from Matsunmawa et al. 1995, and Case-5 Liu and Hiraoka 1997

Figure 1.1.7 Vertical temperature profiles with under-floor displacement ventilation for cooling.

The Japanese applications use 100% fresh air. The ability of the system to remove a cooling load is small. With an air supply temperature of around 66°F (19°C), the maximum cooling load is less than 13 Btu/h ft^2 floor area (40 W/m^2 floor area). According to a survey conducted in the Greater Boston area (Yuan et al. 1998), U.S. offices and workshops have a cooling load around 26 to 40 Btu/h ft^2 floor area (80 - 120 W/m^2 floor area). In addition, European and Japanese office buildings are shallow and are mainly with individual offices. Even if there are large offices in Japan, most of the Japanese designs do not use partition walls. However, U.S. buildings have large interiors. Most offices are partitioned into cubicles. The building size, shape and space configurations in the U.S. are unique. Direct use of the European and Japanese design guidelines of the floor-supply displacement ventilation system for an U.S. building is not appropriate.

On the other hand, the floor-supply displacement ventilation systems do not generate recirculations in the lower part of a space. The floor-supply system with suitable exhausts can minimize the risk of cross contamination between the workers. Mattsson (1998) has demonstrated the positive effect of the exhaust location with displacement ventilation. The system seems superior to other ventilation systems especially for large offices and workshops where the risk of cross contamination between the workers can be high. Therefore, it is necessary to study the floor-supply displacement ventilation systems for U.S. buildings.

1.2 Objective

This research is to improve the design of the floor-supply displacement ventilation system for the removal of a high cooling load without draft risk. The research will propose measures to reduce cross contamination among workers in large offices and workshops. More specifically, the objective of this research is to:

- Improve the design of the floor-supply displacement ventilation system for a higher cooling load while the system can still provide an acceptable comfort level and can be energy effective.
- Optimize the ventilation system to minimize the risk of cross contamination with suitable air supply and exhaust locations.

The floor-supply displacement ventilation system will provide a solution to obtain a good indoor environment for the U.S. workers to improve their health welfare. The system can also be used to reduce cross contamination in patient waiting rooms, wards, and schools with allergic children, homeless shelters, etc., where the health risk is high to the workers.

1.3 Scope of Work

The study will assess the indoor air quality, thermal comfort, and energy consumption of the floor-supply displacement ventilation system. The parameters to be studied include the diffuser type, perforated degree, ventilation rate, supply air temperature, exhaust location, floor insulation, ceiling height, furniture and partition arrangement, etc. The research will use numerical simulations through Computational Fluid Dynamics (CFD) technique to reduce the costs. Nonetheless, detailed and high quality experimental data will be obtained in a full-scale environmental chamber, and the data will be used to validate the CFD results.

2. EXPERIMENTAL STUDY

In general, two main research methods are available to study indoor environment: experimental investigation and computer simulation. In principle, direct measurements give the most realistic information concerning indoor air quality and thermal comfort, such as the distributions of air velocity, temperature, relative humidity, and contaminant concentrations. However, direct measurements are very expensive and time consuming.

To simulate an indoor space properly and obtain reliable results of direct measurements, an environmental chamber which is isolated from the external space is necessary. To obtain accurate results, the airflow and temperature from the HVAC systems and the temperature of the building enclosure must be maintained the same throughout the experiment. This is especially difficult without an isolated experimental chamber because the outdoor conditions change over time and the temperature of the building enclosure and the airflow and temperature from the HVAC systems would change as well. However, such an environmental chamber costs more than $300,000 with necessary equipment for measuring air velocity, temperature, relative humidity, and contaminant concentrations. Furthermore, it may not be easy to change from one spatial configuration to another. In addition, since the measurements must be made at many locations to get useful information, a complete measurement may take a long time of work.

On the other hand, the indoor air quality and thermal comfort can be determined computationally by solving a set of conservation equations describing the flow, energy, and contaminants in the system. Due to the limitations of the experimental approach and the increase in performance and affordability of high-speed computers, the numerical solution of these conservation equations provides a practical option for computing the airflow and pollutant distributions in buildings. This method is the Computational Fluid Dynamics (CFD) technique.

The CFD technique is a powerful tool for solving indoor environment problems, such as airflow pattern and the distributions of air velocity, temperature, relative humidity, turbulent intensity, and contaminant concentrations. Because of the limited computer power and capacity available at present, turbulence models have to be used in the CFD technique in order to solve the flow motion. However, the use of turbulence models leads to uncertainties in the computed results because the models do not have universal validity for all kinds of indoor spaces. Therefore, it is essential to validate a CFD program by appropriate experimental data.

A lot of experimental data are available in the literature but very few of them can be used for validation. It is because experimental data for CFD validation must contain detailed information of flow and thermal boundary conditions as well as flow and thermal parameters measured in the space.

Therefore, we conducted the experiment of the floor-supply displacement ventilation system to obtain the data which can be used to validate the CFD program for the floor-supply displacement system. Since the experimental data are used only for the CFD validation, the measurements were conducted only for a few typical cases.

This chapter presents detailed experimental method and data for the floor-supply displacement system.

2.1 Experimental Facility

Environmental chambers

The measurements for CFD program validation were done in two different chambers. Due to the change of the academic affiliation of the principle investigator, the experiments for the office arrangement was done in the environmental chamber at the Massachusetts Institute of Technology (MIT) while the experiments for the workshop arrangement was later done in the environmental chamber at the Purdue environmental chamber.

According to the tests conducted at MIT environmental chamber for office configuration and the CFD simulation results, it was found that the height of the room has significant impact on the performance of the floor-supply displacement system. The total height of the MIT test chamber was only 8 ft. After installing the raised floor, it was only about 7 ft, which was not realistic for an actual office room. Though the tests for office configuration are acceptable, it would be better to have a high ceiling. The ceiling height of the new test chamber at Purdue University was 9 ft, which was common for most office buildings and it was a more realistic representation for office and workshop.

The chambers are shown in Figure 2.1.1. Both chambers consist of a box which is covered by well-insulated walls. Each chamber has a movable wall, which divides the chamber into two chambers. One is the test chamber, in which the measurements are done and the other is the climate chamber, which can represent different outdoor conditions. The movable wall has a double-grazing window and the rest parts are well-insulated walls. The specifications of the chambers are shown in Table 2.1.1.

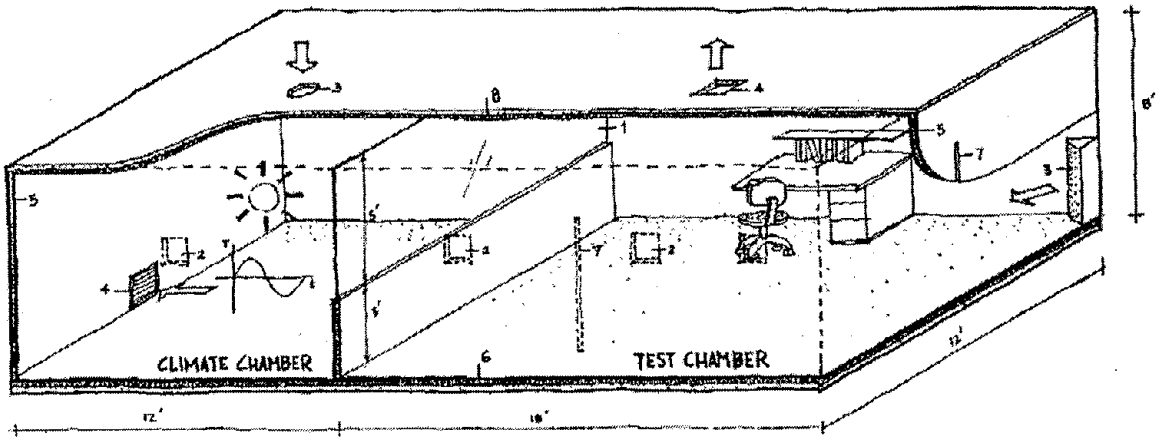

(a) MIT environmental chamber

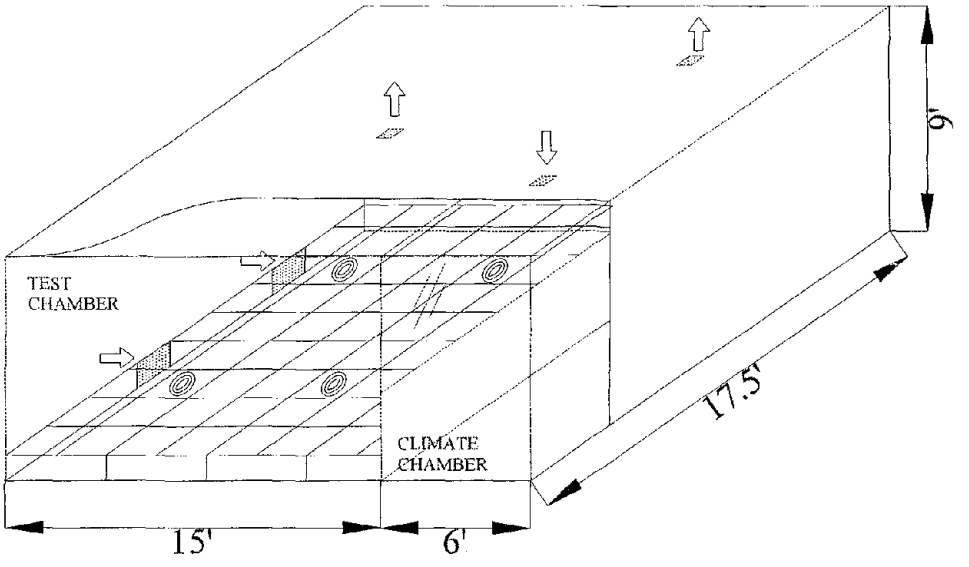

(b) Purdue environmental chamber
Figure 2.1.1. Experimental chambers

Table 2.1.1. The specifications of the experimental chamber
(a) MIT environmental chamber

Dimension	
Test chamber	5.16m * 3.65m * 2.43m (high)
Climate chamber	3.08m * 3.65m * 2.43m (high)
Window	3.45m (wide) * 1.16 m (high)
Thermal resistance	
Walls (including partition)	5.3 Km^2/W
Ceiling, Floor, Door	5.3 Km^2/W
Window	0.27 Km^2/W

(b) Purdue environmental chamber

Internal Dimension	
Test chamber	4.2m * 4.8m * 2.75m (including 0.32m floor plenum height) (high)
Climate chamber	1.83m * 4.8m * 2.75m (high)
Window	4.75m (wide) * 1.48 m (high)
Thermal resistance	
The partition wall	3.64 Km^2/W
Walls	5.45 Km^2/W
Ceiling, Door	5.45 Km^2/W
Floor - 4 in concrete with R-19 insulation form	5.45 Km^2/W (for insulation form)
Window	0.25 Km^2/W

HVAC systems

Each chamber has an individual HVAC system so that different conditions can be made for the test chamber and the climate chamber. Specifications of the HVAC system for each chamber are shown in Table 2.1.2. The schematic figure of the HVAC system is shown in Fig 2.1.2. The temperature sensors, humidity sensors and pressure sensors along the ductwork are also indicated in the ductwork.

Table 2.1.2 Specifications of the HVAC system
(a) MIT environmental chamber

	Test chamber	Climate chamber
Supply Fan	max 930 m^3/h	max 930 m^3/h
Return Fan	max 930 m^3/h	max 930 m^3/h
Preheter	8 kW	8 kW
Reheter	8 kW	8 kW
Humidifier	11 kg/h	None
Chiller	21 kW	

(b) Purdue environmental chamber

	Test chamber	Climate chamber
Supply Fan	max 850 m^3/h	max 850 m^3/h
Return Fan	max 850 m^3/h	max 850 m^3/h
Preheter	8 kW	8 kW
Reheter	8 kW	8 kW
Humidifier	11 kg/h	11 kg/h
Chiller	21 kW	

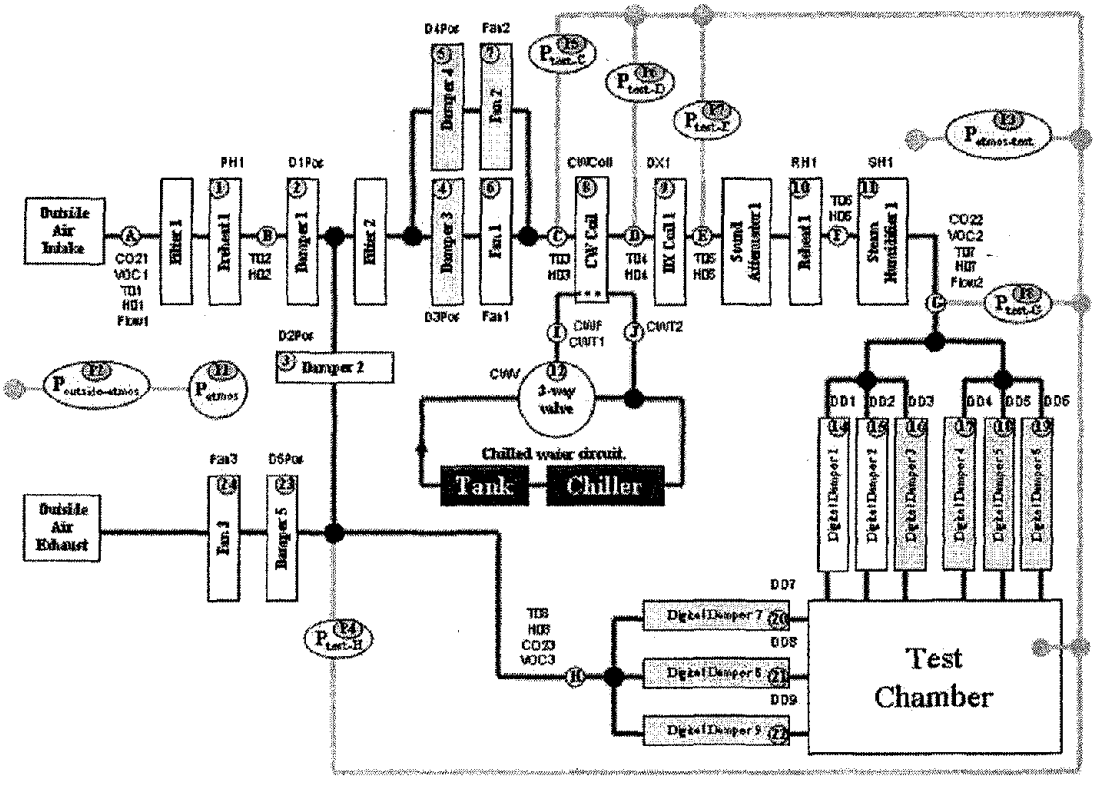

Figure 2.1.2 HVAC system for the experimental chambers at Purdue University

Each HVAC system is controlled using the software "Insight" through the control interfaces on a personal computer. The high precision control enables us to obtain high quality experimental environment in the chambers. Air temperature and air supply rate for both chambers can be well controlled.

Measuring equipment

The measuring equipment used for the research is:

- A hot-sphere anemometer system for measuring air velocity and temperature
- A thermo-couple system for measuring temperature
- A tracer gas system for measuring contaminant concentration
- A flow visualization system for observing airflow patterns

A hot-sphere anemometer system for measuring air velocity and temperature

Hot-sphere anemometers with omni-directional sensors are used for measuring air velocity and temperature in the experimental chambers. The hot-sphere anemometer used in this experiment is shown in Figure 2.1.3 and the specifications are shown in Table 2.1.3. The anemometer probe includes an omni-directional velocity sensor and temperature sensor. The velocity sensor is made of enameled cupper wire pressed into the shape of the sphere, diameter of which is 3 mm. The temperature sensor is made of the thin nickel wire and its shape is cylindrical. The temperature sensor measures the ambient air. Both the sensors are vacuum covered with special aluminum coating that increases their resistance to contamination and decrease the effect of thermal radiation on the readings. The probe is placed in a support, which length is 250 mm. The temperature sensor operates in a constant temperature anemometer bridge with automatic temperature compensation. An ADD board is used for data acquisition. The test chamber at Purdue University has 63 hot-sphere anemometers for simultaneous measurements of air velocity.

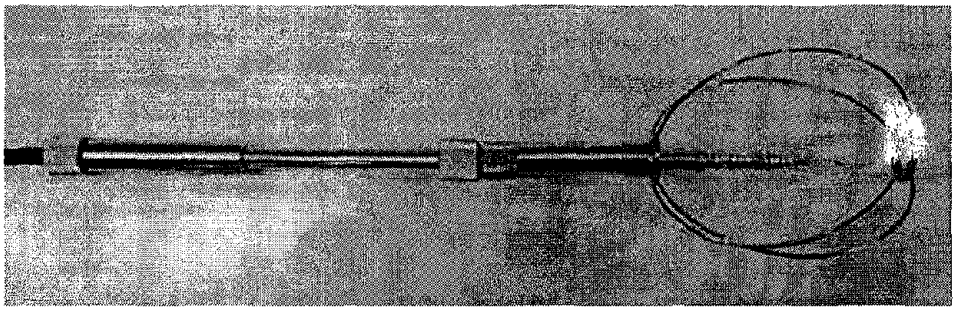

Figure 2.1.3 Anemometer probe

Table 2.1.3 Specifications of the anemometer system

Type	hot-spherical
Velocity sensor	spherical, diameter=3mm
Velocity range	0.05 to 5 m/s
Repeatability	0.01m/s
Temperature range	0 to 60 C
Temperature accuracy	0.3 C
Transducer outputs(voltage)	0-5 V
max length of cable	5 m
Distance between two sensors	25 mm
Diameter of the probe	7 mm

A thermo-couple system for measuring temperature

Thermocouples are used to measure both air and surface temperature in the experimental chamber. Thermocouples are coated with aluminum paint to reduce the radiation. A data logger system is used for a digital data acquisition. The specifications of the thermocouples used in this experiment are shown in Table 2.1.4. Fifty-eight thermocouples are used to measure both wall and floor surface temperatures.

Table 2.1.4. Specifications of the thermocouples

Material	Copper-Constantan
Insulation	PFA
Temperature range	-60 to 100 C
Temperature Accuracy	0.5 C
Size	0.62 mm x 0.10 mm
Weight	2 (lb/1000feet)

A tracer gas system for measuring contaminant concentration

A multi-gas monitor and analyzer system is used to measure contaminant concentration in the test chamber. Its measurement principle is based on the photoacoustic infrared detection method, which can be applied for almost any gas which absorbs infrared light. The multi-gas monitor and analyzer system used in this experiment are shown in Figure 2.1.4 and the specifications are given in Table 2.1.5. The gas-analyzer is controlled by a personal computer

and data are stored also in the computer. In this experiment SF_6 is used to simulate a contaminant because the background concentration of SF_6 in the atmosphere is almost zero.

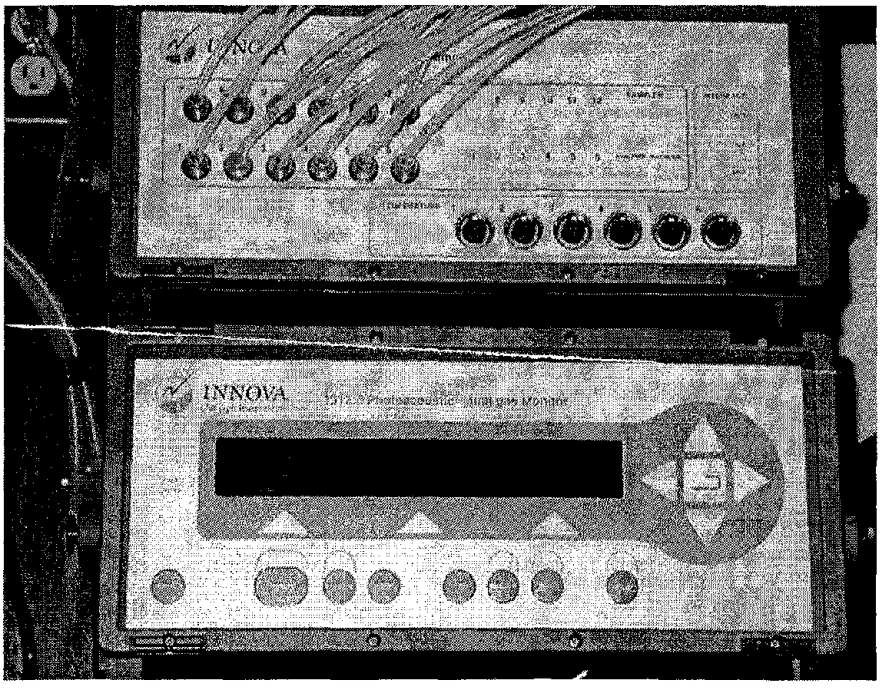

Figure 2.1.4 The multi-gas monitor and analyzer system

Table 2.1.5 Specifications of the multi-gas monitor and analyzer system

Measurement technique	Photoacoustic infrared spectroscopy
Measurement range	Min. 0.001 ppm
Measurement unit	ppm or mg/m^3
Response time	about 30s to 100s
Repeatability	1% of measured value
Operating temperature	5C to 40C

A flow visualization system for observing airflow patterns

The test chamber has two long vertical slots and several observation windows on the walls. Light penetrates through the slots and forms a thin light sheet. By injecting smoke into the test chamber, the airflow pattern can be observed through observation windows normal to the light sheet.

The test facility has two types of smoke sources. One is a theater fog generator and the other is an air current kit. The fog generator and the air kit are shown in Figures 2.1.5 and 2.1.6, respectively. The theater fog generator produces a large amount of smoke and the smoke is

supplied to the chamber or the ducts through a tube which is attached to the generator. This generator is suitable for observing how supply air is distributed into the room. On the other hand, the air current kit is suitable for observing air flow pattern in a particular area. The kit generates a small amount of smoke locally.

Figure 2.1.5 Fog generator

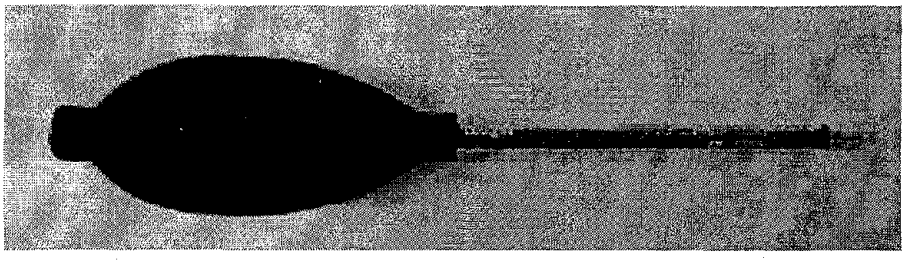

Figure 2.1.6 Air current kit

2.2 Experimental Setup

For the experiments studied in the environmental chamber at Purdue University, six cases were carried out for different diffusers with the room configurations of offices and workshops.

Setup of experimental chamber

The chamber was installed with an accessible raised floor. The cavity under the raised floor is pressurized by the supply air and used as a supply air plenum feeding the floor diffusers. The

raised floor was made of movable floor panels and they were supported by steel frame. The sizes of the panels were 600mm by 600mm.

The round shape swirl floor diffuser used in this experiment is shown in Figure 2.2.1. The diameter is 210mm and the height is 150mm.

After setting up the raised floor in the test chamber the air leakage from the raised floor was checked using smoke visualization before setting up office configuration.

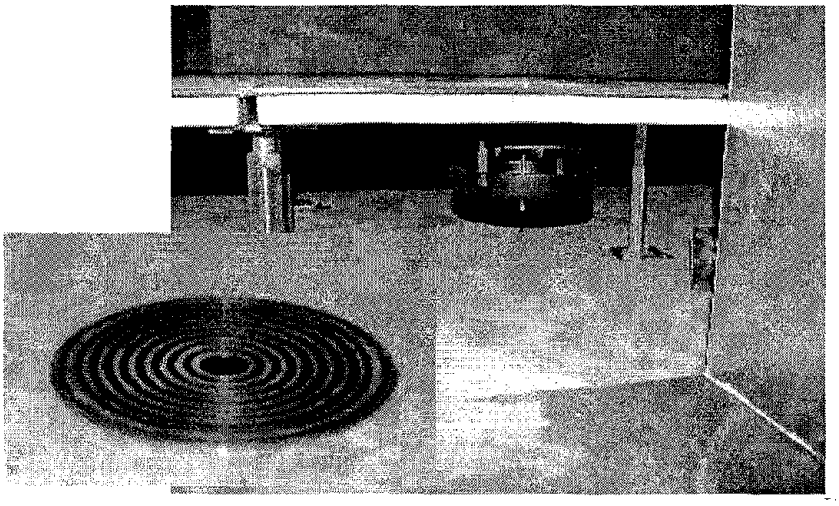

Figure 2.2.1 Round-shape swirl floor diffuser

Experimental configuration

The six measurements were conducted with different configurations. Table 2.2.1 summarizes the arrangements of these six cases.

Table 2.2.1 Summary of the experimental configuration

Case	***Diffuser Type***	***Occupancy***	***Chamber***	***Internal furniture***
Workshop-1	Swirl diffuser	4	Purdue	2 Tables
Workshop-2	Perforated Panel	4	Purdue	2 Tables
Office-1	Swirl diffuser	2	MIT	2 Tables
Office-2	Perforated Panel	2	Purdue	2 Tables
Office-3	Swirl diffuser	2	Purdue	2 Tables with partition
Office-4	Perforated Panel	2	Purdue	2 Tables with partition

The internal heat sources and the tracer gas source used in the six cases are listed in Table 2.2.2.

Table 2.2.2 Internal heat source and the tracer gas source

Heat Sources				
Item	size (m)			Heat (W)
	length	width	height	
Occupant (for workshop cases)	0.4	0.4	1.1	200
Occupant (for workshop cases)	0.4	0.4	1.1	100
Equipment	0.5	0.4	0.25	100
Ceiling lamp	1.2	0.15	0.08	64
Temperature in the climate chamber : 32 (C)				
Tracer gas (SF_6) Source				
Item	Height (m)		SF_6 (ml/min)	
Occupant	1.1		500	

Measurement procedure

The measurements for air velocity, air temperature, and SF_6 concentration were conducted in nine removable poles installed in the chambers. Each pole had seven hot-sphere anemometer probes and six sampling tubes for contaminant concentration measurement. Fifty-eight thermocouples were used to measure temperatures of the walls, the floor, the ceiling, and the window; the temperature in the concrete floor slab; and the supply and exhaust temperature.

The following figures show the configurations used in the corresponding experiments (Figure 2.2.2).

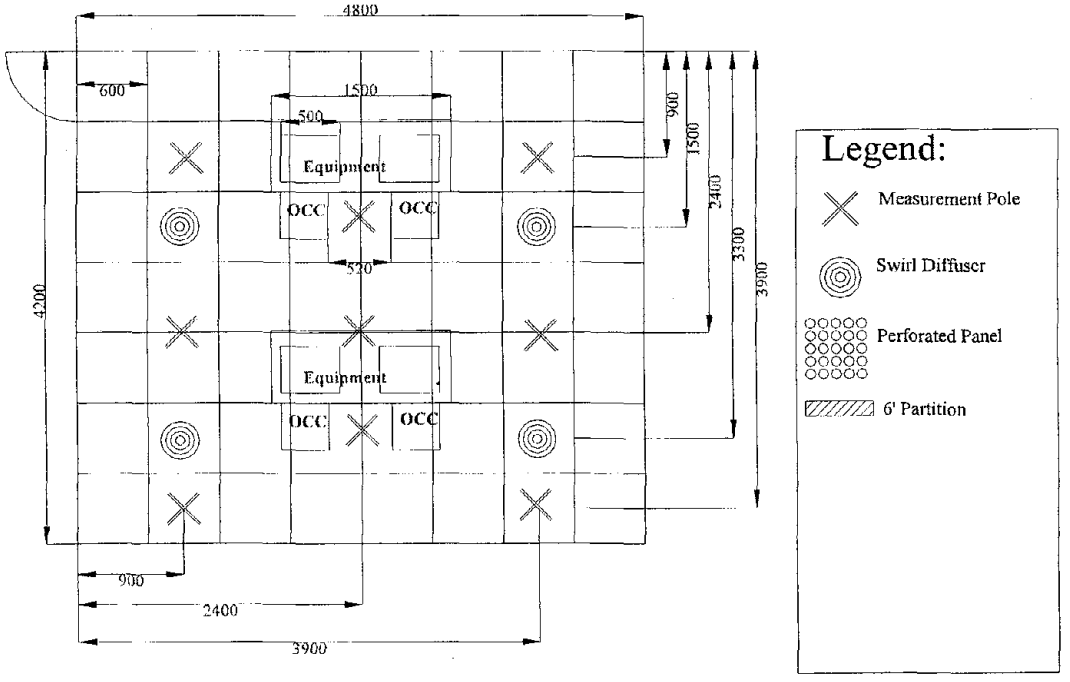

(a) Layout plan of workshop-1 and 2

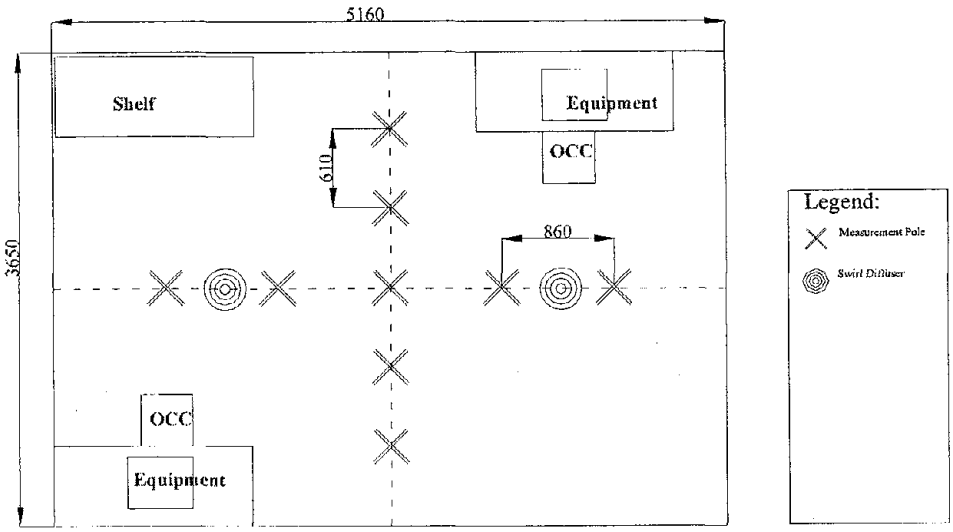

(b) Layout plan of office-1

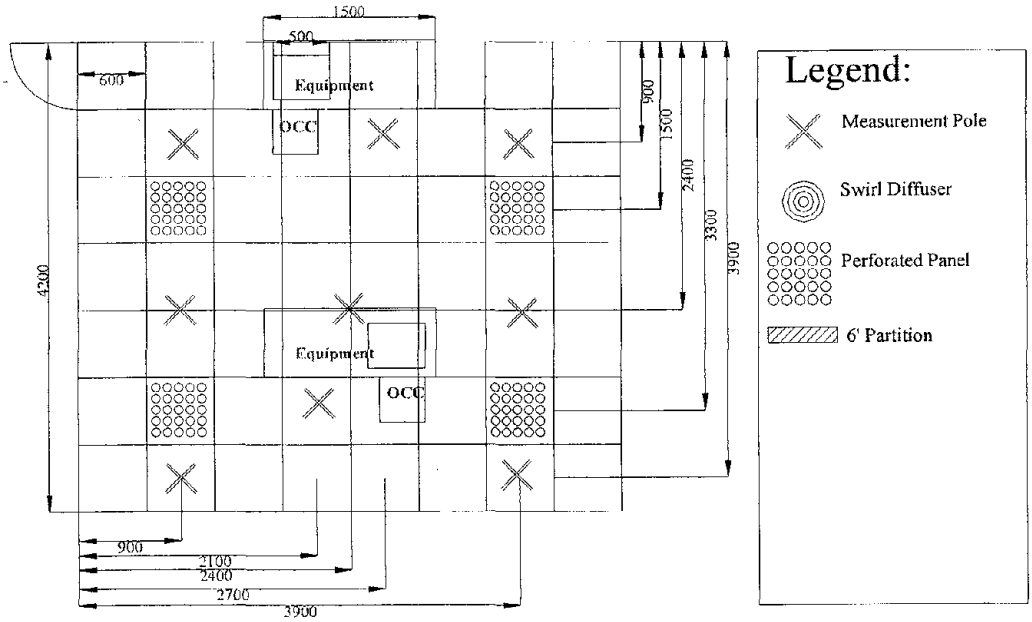

(c) Layout plan of office-2

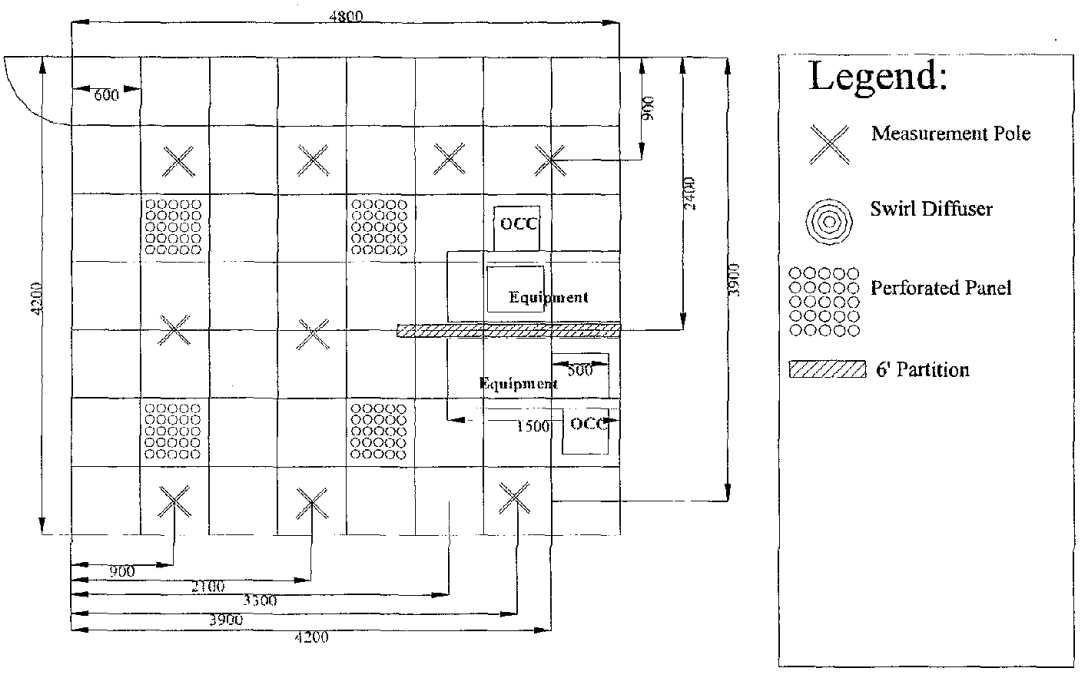

(d) Layout plan of office-4 (with partition and perforated panels)

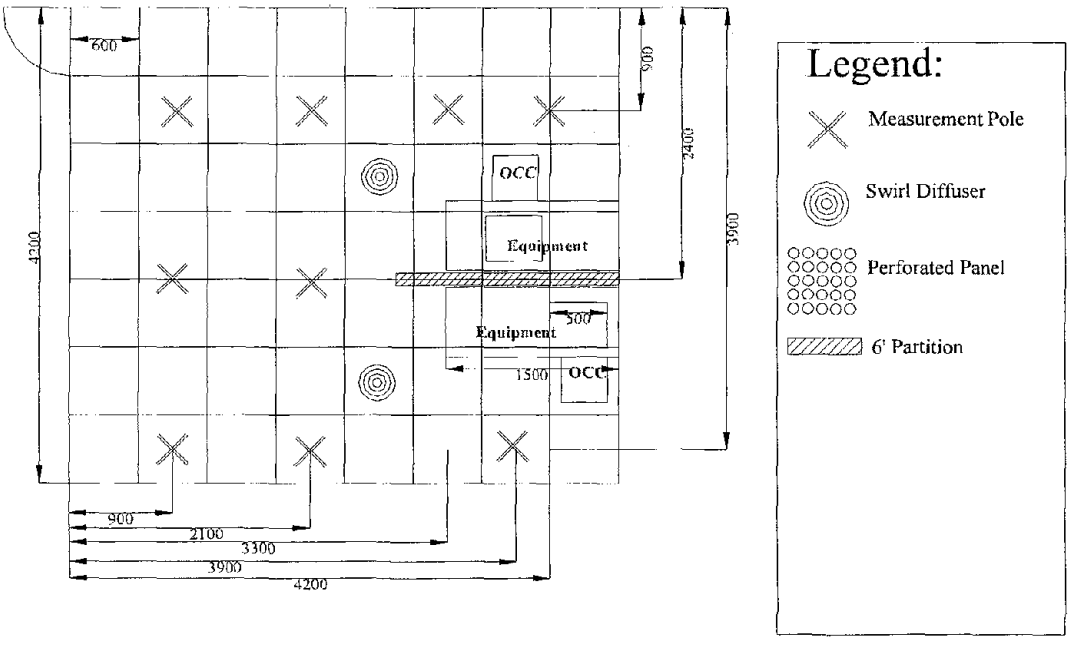

(e) Layout plan of office-3 (with partition and swirl diffusers)

Figure 2.2.2 Layouts used in the environmental chamber at Purdue University.

Measurements were conducted under steady-state conditions by stabilizing the room thermal and fluid conditions for more than 28 hours before starting the measurements. Air velocity, air temperature, and SF6 concentration were measured in nine different locations (poles). Total measuring points on the pole for air velocity were 63, for gas concentration were 54, and for temperature were 63. Figure 2.2.3 shows the experimental set-up.

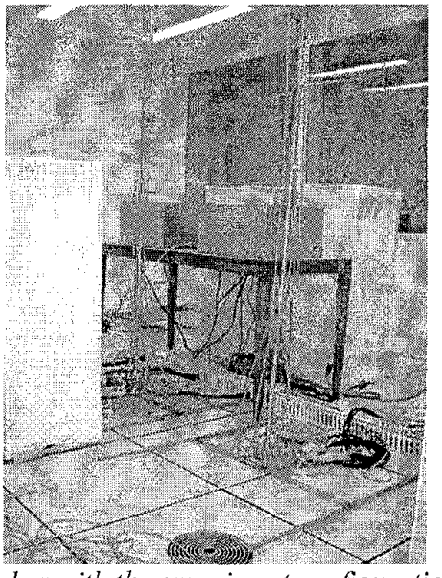

Figure 2.2.3 Test chamber with the experiment configuration and sampling poles

2.3 Experimental Results

Figures 2.3.1 shows smoke visualization of the air flow from the floor diffuser and perforated panel, respectively. The air velocity from the perforated panels was upwards and uniform while the air velocity from the swirl diffuser was a 30 degree bend from vertical axis and with a strong turbulence.

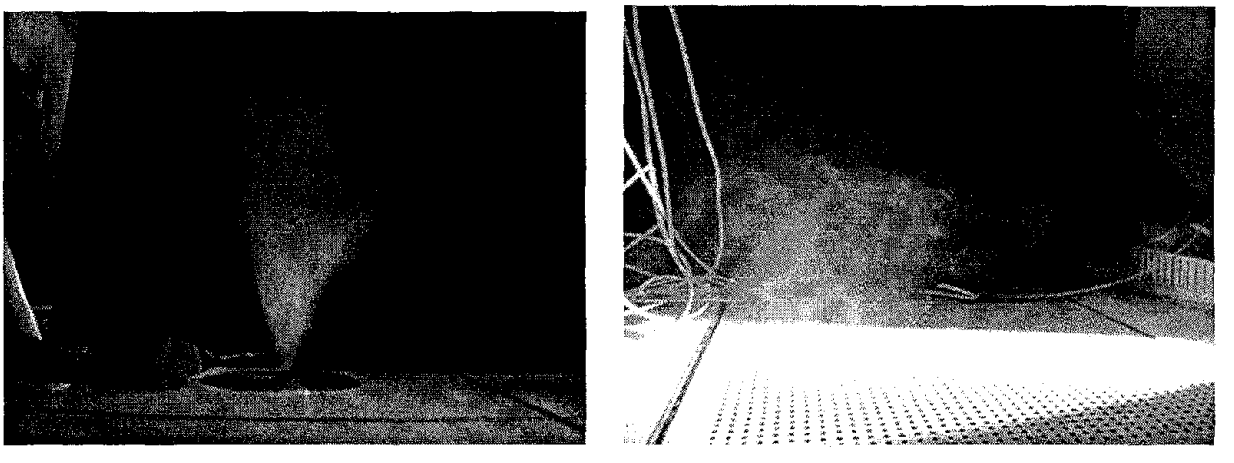

Figure 2.3.1 Smoke visualization of the air flow from the floor diffuser (left) and from the perforated panel (right).

The results of air velocity, air temperature, and tracer gas concentration are shown in Tables 2.3.1a-e. These data will be used to validate the CFD program used in this research in the next chapter.

Table 2.3.1a Experimental results of temperature, velocity, and SF6 concentration for workshop - 1

Room volume	55.44 m3			
Airflow rate	748 m3/h	Air change rate	13.5 times/h	
T07(Supply at the duct)	15.5 °C			
Tdiffuser-1	18 °C	Tdiffuser-2	17.9 °C	
Tdiffuser-3	17.1 °C	Tdiffuser-4	16.8 °C	
Texhaust	22.8 °C	Tclimate	32.2 °C	
SF6 inlet	0.0924 ppm	SF6 return	0.34 ppm	
Heat balance				
Heat-input (W)	= Heat room + Heat window		= 1775.2	% error
Heat-removed(W)	= air flow rate*density*Cp*dT		= 1828.7	3.01

Twall

	W	E	S	N
Upper	24.3	25.1	24.4	24.3
Middle	22.6		22.4	23.1
Lower	19	21.4	19.2	19.6

Twindow

	E
Upper	26.6
Middle	26.5
Lower	26.4

Tfloor/ceiling/pole

	P1	P2	P3	P4	P5	P6	P7	P8	P9
Ceiling	24.4		24.9	23.8		24.4	24.4		24.5
2.2m	24.6	24.9	24.6	23.7	23.4	23.9	24.4	24.6	24.6
1.7m	24	23.8	23.9	23	23.5	23.5	23.7	23.9	23.8
1.4m	22.8	23.2	23.5	22.1	23.1	22.4	22.8	23.2	23.2
1.1m	21.5	21.3	20.9	21.5	21.9	21.8	21.2	21.8	22.3
0.6m	20.9	20.5	20.2	21.5	21.1	21.3	20.5	20.8	19.8
0.3m	21.1	20.9	20.5	21.5	20.9	21.5	20.6	20.7	19.6
0.1m	21.5	20.8	20.5	21.5	21.2	21.1	20.9	20.1	19.4
Floor Penel	21.5	21.4	21.4	22.2	21.2	22.2	20.6	20.4	20.4
floor slab (upper)	17.8		18.2	16.5		17.5	16.5		16.7
floor slab (lower)	17.8		18.2	16.6		17.5	16.7		16.8

Velocity

	P1	P2	P3	P4	P5	P6	P7	P8	P9
2.2m	0	0	0	0.06	0.18	0.05	0	0	0
1.7m	0	0	0	0.05	0.05	0.05	0	0	0
1.4m	0	0	0	0.05	0	0.05	0	0	0
1.1m	0.05	0.08	0.09	0.1	0.06	0.09	0.05	0.05	0
0.6m	0.06	0.08	0.07	0.14	0.08	0.07	0.07	0	0.12
0.3m	0.06	0.05	0.07	0.11	0.08	0.06	0.06	0	0.1
0.1m	0.06	0.05	0.08	0.07	0.08	0	0.07	0.07	0.1

Tracer Gas (ppm)

	P1	P2	P3	P4	P5	P6	P7	P8	P9
2.2m	0.91		0.76	0.22	0.34		0.24		0.24
1.7m	0.93		1.14	0.21	0.29		0.19		0.32
1.4m	0.49		0.42	0.17	0.23		0.15		0.21
1.1m	0.33		0.31	0.23	0.27		0.16		0.23
0.6m	0.26		0.21	0.17	0.24		0.14		0.16
0.1m	0.24		0.2	0.12	0.14		0.13		0.13

Table 2.3.1b Experimental results of temperature, velocity, and SF6 concentration for workshop - 2

Room volume	55.44 m3			
Airflow rate	748 m3/h	Air change rate	13.5 times/h	
T07(Supply at the duct)	14.4 °C			
Tdiffuser-1	17.4 °C	Tdiffuser-2	16.9 °C	
Tdiffuser-3	16.7 °C	Tdiffuser-4	16 °C	
Texhaust	22.8 °C	Tclimate	32.2 °C	
SF6 inlet	0.0925 ppm	SF6 return	0.347 ppm	

Heat balance

Heat-input (W)	= Heat room + Heat window	=	1808	% error
Heat-removed(W)	= air flow rate*density*Cp*dT	=	2102.9	16.31

Twall

	W	E	S	N
Upper	23.9	24.7	24.2	23.9
Middle	22.4		22.1	22.3
Lower	19.5	22	18.8	19.8

Twindow

	E
Upper	26.6
Middle	26.3
Lower	25.8

Tfloor/ceiling/pole

	P1	P2	P3	P4	P5	P6	P7	P8	P9
Ceiling	24.1		24.7	23.1		23.1	24		24.3
2.2m	25.1	25.4	25.1	24.1	24.5	24.3	24.9	25.4	24.8
1.7m	24.5	24.5	24.7	23.5	24.4	24.8	24.7	24.5	24.5
1.4m	24	24.1	24.5	22.9	24.5	24.1	24.3	23.9	24.1
1.1m	22.7	22.9	22.9	21.8	22.6	22.8	22.1	22.4	22.5
0.6m	20.4	20.6	21.3	20.6	20.8	20.3	21	20.4	20.3
0.3m	20.9	20.2	20.9	20	20.7	20	21.2	18.8	18.4
0.1m	21	20.1	21	18.9	20.8	20.7	21.1	17.7	18.4
Floor Penel	20.4	20.4	20.6	21.1	19.9	22.1	19.5	19.2	20
floor slab (upper)	17.8		18.4	16.8		17.8	17		17.1
floor slab (lower)	17.8		18.4	16.9		17.8	16.9		17.2

Velocity

	P1	P2	P3	P4	P5	P6	P7	P8	P9
2.2m	0.0	0.0	0.0	0.0	0.2	0.0	0.0	0.0	0.0
1.7m	0.0	0.0	0.0	0.0	0.0	0.0	0.0	0.0	0.0
1.4m	0.0	0.0	0.0	0.0	0.0	0.0	0.0	0.0	0.0
1.1m	0.0	0.0	0.0	0.0	0.0	0.0	0.0	0.0	0.0
0.6m	0.09	0.05	0.0	0.12	0.06	0.1	0.0	0.0	0.1
0.3m	0.06	0.10	0.0	0.11	0.06	0.1	0.09	0.06	0.1
0.1m	0.00	0.05	0.0	0.06	0.07	0.0	0.06	0.10	0.09

Tracer Gas (ppm)

	P1	P2	P3	P4	P5	P6	P7	P8	P9
2.2m	0.67		0.79	0.17	0.30		0.15		0.16
1.7m	1.66		1.93	0.14	0.30		0.15		0.16
1.4m	0.75		1.06	0.13	0.18		0.11		0.16
1.1m	0.13		0.16	0.11	0.13		0.10		0.10
0.6m	0.10		0.10	0.10	0.10		0.10		0.10
0.1m	0.10		0.10	0.10	0.10		0.10		0.10

Table 2.3.1c Experimental results of temperature, velocity, and SF6 concentration for office - 2

Room volume	55.44 m3			
Airflow rate	340 m3/h	Air change rate	6.1 times/h	
T07(Supply at the duct)	13.3 °C			
Tdiffuser-1	16.5 °C	Tdiffuser-2	16.4 °C	
Tdiffuser-3	17.6 °C	Tdiffuser-4	17 °C	
Texhaust	22.8 °C	Tclimate	32.2 °C	
SF6 inlet	0 ppm	SF6 return	0.34 ppm	
Heat balance				
Heat-input (W)	= Heat room + Heat window	=	1029.8	% error
Heat-removed(W)	= air flow rate*density*Cp*dT	=	1081.0	4.98

Twall

	W	E	S	N
Upper	23.3	22.7	23.7	23.2
Middle	22.6		21.8	21.9
Lower	19.4	21.2	19.1	19.3

Twindow

	E
Upper	25.8
Middle	25.2
Lower	24.5

Tfloor/ceiling/pole

	P1	P2	P3	P4	P5	P6	P7	P8	P9
Ceiling	23.1		23.4	22.5		23.1	23.3		23.3
2.2m	24.4	24.6	24.5	24.1	23.7	24.2	24.1	24.8	24.3
1.7m	23.5	23.5	23.7	23.5	23.5	23.5	23.3	23.4	23.5
1.4m	22.9	22.9	23.2	22.9	22.8	22.7	22.6	22.9	22.9
1.1m	21.8	22	22	21.8	21.8	21.9	21.6	21.9	21.9
0.6m	20.5	20.4	20.6	20.6	20.1	20.5	20.4	20.4	20.6
0.3m	20	20	19.9	20	19.6	20	20.1	19.9	19.8
0.1m	18.6	17.7	18.5	18.9	20.1	18.3	18.3	18.6	17.8
Floor Penel	19.9	20.3	19.3	19.3	19.8	20.5	20	20.2	19.3
floor slab (upper)	16.1		17	16.4		17	16.2		17.6
floor slab (lower)	16.2		17	16.5		17	16.4		17.9

Velocity

	P1	P2	P3	P4	P5	P6	P7	P8	P9
2.2m	0.0	0.0	0.0	0.0	0.11	0.0	0.0	0.0	0.0
1.7m	0.0	0.0	0.0	0.0	0.0	0.0	0.0	0.0	0.0
1.4m	0.0	0.0	0.0	0.0	0.0	0.0	0.0	0.0	0.0
1.1m	0.0	0.0	0.0	0.0	0.0	0.0	0.0	0.0	0.0
0.6m	0.0	0.0	0.0	0.0	0.0	0.0	0.0	0.0	0.0
0.3m	0.0	0.0	0.0	0.0	0.0	0.0	0.0	0.0	0.0
0.1m	0.09	0.0	0.0	0.0	0.07	0.0	0.05	0.06	0.0

Tracer Gas (ppm)

	P1	P2	P3	P4	P5	P6	P7	P8	P9
2.2m	0.71		0.88	0.39	0.67		0.48		0.94
1.7m	1.22		2.60	0.52	1.41		0.39		0.85
1.4m	4.17		3.85	5.67	5.60		0.30		3.93
1.1m	0.20		0.22	0.21	0.24		0.20		0.20
0.6m	0.20		0.23	0.20	0.20		0.20		0.20
0.1m	0.21		0.22	0.22	0.22		0.21		0.21

Table 2.3.1d Experimental results of temperature, velocity, and SF6 concentration for office - 3

Room volume	55.44 m3		
Airflow rate	340 m3/h	Air change rate	6.1 times/h
T07(Supply at the duct)	12.2 °C		
Tdiffuser-1	16.8 °C	Tdiffuser-2	16 °C
Tdiffuser-3	16.7 °C	Tdiffuser-4	15.9 °C
Texhaust	22.8 °C	Tclimate	32.2 °C
SF6 inlet	0.15939 ppm	SF6 return	1.118 ppm

Heat balance

Heat-input (W)	= Heat room + Heat window	=	1108	% error
Heat-removed(W)	= air flow rate*density*Cp*dT	=	1203.7	8.64

Twall

	W	E	S	N
Upper	23.9	24.7	24.2	23.9
Middle	22.4		22.1	22.3
Lower	19.5	22	18.8	19.8

Twindow

	E
Upper	26.6
Middle	26.3
Lower	25.8

Tfloor/ceiling/pole

	P1	P2	P3	P4	P5	P6	P7	P8	P9
Ceiling	23.9		24.3	22.9		23.7	23.6		23.7
2.2m	23.8	24.2	24.2	23.9	23.9	24.1	24	24.6	24.1
1.7m	23.7	23.8	24.1	23.8	23.8	23.8	23.6	23.8	23.9
1.4m	23.1	23.1	23.3	23.1	22.8	22.9	22.8	23.1	23.1
1.1m	21.9	22.1	22.3	21.6	21.9	21.9	21.6	21.6	22
0.6m	20.9	20.9	20.8	21	20.9	20.3	21.2	20.8	20.8
0.3m	21	20.6	20.6	20.7	20.6	20.6	21	20.9	20.8
0.1m	21.1	20.4	20.4	20.6	20.6	20.4	20.5	20.6	20.5
Floor Penel	20.4	20.4	20.8	20.5	20.8	20.6	20.6	20.9	20.9
floor slab (upper)	16.7		17.3	16.1		16.8	16.6		17
floor slab (lower)	16.7		17.3	16.2		16.8	16.7		17

Velocity

	P1	P2	P3	P4	P5	P6	P7	P8	P9
2.2m	0.00	0.00	0.00	0.00	0.07	0.00	0.00	0.00	0.00
1.7m	0.00	0.00	0.00	0.00	0.00	0.05	0.00	0.00	0.00
1.4m	0.00	0.00	0.00	0.00	0.00	0.00	0.00	0.00	0.00
1.1m	0.00	0.00	0.00	0.00	0.00	0.00	0.00	0.05	0.00
0.6m	0.00	0.00	0.00	0.05	0.00	0.06	0.00	0.05	0.07
0.3m	0.00	0.05	0.05	0.00	0.00	0.05	0.00	0.05	0.00
0.1m	0.00	0.00	0.06	0.00	0.09	0.00	0.00	0.05	0.00

Tracer Gas (ppm)

	P1	P2	P3	P4	P5	P6	P7	P8	P9
2.2m	1.23		1.29	1.18	1.11		1.09		1.12
1.7m	1.21		1.39	1.14	1.38		1.05		1.12
1.4m	0.86		3.69	1.55	3.22		7.36		1.41
1.1m	0.63		0.87	1.63	0.91		1.21		0.91
0.6m	0.62		0.66	1.23	0.98		1.19		0.52
0.1m	0.63		0.59	0.91	0.82		0.67		0.52

Table 2.3.1e Experimental results of temperature, velocity, and SF6 concentration for office – 4

Room volume	55.44 m3			
Airflow rate	340 m3/h	Air change rate	6.1 times/h	
T07(Supply at the duct)	13.3 °C			
Tdiffuser-1	18.1 °C	Tdiffuser-2	17.3 °C	
Tdiffuser-3	18 °C	Tdiffuser-4	17.2 °C	
Texhaust	22.8 °C	Tclimate	32.2 °C	
SF6 inlet	0.2052 ppm	SF6 return	1.023 ppm	
Heat balance				
Heat-input (W)	= Heat room + Heat window	=	1008	% error
Heat-removed(W)	= air flow rate*density*Cp*dT	=	1077.2	6.87

Twall

	W	E	S	N
Upper	23.9	24.7	24.2	23.9
Middle	22.4		22.1	22.3
Lower	19.5	22	18.8	19.8

Twindow

	E
Upper	26.6
Middle	26.3
Lower	25.8

Tfloor/ceiling/pole

	P1	P2	P3	P4	P5	P6	P7	P8	P9
Ceiling	23.1		23.7	22.1		23	23.3		22.9
2.2m	23.9	24.3	24.1	23.8	23.8	24	23.9	24.5	24
1.7m	24.6	23.6	23.8	23.5	23.4	23.1	23.3	23.5	22.8
1.4m	23	22.9	23.3	22.8	22.7	22.4	22.6	22.9	22.5
1.1m	21.9	22.1	22	21.7	21.8	21.9	21.7	21.9	21.9
0.6m	20.1	20.3	20.5	20.5	20.1	20.2	20.4	20.4	20.2
0.3m	20	20	19.9	19.3	19.4	19.6	19.6	19.6	19.5
0.1m	20.4	19.4	18.5	18.9	19.8	18.5	18.7	18.4	17.9
Floor Penel	20.4	19.3	19.6	19.6	19.4	19.2	22.9	19.6	19
floor slab (upper)	16.5		17.6	16.2		17.1	16		16.7
floor slab (lower)	16.5		17.6	16.3		17.1	16.2		16.9

Velocity

	P1	P2	P3	P4	P5	P6	P7	P8	P9
2.2m	0.05	0.00	0.05	0.00	0.00	0.06	0.00	0.00	0.00
1.7m	0.00	0.00	0.00	0.00	0.00	0.00	0.00	0.00	0.00
1.4m	0.00	0.00	0.00	0.00	0.00	0.00	0.00	0.00	0.00
1.1m	0.00	0.00	0.00	0.00	0.00	0.00	0.00	0.00	0.00
0.6m	0.00	0.00	0.00	0.00	0.00	0.00	0.00	0.00	0.05
0.3m	0.00	0.00	0.00	0.00	0.00	0.07	0.00	0.00	0.00
0.1m	0.00	0.00	0.00	0.00	0.00	0.06	0.05	0.06	0.05

Tracer Gas (ppm)

	P1	P2	P3	P4	P5	P6	P7	P8	P9
2.2m	1.38		2.02	0.17	0.95		1.45		1.08
1.7m	0.87		1.07	0.14	1.29		1.25		0.45
1.4m	0.32		1.58	0.13	7.73		0.31		0.47
1.1m	0.19		0.19	0.11	0.19		0.19		0.19
0.6m	0.19		0.19	0.10	0.19		0.19		0.19
0.1m	0.20		0.20	0.10	0.21		0.20		0.20

2.4 Conclusions

Since the experimental data are used only for the CFD validation, the measurements were conducted only for the six typical cases. It was found that the floor-supply system created temperature stratification. The temperature gradient in the lower part of the room is much larger than that in the upper part, because most heat sources, such as PCs and occupants, are located in the lower part of the room. Comparing the vertical temperature distributions of workshop-1 with that for workshop-2, the impact of the swirl diffusers and perforated panels were observed. Swirl diffusers induced more turbulence flow near the diffuser region and the temperature, therefore, was less stratified than perforated panels. A similar observation was drawn when the vertical temperature distributions of office-3 and office-4 were compared. However, ASHRAE Standard

55-2004 restricts the vertical temperature difference between the head and the feet of a person to not more than 3°C for thermal comfort. In the experiment, the head level of a sitting person was at 1.1m and the feet level was at 0.1m. For workshop-2, this thermal comfort requirement was not satisfied only at poles 8 and 9. Remediation of this situation was not carried out. It was because the supply air temperature and velocity was not individually controlled by the perforated panels.

With these experiment results, in general, swirl diffusers can achieve thermal comfort better than perforated panels due to the less stratification in temperature. Swirl diffusers should be, therefore, suggested to be used for the space with huge heat sources as it can handle higher cooling load without the problem of steep stratification in the occupied zone.

The experimental data obtained will be used for a CFD program validation in next chapter.

3. VALIDATION OF CFD PROGRAM

The validation is to demonstrate the ability of the CFD program to accurately predict representative indoor environmental applications for which reliable data is available. It shows how accurately the CFD simulations can predict indoor environment problems in the real world. Therefore, the validation process is necessary to apply the CFD program for design and evaluation of a similar indoor environment category.

The fundamental strategy of validation is to identify suitable experimental data, to make sure that all the important physical phenomena in the problem interested are correctly modeled, and to quantify the error and uncertainty in the CFD simulation. Since the primary role of CFD in indoor environment modeling is to serve as a useful tool for design and analysis, it is essential to have a systematic and affordable program validation process.

With the detailed experimental data obtained in Chapter 2, the CFD program used in this research can be validated. The validated CFD program can be used to simulate and evaluate the design and performance of the floor-supply displacement ventilation system. The CFD program used in this research is a commercial program, "PHOENICS". The CFD model used is a RNG (re-normalization group) k-ε model.

Since new office and workshop buildings are becoming highly airtight and insulated, occupied by a high density of electric equipment, most rooms need cooling even in the winter. In addition, floor-supply ventilation systems are generally suitable for heating in the winter, because warm conditioned air is supplied from the floor and exhausted from the ceiling grills which is in accordance with the direction of buoyancy effects. Therefore, the most challenging situation in applying floor-supply ventilation will be cooling in summer condition. As the result, all the experiments were carried out and investigated under the steady-state simulations of cooling in summer conditions.

3.1 CFD Model

In general, the Reynolds stress models are used for complex flows. Among several kinds of k-ε models, the Re-Normalization Group (RNG) k-ε model (Yakhot and Orszag 1986, Yakhot 1992) is stable and is slightly more accurate than the standard k-ε model (Launder and Spalding 1974) for indoor airflow simulations. (Chen 1995, Loomans 1998) Therefore, the RNG k-ε model is used in this study.

The Re-normalization group (RNG) k-ε model

CFD is the application of numerical techniques to solve the Navier-Stokes equations for fluid flow. The Navier-Stokes equations are derived by applying the principles of conservation laws of mass and momentum to a control volume of fluid. When applying CFD to the indoor air quality and thermal comfort problem, conservation of mass for a contaminant species and energy for thermal responses also may be applied. All of the conservative governing equations can be expressed in a common form in Equation (3.1.1).

$$\frac{\partial}{\partial t}(\rho\phi)+\frac{\partial}{\partial x_j}(\rho u_j\varphi)=\frac{\partial}{\partial x_j}(\Gamma_\varphi\frac{\partial\varphi}{\partial x_j})+S_\varphi \qquad (3.1.1)$$

where

t	=	time
ρ	=	air density (kg/m^3)
ϕ	=	dependent variable: 1 for mass continuity u_j (j=1,2, and 3) for three components of momentum k for kinetic energy of turbulence ε for dissipation rate of turbulence energy T for temperature C for contaminant concentration
x_j	=	coordinate
Γ_ϕ	=	effective diffusion coefficient
S_ϕ	=	source term

For buoyancy flows, the Buossinesq approximation, which relates density change with temperature difference, is usually employed. Since most practical flows are turbulent, a certain turbulence theory must be applied in order to close the equation system. For most of the industrial cases, turbulence modeling theory is a more practical and effective way to simplify the turbulence terms in the Navier-Stokes equations.

However, due to the complexity of turbulent flow, it is difficult to obtain a universal turbulence model for all types of indoor airflow. Many efforts have been made to identify the most suitable turbulence model for indoor airflow. A general conclusion from several studies of different models for indoor airflow is that turbulent models perform differently from one case to another, although all simulated flows are indoor airflows.

In general, the standard k-ε model performs well among many turbulent models. The standard k-ε model is stable, easily implemented, widely validated, and reasonably accurate for many applications. This feature makes the standard k-ε model one of the most widely used turbulence models in practice for indoor flows. However, in many HVAC applications, the standard k-ε model has problem in predicting strong buoyancy, separated flows, axisymmetric jets, swirl flows, and heat transfer from a wall. Therefore, many modified k-ε models, such as the RNG (Re-Normalization Group) k-ε model (Yakhot and Orszag 1986, Yakhot et al. 1992), have been developed to improve performance for certain cases of problems.

Table 3.1.1 Values of ϕ, Γ_ϕ, and S_ϕ

ϕ	Γ_ϕ	S_ϕ
1	0	0
u_j	$\mu+\mu_t$	$-\partial p/\partial x_i - \rho g_i \beta(T-T_0)$
k	$(\mu+\mu_t)/\sigma_k$	$G-\rho\varepsilon+G_B$
ε	$(\mu+\mu_t)/\sigma_\varepsilon$	$(C_{\varepsilon 1}G - C_{\varepsilon 2}\rho\varepsilon + C_{\varepsilon 3}G_B)\varepsilon/k + R$
T	$\mu/\sigma_l + \mu_t/\sigma_t$	S_T
C	$(\mu+\mu_t)/\sigma_c$	S_C

where

μ is laminar viscosity

$\mu_t = \rho C_\mu \frac{k^2}{\varepsilon}$ is turbulent viscosity

$G = \mu_t \frac{\partial u_i}{\partial x_j}\left(\frac{\partial u_i}{\partial x_j} + \frac{\partial u_j}{\partial x_i}\right)$ is turbulent production

$G_B = -g_i \beta \frac{\mu_t}{Pr_t}\frac{\partial T}{\partial x_i}$ is turbulent production due to buoyancy

$R = \frac{C_\mu \eta^3 (1-\eta/\eta_0)}{1+\beta\eta^3}\frac{\varepsilon^2}{k}$ is the source term from renormalization

$\eta = S\frac{k}{\varepsilon}$, $S = (2S_{ij}S_{ij})^{1/2}$, $S_{ij} = \frac{1}{2}\left(\frac{\partial u_i}{\partial x_j} + \frac{\partial u_j}{\partial x_i}\right)$

$C_\mu = 0.0845$, $C_{\varepsilon 1} = 1.42$, $C_{\varepsilon 2} = 1.68$, $C_{\varepsilon 3} = 1.0$ are the model constants

$\sigma_k = 0.7194$, $\sigma_\varepsilon = 0.7194$, $\sigma_l = 0.71$, $\sigma_t = 0.9$, $\sigma_c = 1.0$ are Prandtl or Schmidt numbers

The differences between the standard k-ε model and the RNG k-ε model are:

- The model coefficients assume different values.
- The dissipation rate transport equation includes an additional source term R.

The additional term R improves flow prediction for regions with large strain rates, and the term is negligible for small strain rates. Therefore, the model can better predict separate flows, which are commonly present in door airflow.

Wall functions

Since the RNG k-ε model is valid for high Reynolds number turbulent flow, wall functions are needed for near wall region where flow Reynolds number is low. This study uses the following wall functions.

Velocity

$$U = \left(\frac{\tau}{\rho}\right)^{1/2} \frac{1}{\kappa} \log\left(\frac{y}{y^*} E\right) \qquad (3.1.2.)$$

where

U	=	velocity parallel to the wall
τ	=	wall share stress
κ	=	von Karman constant (= 0.41)
y	=	distance between the first grid node and the wall
E	=	an integration constant (=9.0)
y*	=	a length scale

Kinetic energy of turbulence

$$k = \frac{1}{C_\mu^{1/2}} \left(\frac{\tau}{\rho}\right) \qquad (3.1.3)$$

Dissipation rate of turbulent kinetic energy

$$\varepsilon = \left(\frac{\tau}{\rho}\right)^{3/2} \frac{1}{\kappa y} \qquad (3.1.4)$$

Temperature

$$q = h_c (T_W - T_{air}) \qquad (3.1.5)$$

where

q	=	heat flux
h_c	=	convective heat transfer coefficient
T_W	=	wall temperature
T_{air}	=	air temperature

Numerical technique

The Navier-Stokes equations are highly non-linear and self-coupled, which are impossible to have analytical solutions in most real cases. Therefore, in CFD the Navier-Stokes equations are solved by discretizing the equations using finite difference or finite element techniques that eventually lead to solve a set of algebraic equations numerically. The simulations use the finite volume method and SIMPLE algorithm.

After generating a numerical grid on which the discrete algebraic equations are solved and specifying a set of problem-dependent boundary conditions, the calculation is iterated until a

prescribed convergence criterion is met. The convergence criterion was set such that the respective sum of the absolute residuals of p, u_j, T, c, k, and ε is less than 10^{-3}.

3.2 Validation

The CFD program used in this research is validated by comparing the distributions of temperature, velocity, and tracer gas concentration between measured data and computed results for the cases mentioned in chapter 2. The measurements were conducted with office and workshop configurations. The details of the experiments were presented in Chapter 2.

Boundary conditions

The CFD validation requires the specification of boundary conditions for heat transfer from heated objects and walls, sources of the tracer gas, supply airflow, and exhaust airflow.

Walls

The surface temperatures on the ceiling, floor, side walls, and window were measured in the experiment and are used for the boundary conditions for the walls and the window. The important parameter of the boundary conditions of the walls is the convective heat transfer coefficient for each wall, h_c. The convective heat transfer coefficient is defined in the Newton's law (3.2.1).

$$q = h_c(T_W - T_{air}) \qquad (3.2.1)$$

where

q	=	heat flux due to convection (W/m^2)
h_c	=	convective heat transfer coefficient (W/m^2K)
T_W	=	wall surface temperature(°C)
T_{air}	=	air temperature (°C)

As in the equation, the coefficient is defined based on the temperature difference between the wall surface temperature and the air temperature. The air temperature is taken at a point which is far enough from the wall (more than 0.3 m). For indoor conditions, h_c for walls is between 3 ~ 6 W/m^2K, although it is related to the localized flow.

However, in the CFD program, the heat transfer coefficient which is an input for the program uses the temperature difference between the wall surface and the first cell from the wall. Since the grid should be fine near the walls, the distance between the wall and the first cell is less than 0.3 m in most cases. Therefore, to find appropriate heat transfer coefficient, it is necessary to check whether the h_c for the temperature difference between the wall surface temperature and the air temperature is between 3 ~ 6 W/m^2K in the result. It may take a few iterations to obtain the appropriate coefficient input for the program. The equation (3.2.2) may be used for this procedure.

$$q = h_c(T_W - T_{air}) = h_{CFD}(T_W - T_{firstcell}) \quad (3.2.2)$$

where

h_{CFD} = convective heat transfer coefficient input in the CFD program

$T_{firstcell}$ = air temperature at the first cell from the wall

In addition to the procedure above, to get the appropriate values of h_{CFD}, it is necessary to compare the computed results to the experiment data and to adjust the coefficients if it is needed. This may also need some iterations. The heat transfer coefficients which were used in the CFD program as input values are shown in Table 3.2.1.

Table 3.2.1 The heat transfer coefficients which were used in the CFD program

	Ceiling	Side Wall	Floor	Window
h_{CFD}	10	20	20	20

Heated objects

The surface temperatures of the heated objects, such as persons, PCs, and ceiling lamps, were also measured in the experiments by an infra-red temperature sensor. Therefore, the boundary conditions of heated objects were similar to the walls.

The known values also include the total heat from the objects. However, the total heat consisted of both the convective heat and the radiative heat as shown in Equation 3.2.3. The radiative heat was considered to be included in the wall temperatures around the objects, which released heat to the room by convection from the wall. Therefore, in the CFD program, the convective heat flow boundary condition was used for the heated objects.

Since the total heat consists of both the convective heat and the radiative heat and only the total heat was known, it is necessary to estimate both the convective heat and the radiative heat in order to specify the boundary condition. With the known surface temperature of the heated object, the h_{CFD} was adjusted case by case to give a reasonable convective heat output to match with the experimental condition. The estimation of the h_{CFD} used Equations 3.2.4 and 3.2.5 for radiative and convective heat transfer.

$$Q_{total} = q_{convection} + q_{radiation} \quad (3.2.3)$$

$$q_{radiation} = \varepsilon_{object}\varepsilon_{wall}\sigma(T_{object}^4 - T_{walls}^4)A_{object} \quad (3.2.4)$$

$$q_{convection} = h_c(T_{object} - T_{air}) \quad (3.2.5)$$

where

ε_{object} = surface emissivity of the heated objects
ε_{wall} = surface emissivity of the surrounding walls
σ = Stefan-Boltzmann constant
T_{object} = surface temperature of the heated objects
T_{air} = air temperature around the heated objects
T_{walls} = surface temperature of the surrounding walls
A_{object} = surface area of the heated objects

By assuming h_c and T_{air} at first, T_{object}, $q_{convection}$ and $q_{radiation}$ can be calculated from the equations above. After the first simulation with the calculated the convective heat flow from the objects, it was necessary to compare T_{air} in the result to T_{air} which was assumed before the simulation. If the difference is large, another calculation with the corrected T_{air} is necessary in order to get the appropriate T_{object}, $q_{convection}$, and $q_{radiation}$. In addition, it was also necessary to compare the computed results of the room to the experiment data and to adjust the convective heat flow values from the objects if it is needed. These procedures need about five iterations.

The convective heat coefficient was assumed to be uniformly distributed on the entire surface for most of the heated object surfaces. In the case that the certain surfaces were considered to have more convective heat than the other surfaces based on the real situations, it was represented by the different surface temperature measured from the experiments.

The ratios of convective heat and radiative heat which were used in the CFD program are shown in Table 3.2.2. They were summarized in range since they were varied case by case.

Table 3.2.2 Ratios of convective heat and radiative heat for heated objects

	Ratio of convection (%)	Ratio of radiation (%)	Total heat (W)
Person	70-90	10-30	100-200
Equipment	45-65	35-55	100
Ceiling lamp	50-60	40-50	64

Diffusers and perforated panels (Inlets)

Round swirl diffusers and perforated panels were used in the experiments. Simulating the inlets was a challenge for indoor simulation, since the complicated geometry of the diffusers, the tiny wholes of the panel and high turbulence near the inlet. The model of the boundary conditions for the diffuser was investigated.

The round floor diffusers used in the experiment discharges a swirl jet. Serbric (2000) simulated the vortex ceiling diffuser using CFD. In the study, the diffuser was simulated as the rectangular shape which was divided into sixteen small cells, each having a different airflow direction which was obtained from the smoke visualization. The momentum method was used to simulate the diffusers.

For this research, the floor round diffusers and perforated panels were also simulated by the momentum method. The perforated panels were represented as a 0.6m x 0.6m square opening with a fixed mass inflow and velocity while the diffusers were represented as the rectangular shape which was divided into nine small cells, shown in Figure 3.2.1. Each cell except for the center cell has a different airflow direction. Because the center of the diffuser does not have an opening, the center cell does not have airflow. The important things to consider for this kind of diffuser were the airflow direction and velocity from the diffuser.

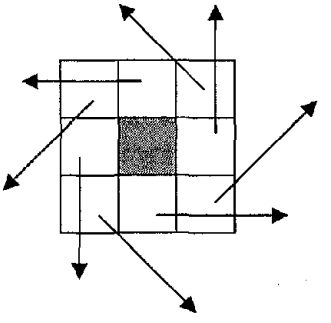

Figure 3.2.1 Floor diffuser simulation

Both horizontal and vertical airflow directions were obtained from the smoke visualization. However, it was difficult to find an exact direction or angle, since they are not so clear. Therefore, several angles were chosen and simulated. By comparing the computed results with different angles to the experiment data, the appropriate airflow angle was determined.

Since the opening shape of the diffuser is complex, even though the opening area and the total airflow rate from the diffuser are known, it is difficult to find the accurate velocity from the diffuser openings by calculation. Therefore, directly measured velocities at the diffusers by the anemometer were used. The turbulence intensities of the diffusers were also specified as the measurements of the anemometer.

For the experimental set-up, the conditioned air went to the floor plenum and then went to each diffuser or each perforated panel. Since the pressure of the floor plenum was not evenly distributed and diffusers or panels were not individually controlled, the velocity of each diffuser or perforated panel is not the same. The values used in the CFD program are in Table 3.2.3.

Table 3.2.3 Values used for the diffuser simulation

	Vertical angle	range of air velocity range (m/s)
Workshop-1	60	1.2-2.0
Workshop-2	N/A	0.16-0.43
Office-1	60	2.0
Office-2	N/A	0.11-0.14
Office-3	75	0.88-1.51
Office-4	N/A	0.05-0.14

Exhaust (Outlets)

Zero pressure and zero gradient for all the flow parameters were used as the boundary conditions for the exhaust.

Source of tracer gas

The tracer-gas, SF_6, source was set as a zero-momentum source. Considering the amount of total mass is very small and it does not affect the results much, a zero-momentum assumption is reasonable.

Results

Cases of Workshop-1 and Office-1 were employed as the reference cases for the performance analysis in Chapter 4. These two cases were also used for validating the CFD calculations. The other four experimental cases were used as further comparison under different geometries and diffusers types. The conclusions are similar to those obtained for cases of Workshop-1 and Office-1. Appendix A shows more detailed results for the other four cases.

Figures 3.2.2 to 3.2.3 present, respectively, the measured and computed temperature, velocity, and SF_6 concentration for cases of Workshop-1 and Office-1. The measurements were done at nine different pole locations. Each pole has sensors at different heights to measure temperature, velocity, and SF_6 concentration. Table 3.2.4 summarized the figure number and the corresponding results shown in the figures.

Table 3.2.4 Figure number and the corresponding cases

Case	*Figure number*	*Remark*
Workshop-1	3.2.2	(a) – Velocity
Office-1	3.2.3	(b) – Temperature
		(c) – SF_6 concentration

Figures 3.2.2 (a) and 3.2.3 (a) present velocity distributions of these two cases. The velocities in the room were generally low for both cases. The velocity is less than 0.2 m/s except around the diffusers and exhaust. The agreements between the computed velocity and measured data are

acceptable in both cases. Except in pole 1, 6 and 7 of Workshop-1 (Figure 3.2.2(a)), there are discrepancies at the region higher than 1.1 m. It is because the RNG k-ε model tends to over-estimate the convective plume of heat sources (Chen 1995). Reynolds stress turbulence model was suggested by Chen (1995) for calculating convective plumes velocity. Reynolds stress turbulence model has six additional stress equations to calculate compared with the RNG k-ε model. Reynolds stress turbulence model accounts for the effects of streamline curvature, swirl, rotation, and rapid changes in strain rate than the RNG k-ε model, it has greater potential to give accurate predictions for complex flows. However, Reynolds stress turbulence model is not adopted in this research due to the restricted convergence in complex geometry and high computational effort.

Figures 3.2.2 (b) and 3.2.3 (b) clearly show that the floor-supply system created temperature stratification in both cases. The cold supply air tended to spread over the room and stayed at the lower level and swirl diffusers induced a strong turbulence and mixing effect. The computed temperature and measured data were generally in agreement except at the pole near the swirl diffusers. At poles 1 and 7 of Workshop-1 (Figure 3.2.2(b)), there are discrepancies at the region higher than 1.1m. It is the same cause due to the over-estimation of velocity in those regions and explained above.

Figures 3.2.2 (c) and 3.2.3 (c) present tracer gas distributions. In most of the cases, the agreements between the computed tracer-gas concentration and measured data are not as good as the temperature and velocity. Since the tracer-gas is a point source and the concentration is very sensitive to the position, it is difficult to get good agreement between the computed tracer-gas concentration and measured data at every point. For example, the computed data of pole 3 was being moved 15 cm apart and the concentration was changed significantly. Nevertheless, the accuracy of the computed concentration seems still acceptable.

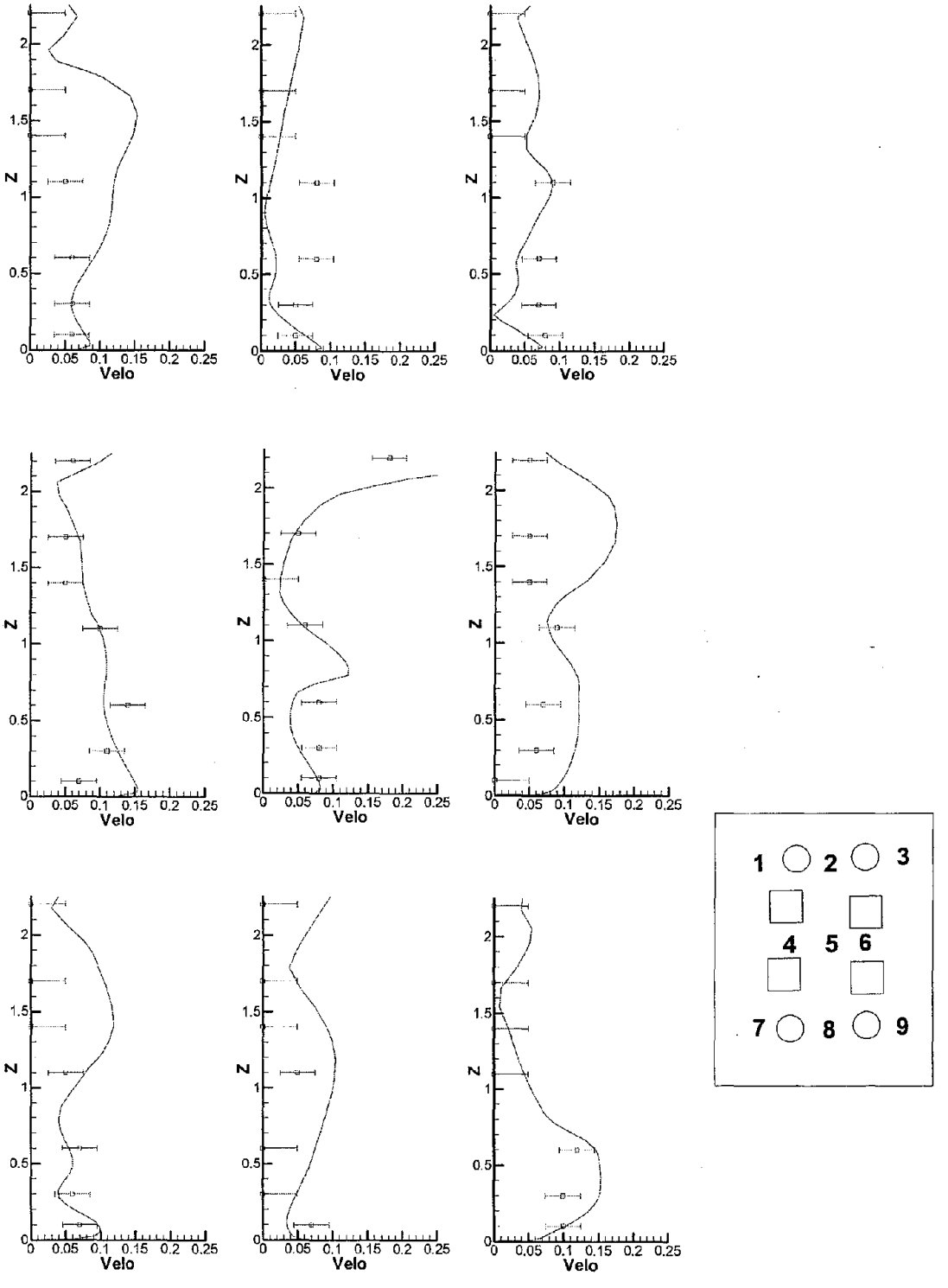

Figure 3.2.2(a) Comparison of the vertical velocity profiles of Workshop-1 units: (m/s), Symbols: measurement, Lines: computation

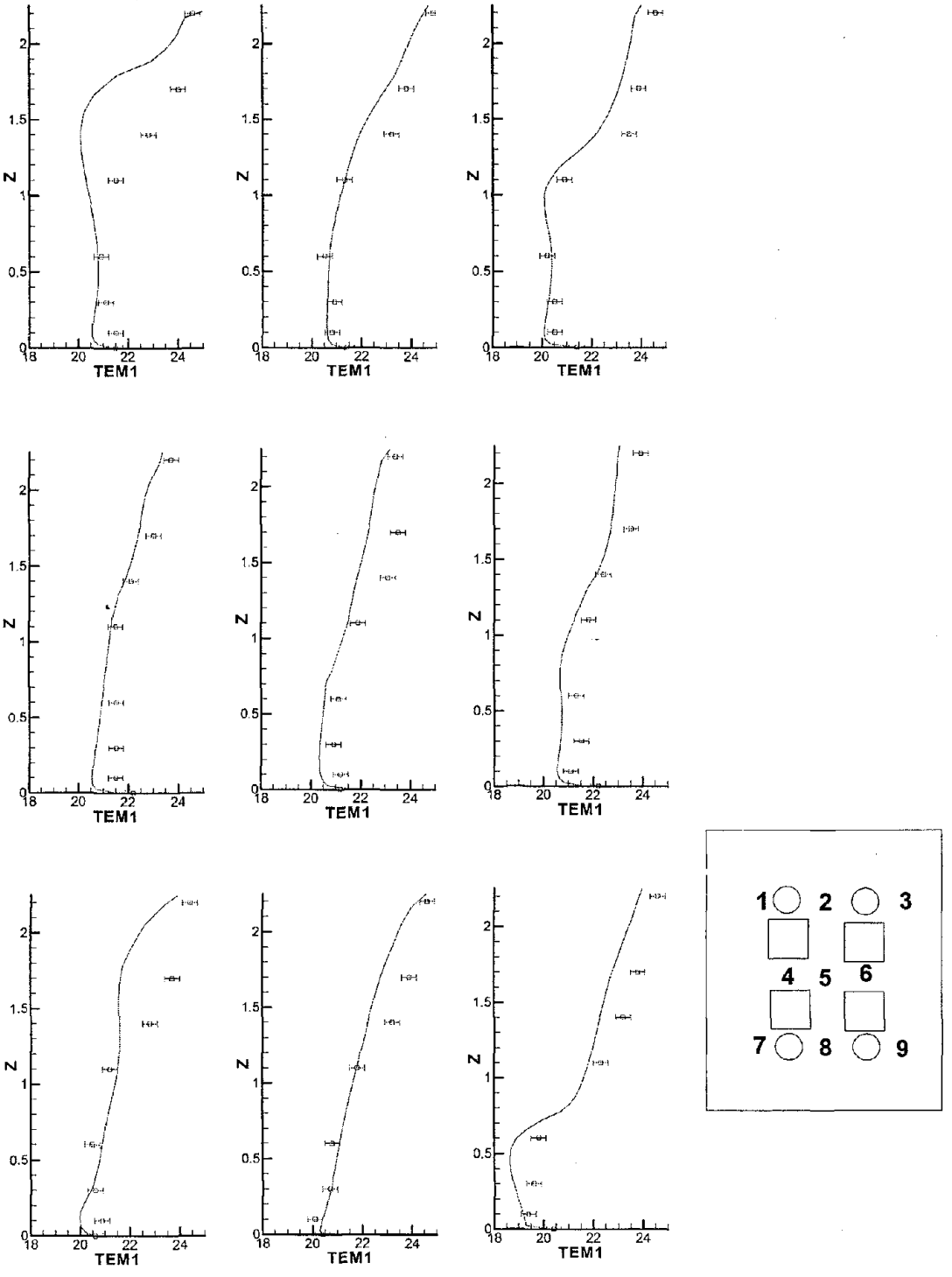

Figure 3.2.2(b) Comparison of the vertical temperature profiles of Workshop-1 units: (^{O}C), Symbols: measurement, Lines: computation

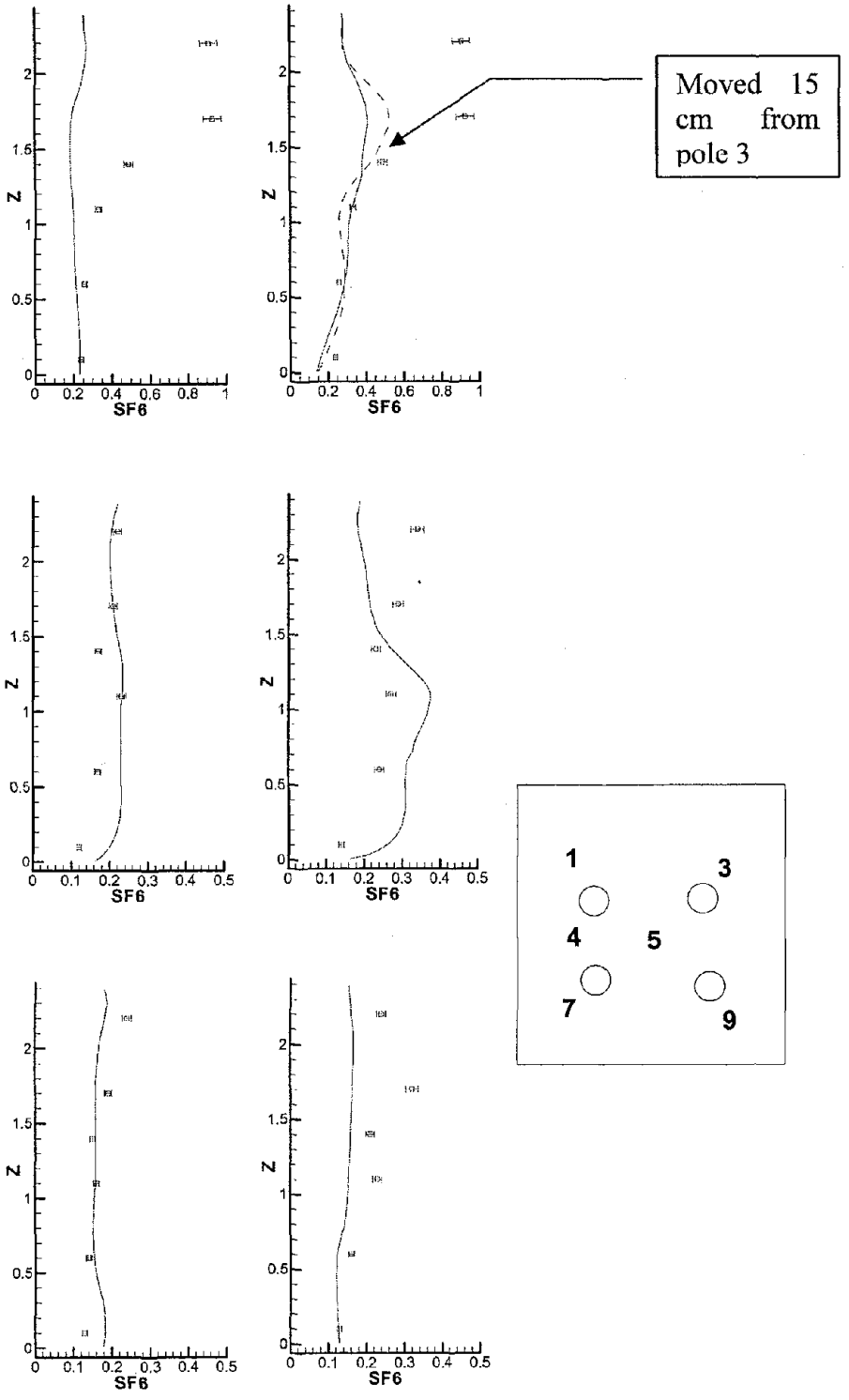

Figure 3.2.2(c) Comparison of the vertical SF_6 concentration profiles of Workshop-1 units: (ppm), Symbols: measurement, Lines: computation

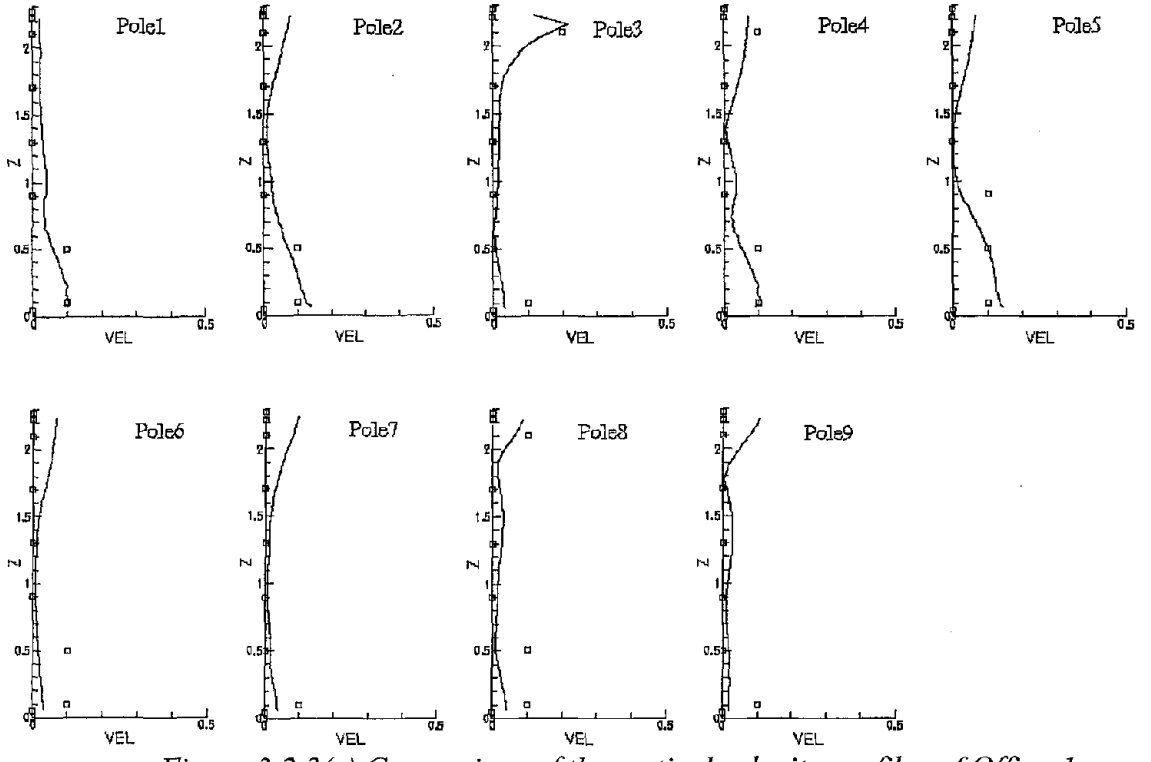

Figure 3.2.3(a) Comparison of the vertical velocity profiles of Office-1
Symbols: measurement, Lines: computation

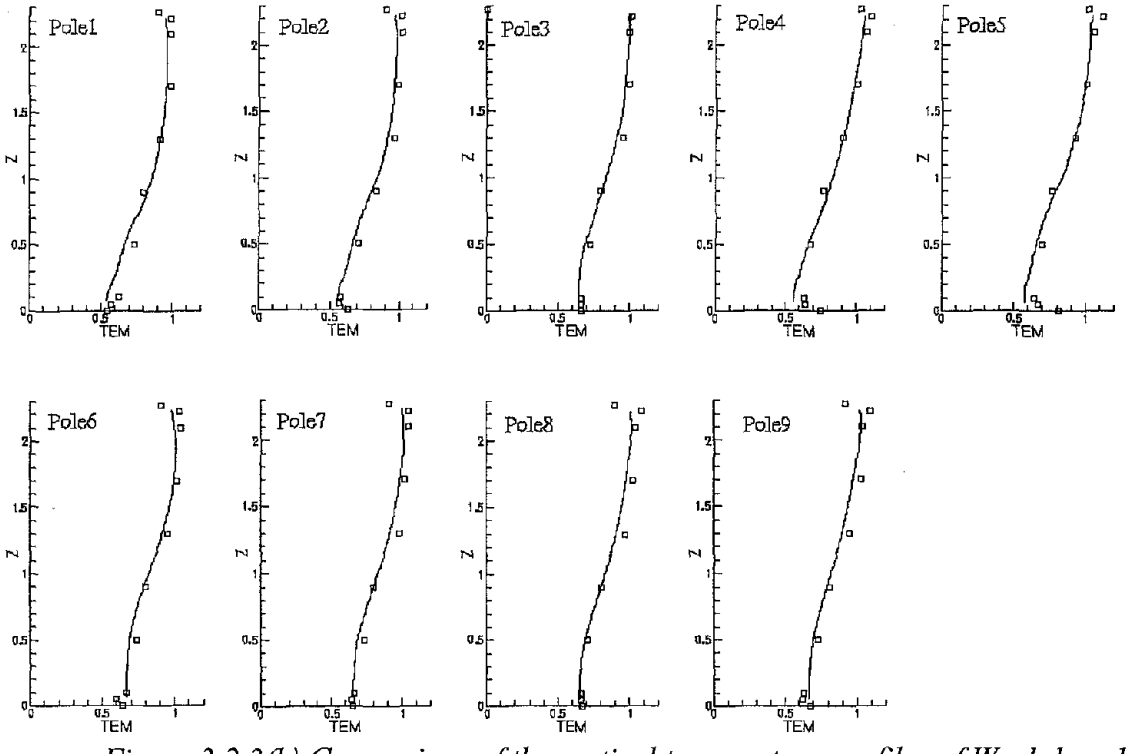

Figure 3.2.3(b) Comparison of the vertical temperature profiles of Workshop-1
units: (^{O}C), Symbols: measurement, Lines: computation

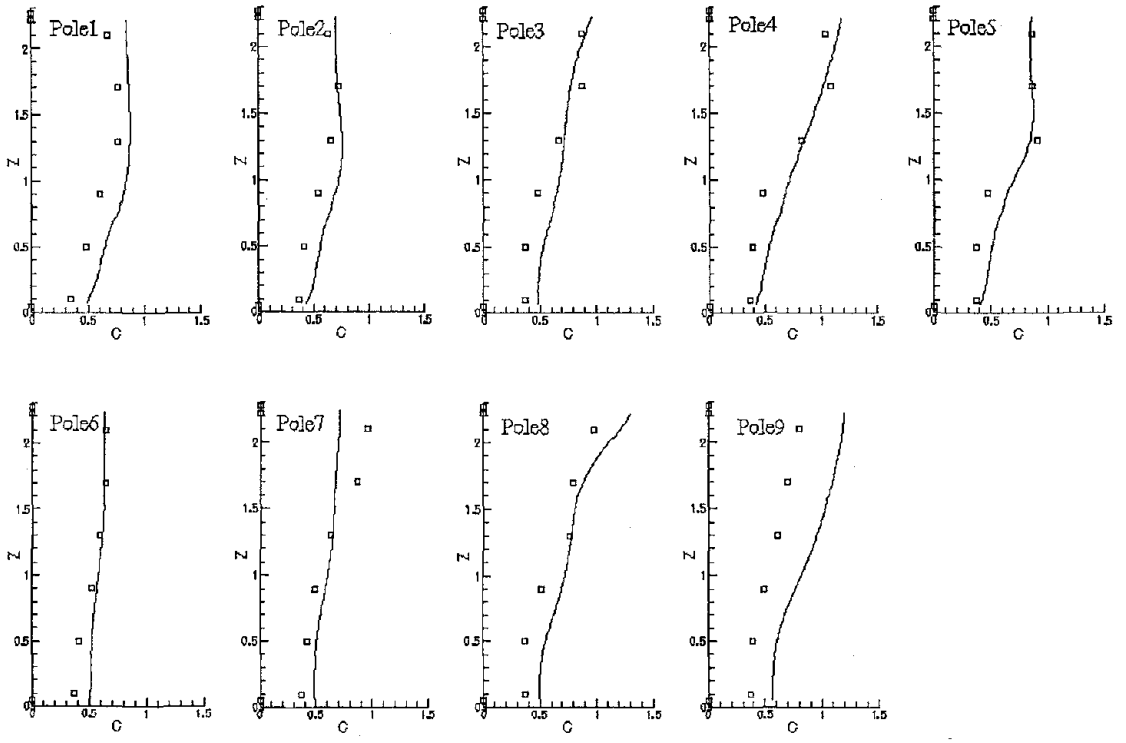

Figure 3.2.3(c) Comparison of the vertical SF_6 concentration profiles of Office-1 C=(c-c,inlet)/(c,exhaust-c,supply), Symbols: measurement, Lines: computation

3.3 Conclusions

A CFD program with the RNG k-ε model of turbulence has been used to predict the airflow, air temperature, and tracer gas concentration distributions in the settings of an office and an industrial workshop. The CFD program was validated by comparing computed results to the experimental data obtained in Chapter 3.

The computed air temperature and air velocity agreed well with the measured data. However, some discrepancies were found between the computed and measured tracer gas concentration. Despite the discrepancies, the validated CFD program predicts the room environment well so that it can be used for indoor simulation in a room with floor-supply displacement ventilation.

4. PERFORMANCE EVALUATION OF THE FLOOR- SUPPLY DISPLACEMENT VENTILATION

This chapter evaluates the performance of the floor-supply displacement system, based on thermal comfort and indoor air quality. The CFD program validated in Chapter 3 is used as a tool for the performance evaluation.

For the office case, we investigated the impacts of the supply airflow rate (air change rate), supply air temperature, number of diffusers, diffuser location, exhaust location, occupant location, and furniture arrangement on the system performance. Then we studied the influence of different cooling loads on the system design.

For the workshop case, we investigated the impacts of the room size and diffuser type on the system performance. Based on the case with an increased room size, the impacts of supply airflow rate (air change rate), supply air temperature, number of diffusers, diffuser location, exhaust location, occupant location, partition arrangement, furniture arrangement and room size were further studied.

4.1 Evaluation Criteria

Thermal comfort level

The current study used the following parameters to evaluate the thermal comfort in a room with the floor-supply displacement ventilation.

- Temperature gradient
- Percentage dissatisfied people due to draft (PD)
- Percentage predicted dissatisfied people (PPD)

The CFD program can calculate the three-dimensional airflow pattern and air velocity, air temperature, and turbulence distributions. With the distributions of air velocity, temperature and turbulence, it is easy to calculate the PD and PPD.

The percentage of dissatisfied people due to draft (PD)

Fanger et al. (1989) developed a model to calculate the PD as:

$$PD = (34 - T)(u - 0.05)^{0.62}(3.14 + 0.37u\,Tu) \quad [\%] \qquad (4.1.1)$$

for PD>100%, PD=100%

where

T = air temperature [°C]
u = air velocity [m/s]
Tu = turbulence intensity [-].

We use

$$Tu=100(2k)^{0.5}/u\ [\%] \qquad (4.1.2)$$

where

k = turbulent kinetic energy.

The predicted percentage of dissatisfied people for the thermal comfort (PPD)

The PPD can be calculated via (ISO 1993):

$$PPD = 100 - 95\exp(-0.03353PMV^4 - 0.2179PMV^2)\ [\%] \qquad (4.1.3)$$

The predicted mean vote, PMV, in the equation is determined by:

$$PMV = [0.303\exp(-0.036M) + 0.028]\ L \qquad (4.1.4)$$

where

L = the thermal load on the body.

Temperature gradient

Especially with the floor-supply displacement ventilation, there is a vertical temperature gradient in the room. According to the ASHRAE standard 55-2004, the temperature difference between the foot level and the head level should be less than 3 °C .

Indoor air quality

The following parameters were used to evaluate the indoor air quality in the room with the floor-supply displacement ventilation system.

- Contaminant concentration distributions
- Mean age of air
- Ventilation effectiveness

The CFD program validated in Chapter 3 can directly calculate these parameters.

Contaminant concentration distributions

In this study, CO_2 is used as an indicator for contaminant concentration. The CO_2 concentration at the supply air is assumed to be 400 ppm in the CFD study. The indoor CO_2 sources are from the occupants. According to the ASHRAE Standard 62-2001, the CO_2 concentration should be less than 1000 ppm in the room.

Mean age of air

The mean age of air, τ, is defined as the average time for all air particles travel from the supply diffuser to that point. It can be derived from the measured transient history of the tracer-gas concentration. Li and Jiang (1996) showed that the mean age of air is governed by a transport equation:

$$\frac{\partial}{\partial t}(\rho\tau)+\frac{\partial}{\partial x_j}(\rho u_j\tau)=\frac{\partial}{\partial x_j}\left(\Gamma_\tau\frac{\partial\tau}{\partial x_j}\right)+\rho \qquad (4.1.5)$$

with the following as the boundary conditions:

$\tau=0$ at the supply diffuser

$\frac{\partial\tau}{\partial x_j}=0$ at the exhaust and walls

Ventilation effectiveness

The ventilation effectiveness is defined as:

$$\eta=\frac{c_e-c_s}{c-c_s} \qquad (4.1.6)$$

where

η = ventilation effectiveness [-]
c_e = contaminant concentration in the exhaust air [ppm]
c_s = contaminant concentration in the supply air [ppm]
c = contaminant concentration in the room air [ppm]

In the condition of complete mixing ventilation, the ventilation effectiveness is 1.

4.2 Floor Displacement Ventilation for Offices

This section focuses on the impacts of several parameters for an office. With the validated CFD program, we investigate numerically the impacts of the following parameters on the indoor air quality and thermal comfort of the floor-supply displacement ventilation systems:

- Supply airflow rate (Air change rate)
- Supply air temperature
- Number of diffusers
- Partition arrangement
- Distance between the workers
- Furniture arrangement
- Exhaust location and number

- Diffuser location

Table 4.2.1 shows the conditions studied. Case R, the reference case (experimental case – Office-1), has a typical office configuration. Although it looks like a small office but it can be interpreted as a part of a large office. Seven different cases are made from the reference case, and each case has two variations. The different parameters of each case are marked as bold letters, and the results of each case are compared to those of the reference case.

Table 4.2.1 Conditions of Parameter Studies for Offices

Conditions

Room Size:	5.16m x 3.65m x 2.7m(H)		
Heat source:	Occupant x 2:	75W(total) x 2	(Convection: 60W/80%)
	PC x2:	108.5W(total)x1	(Convection: 61W/56%)
		173.4W(total)x1	(Convection: 97W/56%)
	Ceiling Light x 4:	68W(total) x 4	(Convection: 41W/60%)

Study Case

	ach	supply air temperature	# of diffusers	partition	occupants location	furniture	Exaust location	diffuser location
Case R	**4**	**19**	**2**	**0**	**far(3m)**	**1 box**	**center**	**regular**
Case-1-1	**2**	**16**	2	0	far(3m)	1 box	center	regular
Case-1-2	**8**	**22**	2	0	far(3m)	1 box	center	regular
Case-2-1	4	19	**1**	0	far(3m)	1 box	center	regular
Case-2-2	4	19	**4**	0	far(3m)	1 box	center	regular
Case-3-1	4	19	2	**2**	far(3m)	1 box	center	regular
Case-3-2	4	19	2	**4**	far(3m)	1 box	center	regular
Case-4-1	4	19	2	0	**near(1m)**	1 box	center	regular
Case-4-2	4	19	2	0	**middle(2m)**	1 box	center	regular
Case-5-1	4	19	2	0	far(3m)	**6 boxes**	center	regular
Case-5-2	4	19	2	0	far(3m)	**6boxes+1table**	center	regular
Case-6-1	4	19	2	0	far(3m)	1 box	**near window**	regular
Case-6-2	4	19	2	0	far(3m)	1 box	**2 exhausts**	regular
Case-7-1	4	19	2	0	far(3m)	1 box	center	**near**
Case-7-2	4	19	2	0	far(3m)	1 box	center	**far**

Reference case (Case R)

The configuration of Case R is shown in Figure 4.2.1. The configuration is almost the same as the case used for validation. In this chapter, this case will be used for the comparison with all other case studies.

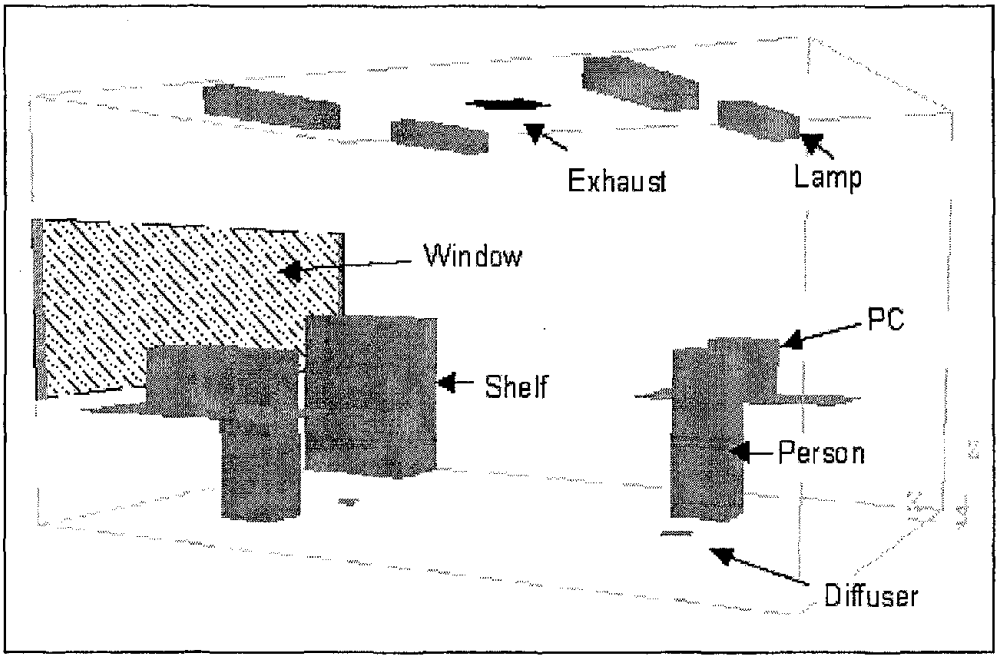

Figure 4.2.1 Configuration of Case R

With this condition, following values in the room are calculated using CFD:

- Temperature
- Velocity
- PD
- PPD
- CO_2 Concentration
- Mean age of air
- Ventilation effectiveness

Since this case will be a reference case, which will be compared to the different cases, two section figures and brief explanation for each parameter are given here. Two section figures, at Y=1.825m and Y=2.635m, are selected. Section at Y=1.825m is at the center of the room in Y direction and section at Y=2.635m is a section where an occupant is sitting.

Temperature

The temperature distributions at section of Y=1.825m and Y=2.635m are shown in Figure 4.2.2. There is temperature stratification in vertical direction, which indicates that the floor- supply system provides displacement ventilation. In general, the vertical temperature gradient depends on the airflow from the floor diffusers and the distribution of the heat sources in the room. The gradient in the occupied zone is larger than that above the occupied zone because it is where most of the heat sources are located. Therefore, the system should be carefully designed so that

the temperature difference between the ankle level and the head level can be maintained to be less than 3 °C , which is the ASHRAE standard's criterion.

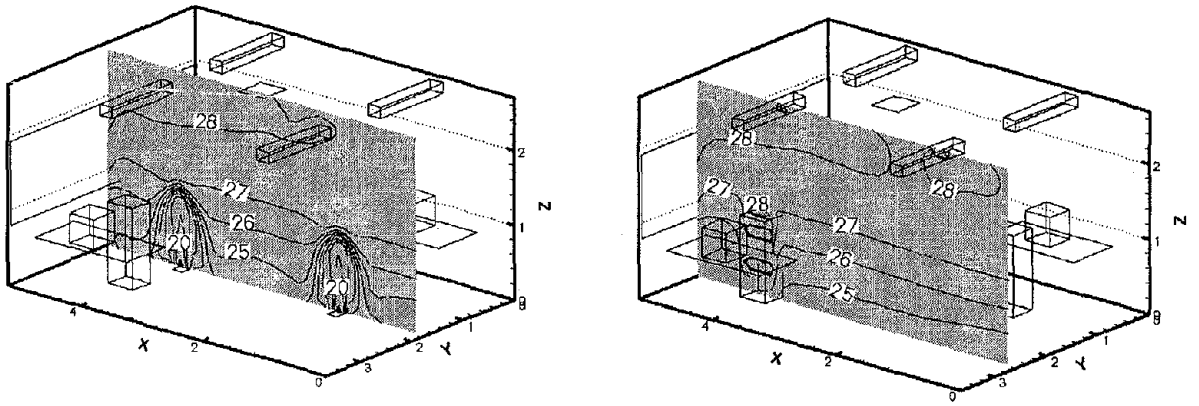

Y=1.825m Y=2.635m

Figure 4.2.2 Temperature distributions at Y=1.825m and Y=2.635m for Case R

Velocity

The velocity distributions at section of Y=1.825m and Y=2.635m are shown in Figure 4.2.3. The supply air velocity from a diffuser is about 2m/s in this condition. It can be seen that supply air velocity is quickly reduced around the diffuser. The area where the air velocity is more than 0.1m/s is only within about 0.5m from the diffuser. Therefore, the risk of draft due to the high air velocity is considered to be small.

In addition to the area near the diffusers, above the heat sources, such as PCs and persons, plumes due to the heat from the objects can be seen.

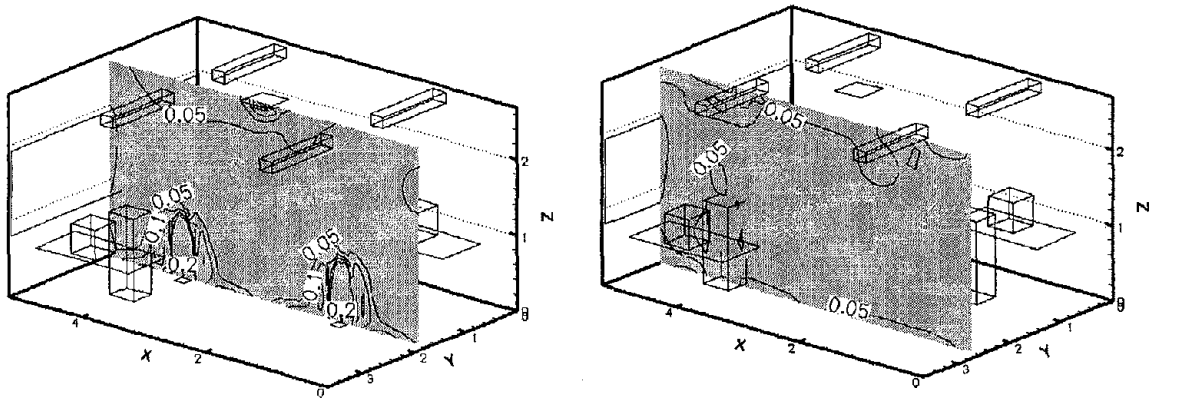

Y=1.825m Y=2.635m

Figure 4.2.3 Velocity distributions at Y=1.825m and Y=2.635m for Case R

Percentage dissatisfied people due to draft (PD)

The PD distributions at section of Y=1.825m and Y=2.635m are shown in Figure 4.2.4. PD is generally less than 10% in the room. Only around diffuser is PD more than 10% due to the supply air velocity from the diffusers. The area where PD is more than 10% is similar to the area where air velocity is more than 0.1m/s.

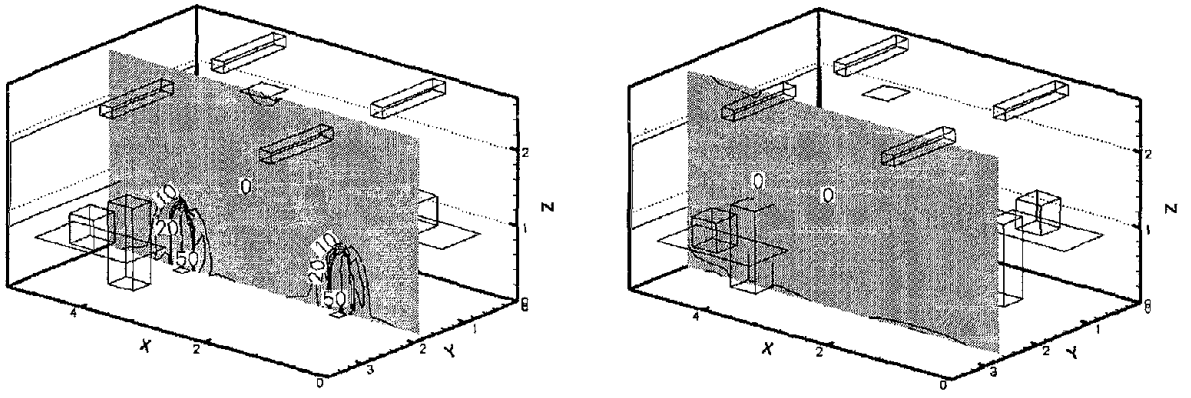

Figure 4.2.4 PD distributions at Y=1.825m and Y=2.635m for Case R

Percentage predicted dissatisfied people (PPD)

The PPD distributions at section of Y=1.825m and Y=2.635m are shown in Figure 4.2.5. The PPD has a vertical stratification similar to the temperature due to the fact that PPD is a temperature related value. The PPD is generally less than 12% in the room, which can be considered to be acceptable comfort level.

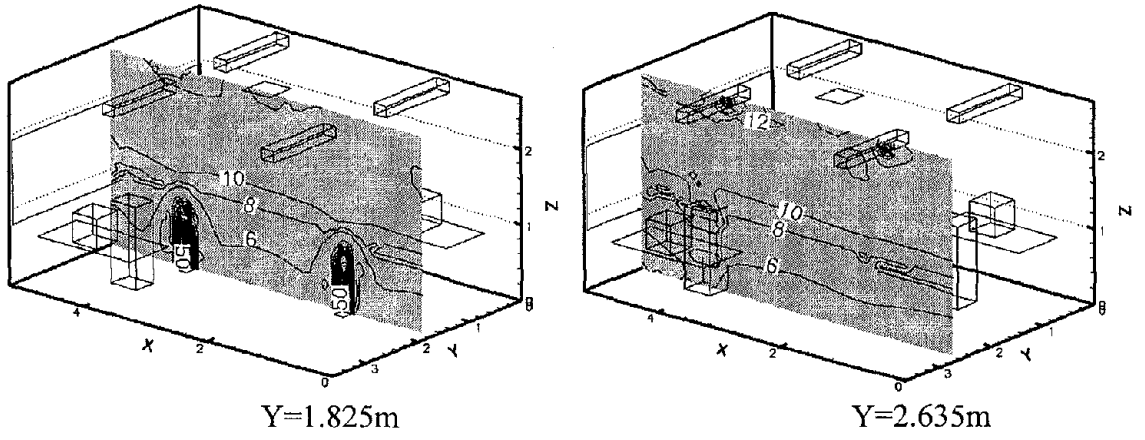

Figure 4.2.5 PPD distributions at Y=1.825m and Y=2.635m for Case R

CO_2 Concentration

The CO_2 distributions at section of Y=1.825m and Y=2.635m are shown in Figure 4.2.6. In this study, CO_2 is used as an indicator for contaminant concentrations. The CO_2 distributions also have a vertical stratification in that the CO_2 concentration in the lower zone is lower than that in the upper zone. The stratification occurs because the fresh air is supplied directly to the occupied zone from the diffusers on the floor and because the heat from the heat sources generates thermal plumes which can bring the CO_2 to the upper zone. The average CO_2 concentrations at the height of 0.1m, 1.1m, and 1.7m are approximately 520ppm, 590ppm, and 620ppm, respectively.

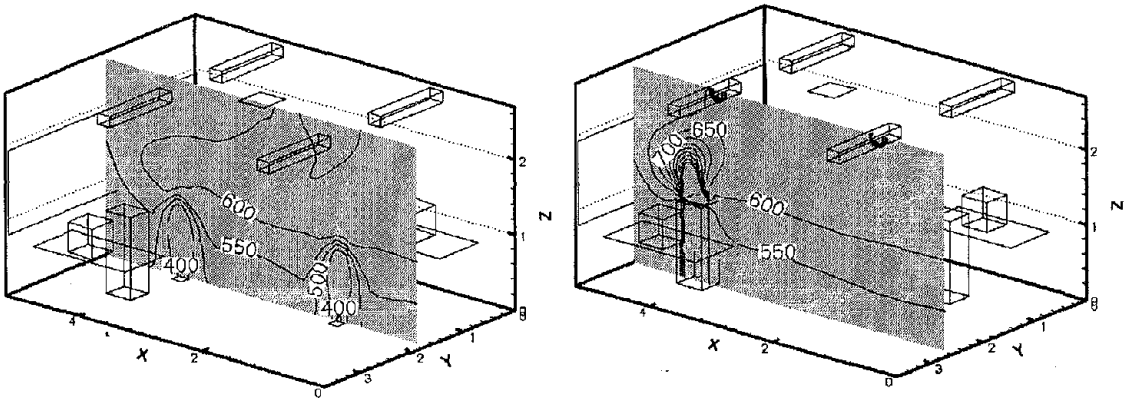

Y=1.825m Y=2.635m

Figure 4.2.6 CO_2 distributions at Y=1.825m and Y=2.635m for Case R

Mean age of air

The mean age of air distributions at section of Y=1.825m and Y=2.635m are shown in Figure 4.2.7. The mean age of the air in the lower part of the room is much younger than that in the upper part of the room. The averaged mean age of air at the height of 0.1m, 1.1m, and 1.7m are approximately 575 s, 810 s, and 845 s, respectively. For complete mixing ventilation, the mean age of air in the room is about 900-1000 s. The floor-supply ventilation systems thus provide better indoor air quality to the occupied zone than mixing ventilation systems.

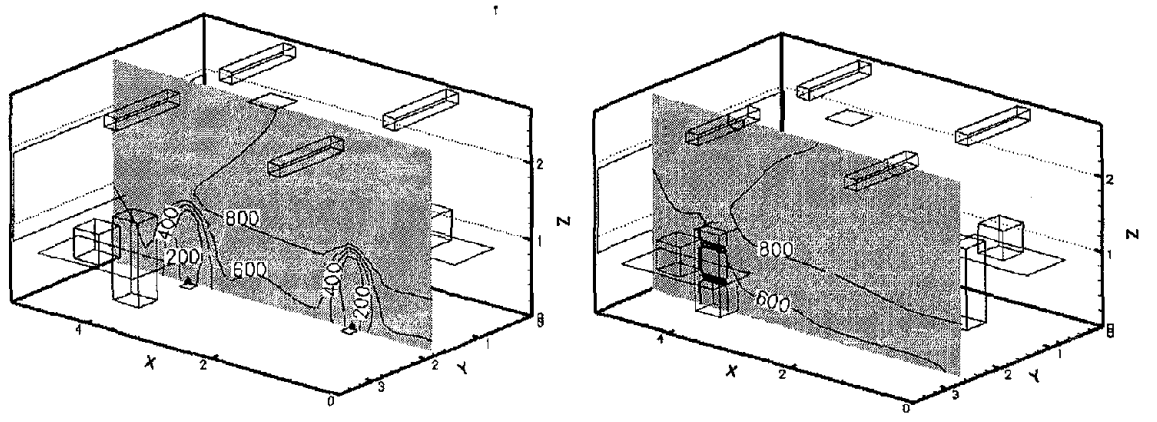

Y=1.825m Y=2.635m

Figure 4.2.7 Mean age of air distributions at Y=1.825m and Y=2.635m for Case R

Ventilation effectiveness

The ventilation effectiveness distributions at section of Y=1.825m and Y=2.635m are shown in Figure 4.2.8. The occupied zone in the room has higher ventilation effectiveness than that of the complete mixing system, which has a value of 1.0.

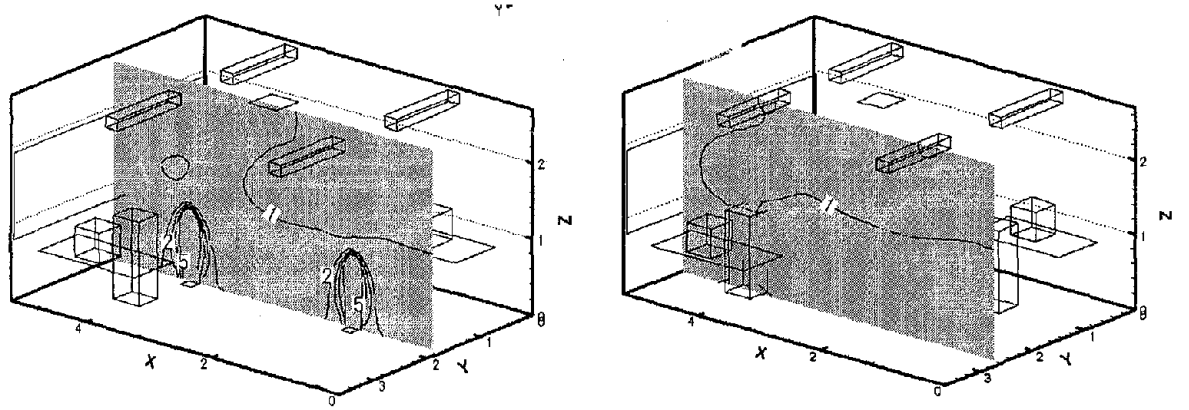

Y=1.825m Y=2.635m

Figure 4.2.8 Ventilation effectiveness distributions at section of Y=1.825m and Y=2.635m

In the following sections, the thermal and fluid conditions will be changed one by one to study their impact on thermal comfort and air quality in the office.

Change of air change rates and supply temperature (Case 1)

In Case 1, the air change rates and supply temperature are changed and the rest remain unchanged. An air change rate is one of the most important parameters for indoor environments. In general, higher air change rates can obtain better indoor environments. However, higher air

change rate consume more energy because of increased fan powers and cooling or heating heat sources. Therefore, if the indoor environment is acceptable, lower air change rates would be better in terms of a lower energy consumption. The supply air temperature is usually determined from the cooling load and the air change rate. Case 1-1 has lower air change rate (2 ach) and lower supply air temperature (16 °C) than that of Case R. Case 1-2 has higher air change rate (8 ach) and higher supply air temperature(22 °C) than that of Case R.

The temperature difference between the foot level and the head level of the reference case and Case 1-1 is around 3.0 °C, which is almost maximum of the acceptable range. On the other hand, in Case 1-2, the temperature is almost uniform in the occupied zone and the temperature difference is about 1 °C. This indicates that with 8 ach, because of the high airflow rate and the supply air velocity (about 2.4m/s), the ventilation is a mixing ventilation rather than a displacement ventilation.

In Case 1-2, the area where PD is higher than 10% is much larger than the other two cases, due to the higher air velocity from the diffusers. Except for the area around diffusers, PD is less than 10%. The area where PD is more than 10% in Case 1-2 is about 1.5m wide and 2m high. If an occupant stays within this area, the occupant would feel a draft. Therefore, with 8 ach, occupants have to avoid sitting within 1.5 m from the diffusers.

The mean age of air corresponds to the air change rate. The higher the air change rate, the younger the age of air. The averaged mean ages of air at Z=1.1m in Case 1-1, Case R, and Case 1-2 are approximately 400 s, 800 s, and 1600 s, respectively. These values are almost proportional to the air change rates.

Similar to the mean age of air, both the CO_2 Concentration and the ventilation effectiveness correspond to the air change rate. The higher the ACH, the lower the CO_2 Concentration and the higher the ventilation effectiveness.

Change of diffuser number (Case 2)

In Case 2, the diffuser number is changed that implies the change of airflow rate or supply air velocity from each diffuser. More diffusers can obtain a more uniform indoor environment, especially horizontally. However, the air change rate is generally determined from the supply air temperature needed to counteract the cooling load. Therefore, the total air change rate is fixed (4 ach) and only the number of diffusers is changed. This means that the airflow rates, or supply air velocity from each diffuser are different in the three cases. The configurations of the Cases 2-1 and 2-2 are shown in Figures 4.2.9 and 4.2.10, respectively. Case 2-1 has one diffuser, Case R has two diffusers, and Case 2-2 has four diffusers. The supply air velocity from each diffuser is 2.4m/s in Case 2-1, 1.2m/s in Case R, and 0.6m/s in Case 2-2.

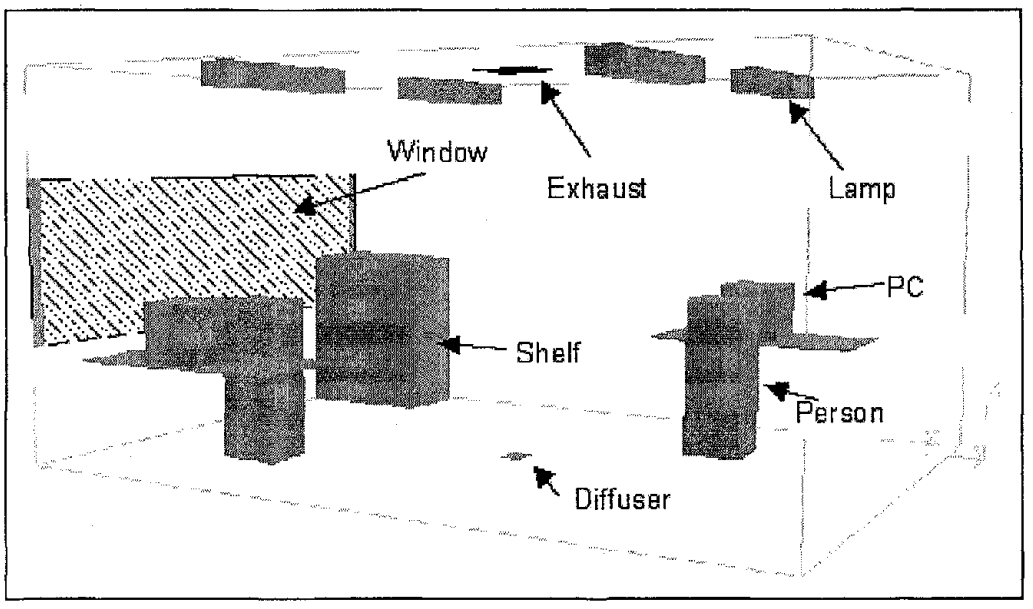

Figure 4.2.9 Configuration of Case 2-1

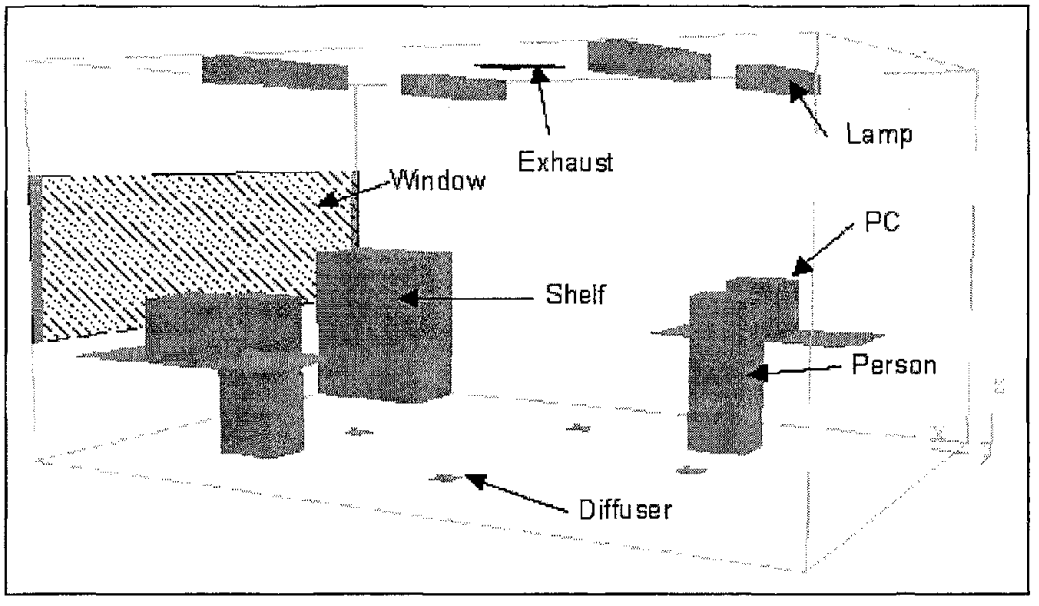

Figure 4.2.10 Configuration of Case 2-2

Table 4.2.2 shows the averaged temperature at the height of 0.1m (ankle level), 1.1m (sitting head level), and 1.7m (standing head level), and the temperature differences between 0.1m and 1.7m (DT1), 0.1m and 1.1m (DT2). The temperature gradient in Case 2-2 is larger than the other two cases, while Case R and Case 2-1 have almost same temperature gradient. Also, DT1 and DT2 in Case 2-2 are about 20-40% larger than those in Case R and Case 2-1. DT1 in Case 2-2 is 3.5 °C , which is larger than the acceptable value. The lower supply air velocity (less than 1.0m/s in this study) generates a greater temperature gradient in the vertical direction, even though total

airflow rate to the room is same. Therefore, the air velocity should not be too low in order to avoid the unacceptable temperature gradient. However, the temperature gradient also depends on the heat sources in the room and the acceptable lowest velocity depends on the internal heat condition.

Table 4.2.2 Averaged temperatures at 0.1m, 1.1m, and 1.7m high

	Height (m)	**TEM (°C)**	**DT1 (1.7m-0.1m)**	**DT2 (1.1m-0.1m)**
Reference Case	**0.1**	24.6	3.1	2.2
	1.1	26.8		
	1.7	27.7		
Case 2-1	**0.1**	24.8	2.9	2.0
	1.1	26.8		
	1.7	27.7		
Case 2-2	**0.1**	24.5	3.5	2.8
	1.1	27.3		
	1.7	28.0		

Table 4.2.3 shows that the averaged mean ages of air at the height of 0.1m, 1.1m, and 1.7m. The age of air at 1.1m and 1.7m high in Case 2-2 is older than those in other two cases, which is attributable to a low supply air velocity. With low supply air velocity, the air spends more time to traveling from the diffusers to the outlet than that with high velocity. On the other hand, in the horizontal direction, less number of diffusers is worse because it is difficult to cover the entire room. Both vertical and horizontal directions must be considered to obtain the best balance of the number of diffusers and supply air velocity for the best indoor air quality. In this case, Case R is the best one and it has the youngest average mean age of air at 1.1m in all three cases.

Table 4.2.3 Averaged age of air at 0.1m, 1.1m, and 1.7m high

	Height (m)	**MAA (sec)**
Reference Case (2 diffusers)	**0.1**	576.3
	1.1	810.5
	1.7	846.6
Case 2-1 (1 diffuser)	**0.1**	659.9
	1.1	852.4
	1.7	880.5
Case 2-2 (4 diffusers)	**0.1**	513.1
	1.1	866.4
	1.7	901.4

Change of partitions (Case 3)

In most offices, partitions are used, which might be a problem to floor-supply systems, because they would be obstacles for air movement in the occupied zone. Therefore, Case 3 is design to study the influence of the number of partitions on the indoor environment with a floor-supply system. The configurations of Cases 3-1 and 3-2 are shown in Figure 4.2.11 and 4.2.12, respectively. All other parameters are the same in these cases. In both Cases 3-1 and 3-2, the floor diffusers are installed within the partition area and there is no heat source in the hallway except for ceiling lamps.

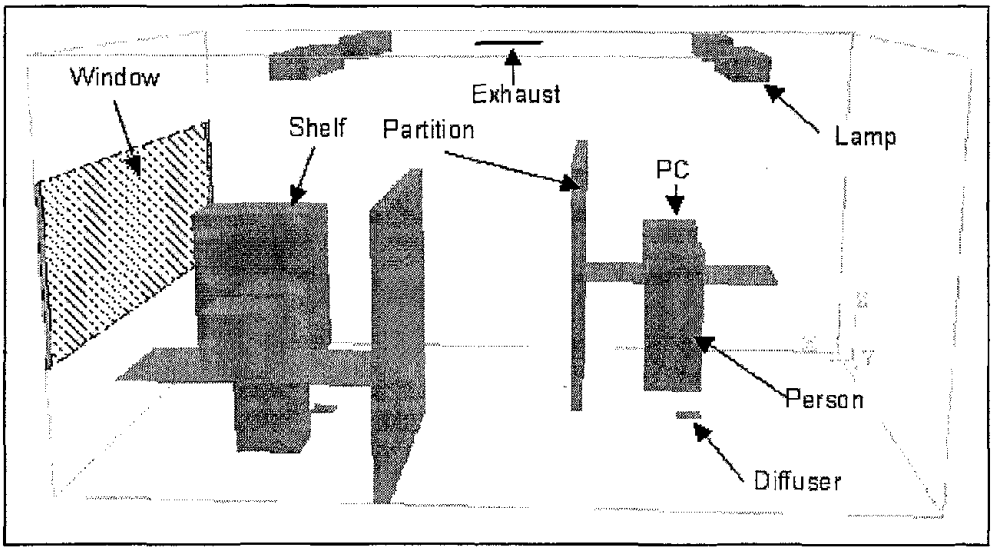

Figure 4.2.11 Configuration of Case 3-1

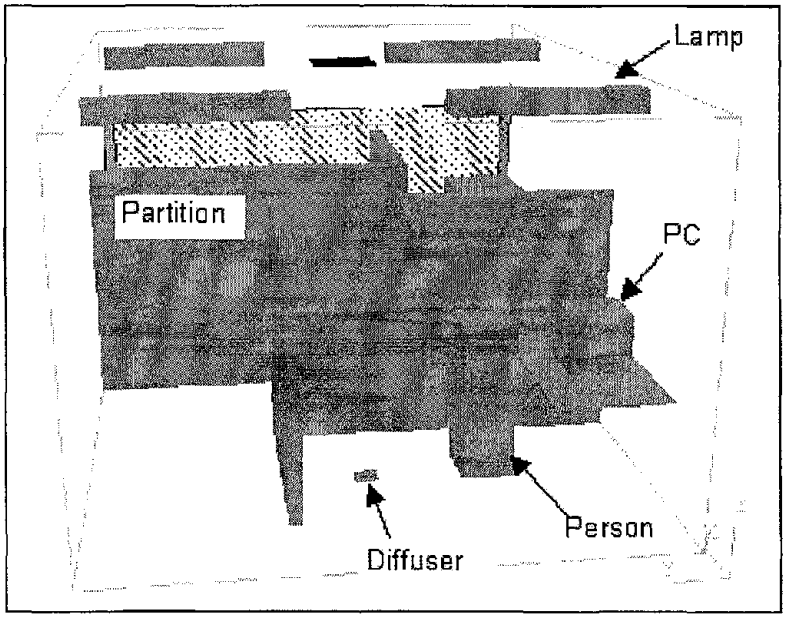

Figure 4.2.12 Configuration of Case 3-2

The distributions among Case 3-1, Case R, and Case 3-2 are almost same. Similarly, PD and PPD distributions are almost same in the three cases. This is because all the heat sources except for the ceiling lamps are within the partition are and the diffusers are also installed within the partition area. For example, if there are heat sources in the hallway, another floor diffuser would be necessary to account for the additional cooling load. The partitions did not appreciably affect the thermal comfort in the room in this case.

The averaged CO_2 concentrations and ages of air at the height of 0.1m, 1.1m, and 1.7m are shown in Table 4.2.4. In all three cases, the CO_2 concentration is around 600 ppm in the occupied zone. However, in Case 3-2, the average CO_2 concentration at 1.7m is smaller than other two cases. This is because the CO_2 sources are at the persons' heads, which are 1.1m high, and the partitions prevent CO_2 from the persons' heads from diffusing to the entire room and CO_2 stratification causes to use upward by the airflow from the floor to the ceiling.

Table 4.2.4 Averaged CO_2 concentrations and ages of air at 0.1m, 1.1m, and 1.7m high.

	Height (m)	**C (PPM)**	**MAA (sec)**
Reference Case	**0.1**	520.2	576.3
	1.1	589.0	810.5
	1.7	622.8	846.6
Case 3-1	**0.1**	524.5	555.7
	1.1	589.7	773.8
	1.7	620.6	807.1
Case 3-2	**0.1**	526.7	515.8
	1.1	589.3	700.1
	1.7	614.3	765.8

The average age of air is the youngest in Case 3-2, and oldest in Case R. This is also because the supply air from the diffuser does not diffuse too far horizontally because of the partitions, but goes upward faster and reaches to the exhaust than in the case without partitions. Therefore, the age of air is younger with partitions than without.

If the floor diffusers are installed appropriately inside the partition area, the indoor air quality could be better than that without partitions.

Change of occupants' location (Case 4)

The occupants' location in the room often could change without changing the location of floor diffusers. The configurations of the Case 4-1 and Case 4-2 are shown in Figure 4.2.13 and 4.2.14, respectively, which are designed to study the impact of occupant's location on the thermal comfort and air quality in the room. In case 4-1, two occupants sit near each other and the distance between two occupants is about 1 m. The distance between two occupants is about 2 m in Case 3-2, about 3 m in Case R. All the other parameters are the same in these cases.

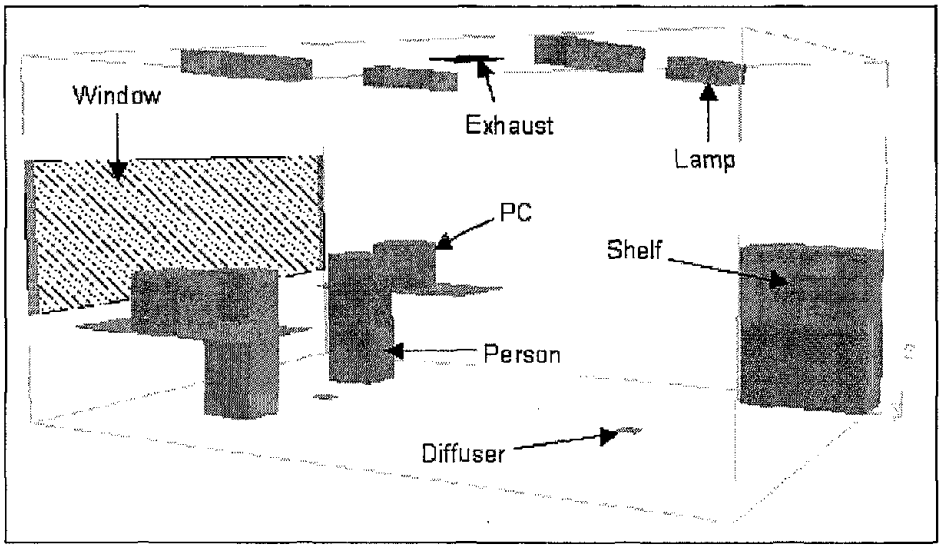

Figure 4.2.13 Configuration of Case 4-1

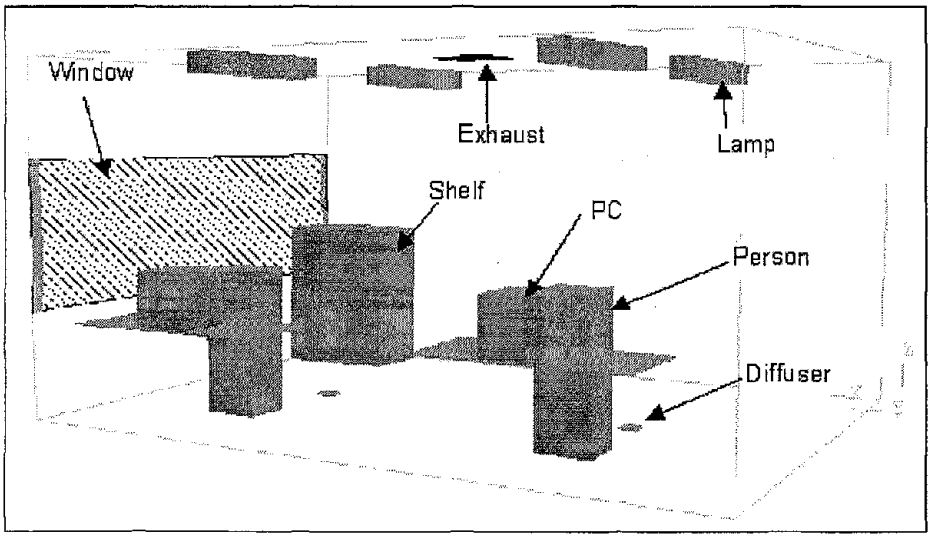

Figure 4.2.14 Configuration of Case 4-1

The temperature distributions are almost same in all the three cases and no large difference can be seen. This indicates that in Case 4-1, one diffuser can remove the heat from two occupants and two PCs. In addition to thermal comfort parameters, indoor air quality parameters, such as CO_2 concentration, mean age of air, and ventilation effectiveness, have almost the same vertical distributions and averaged values in the three cases.

In this case only two occupants are in the room. If heat source density is much higher in a certain area in a room and the capacity of diffusers near that area is not enough to remove the heat, the temperature and contaminant concentration would be than other areas in the room.

Change of furniture (Case 5)

Almost all the rooms have some furniture. They could be located near the occupants or above the floor diffusers, etc. Furniture could have an influence on indoor air movement. Therefore, Case 5 is used to study the influence of furniture on the indoor environment with a floor-supply system. The configuration of Cases 5-1 and 5-2 are shown in Figure 4.2.15 and 4.2.16, respectively. In Case 5-2, a large table is installed above the floor diffusers at a height of 0.75m. All other parameters are the same in these cases.

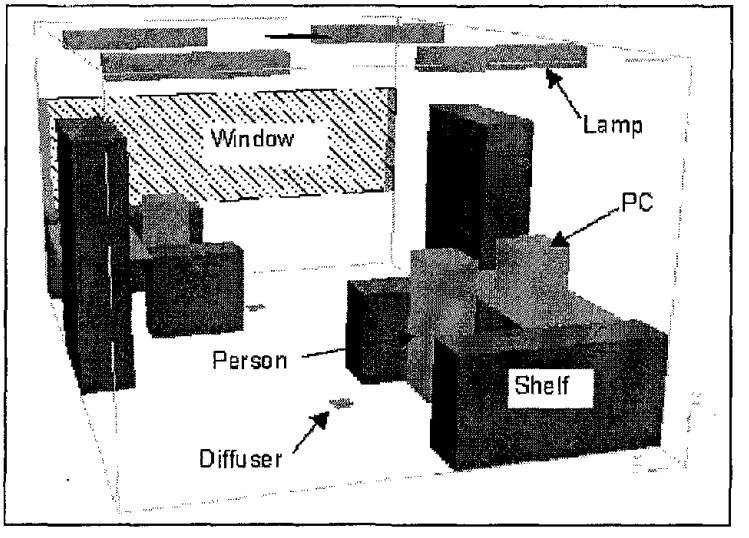

Figure 4.2.15 Configuration of Case 5-1

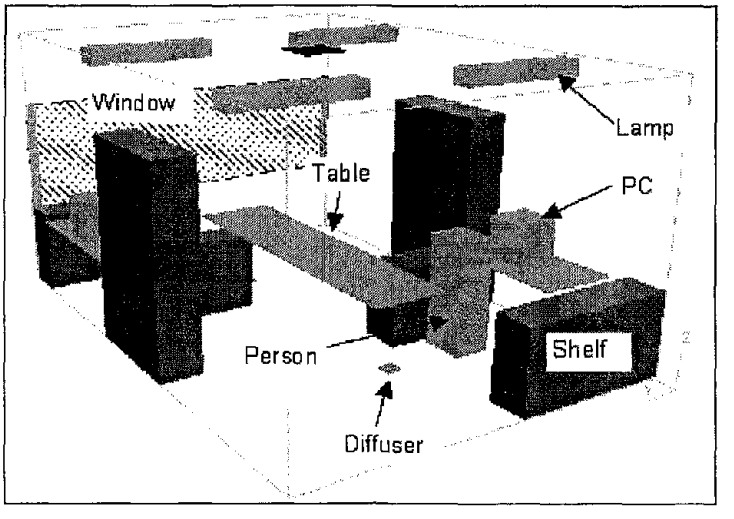

Figure 4.2.16 Configuration of Case 5-2

Table 4.2.5 shows the averaged temperature at the height of 0.1m, 1.1m, and 1.7m, and the temperature differences between 0.1m and 1.7m (DT1), 0.1m and 1.1m (DT2). In Case 5-2, the supply air from the diffusers cannot go higher than the table. The corresponding air temperature

under the table is low and temperature above the table is high. DT1 and DT2 are larger than those in the other two cases and DT1 exceeds the acceptable value. Therefore, if any furniture, such as tables, is installed above the floor diffusers, those obstacles disturb the airflow from the diffusers and thermal comfort in the room would be worse. Except for the table above the floor diffusers, no large influence of the furniture on the thermal comfort parameters can be found. This is probably because furniture is not installed close to the diffusers in this case and if furniture does not disturb the airflow very much.

Table 4.2.5 Averaged temperatures at 0.1m, 1.1m, and 1.7m high

	Height (m)	**TEM (°C)**	**DT1 (1.7m-0.1m)**	**DT2 (1.1m-0.1m)**
Reference Case	**0.1**	24.6	3.1	2.2
	1.1	26.8		
	1.7	27.7		
Case 5-1	**0.1**	24.6	3.2	2.3
	1.1	26.9		
	1.7	27.8		
Case 5-2	**0.1**	24.5	3.4	2.7
	1.1	27.1		
	1.7	27.9		

The averaged CO_2 concentrations and ages of air at the height of 0.1m, 1.1m, and 1.7m are shown in Table 4.2.6. Age of air is younger with furniture than that without furniture. Because of the volume of many pieces of furniture in Case 5-1, 5-2, the actual room volume is about 10% smaller with furniture than the volume in Case R. Therefore, actual air change rate is higher and age of air is younger in Case 5-1 and 5-2. Because of the table, the age of air under the table is young, and that above the table is slightly higher. As for CO_2, because the sources are at the persons' heads, which are 1.1m high and higher than the table, no large influence of the furniture can be seen.

Table 4.2.6 Averaged CO_2 concentrations and ages of air at 0.1m, 1.1m, and 1.7m high

	Height (m)	**C (PPM)**	**MAA (sec)**
Reference Case	**0.1**	520.2	576.3
	1.1	589.0	810.5
	1.7	622.8	846.6
Case 5-1	**0.1**	509.9	542.9
	1.1	581.2	740.2
	1.7	614.5	778.9
Case 5-2	**0.1**	489.0	470.4
	1.1	581.6	745.8
	1.7	612.4	781.6

Change of exhaust location (Case 6)

The parameter changed in Case 6 is the exhaust location. This case was designed to study the influence of exhaust location on thermal comfort and air quality in the office with the floor-supply system. The configurations of Cases 6-1 and 6-2 are shown in Figure 4.2.17 and 4.2.18, respectively. In Case 6-1, the exhaust is installed near the window, because the temperature near the window is high. Placing the exhaust near the window is expected to remove the warm air more effectively. In Case 6-2, two smaller exhausts are used. All other parameters are the same in these cases.

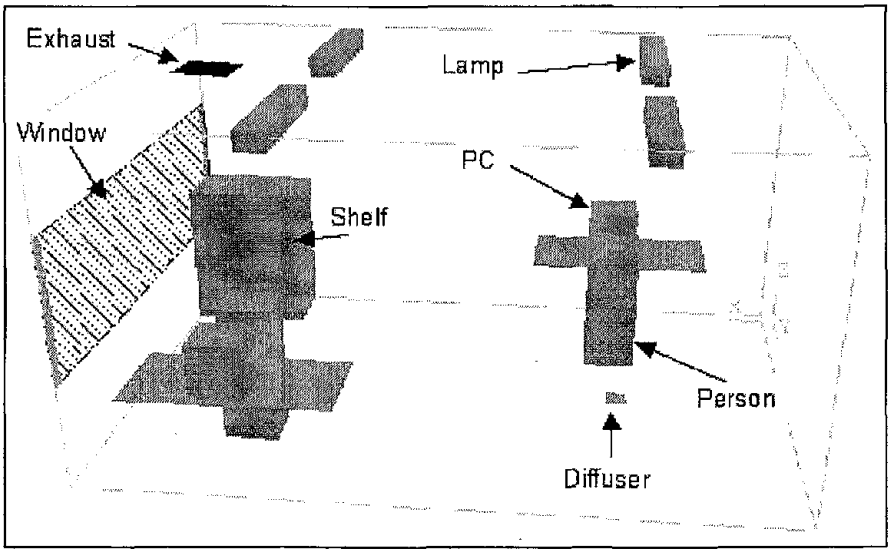

Figure 4.2.17 Configuration of Case 6-1

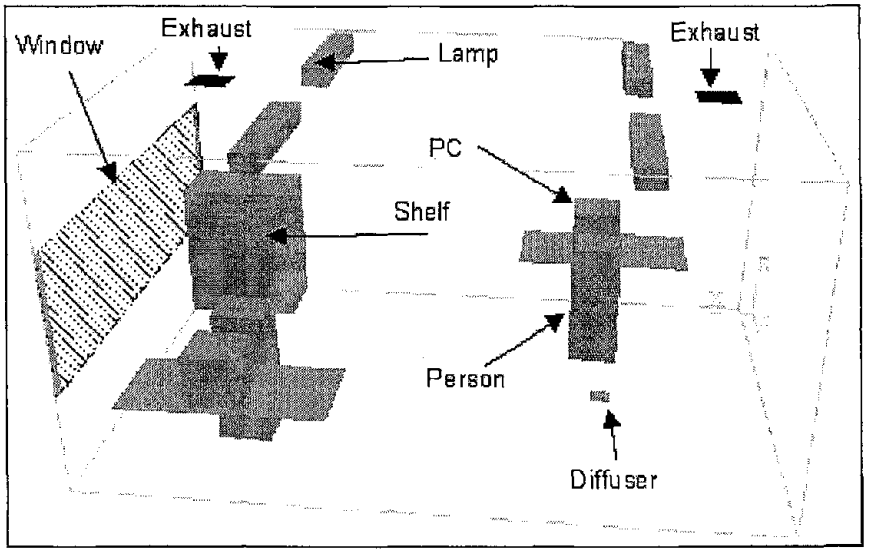

Figure 4.2.18 Configuration of Case 6-2

The vertical temperature distributions are almost same in the three cases. The results do not show large influence of the different exhaust location on the temperature distributions, although the exhaust near the window is expected to remove the warm air effectively in Case 6-1.

The averaged CO_2 concentrations and ages of air at the height of 0.1m, 1.1m, and 1.7m are shown in Table 4.2.7. The averaged CO_2 concentration at 1.7m is the highest in Case 6-1 among three cases, while it is the lowest in Case 6-2. This is because the exhaust location in case 6-1 is far from one of two occupants, and CO_2 cannot be removed effectively. Conversely, in Case 6-2, because each exhaust grill is near each occupant, CO_2 is removed effectively.

Similar to the CO_2 concentration, the averaged mean age of air in Case 6-2 is the oldest among the three cases, while the averaged value in Case 6-1 is the youngest. Because only one exhaust grill is located near the window in case 6-1, the traveling path of the air to the exhaust is longer than that of Case R. On the contrary, in Case 6-2, because there are two exhaust grills, the traveling path is shorter.

Table 4.2.7 Averaged CO_2 concentrations and ages of air at 0.1m, 1.1m, and 1.7m high

	Height (m)	**C (PPM)**	**MAA (sec)**
Reference Case	**0.1**	520.2	576.3
	1.1	589.0	810.5
	1.7	622.8	846.6
Case 6-1	**0.1**	528.9	615.1
	1.1	605.4	875.7
	1.7	644.1	936.5
Case 6-2	**0.1**	511.7	546.3
	1.1	579.3	774.6
	1.7	614.1	816.6

Change of diffuser location (Case 7)

The parameter changed in Case 7 is the diffuser location. In Case 7-1, two diffusers are located near the center of the room and the distance between them is about 1 m. The radius of the area where air velocity is higher than 0.1 m/s around diffuser is approximately 0.5m in Case R. Therefore, 1 m is considered to be the nearest location of two diffusers without interfering with each other. In Case 7-2, the diffusers are located far from each other and the distance between them is about 3 m. In this case the distance between the occupant and the diffuser is about 2 m, while it is 1 m in Case R. The distance between the diffuser and the nearest wall is 1 m. The configurations of the Case 7-1 and Case 7-2 are shown in Figures 4.2.19 and 4.2.20, respectively. All other parameters are the same in these cases.

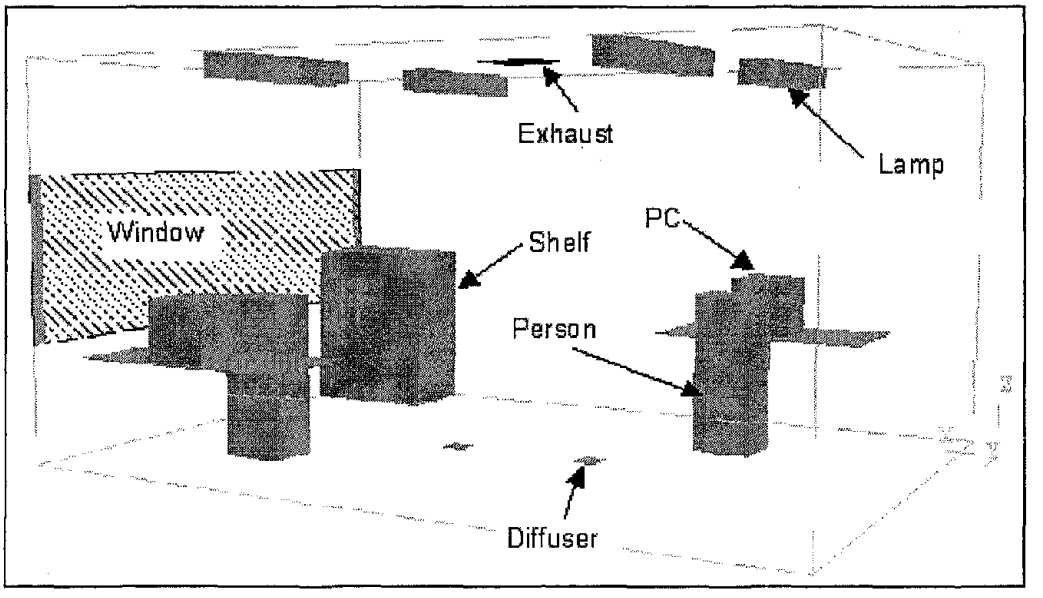

Figure 4.2.19 Configuration of Case 7-1

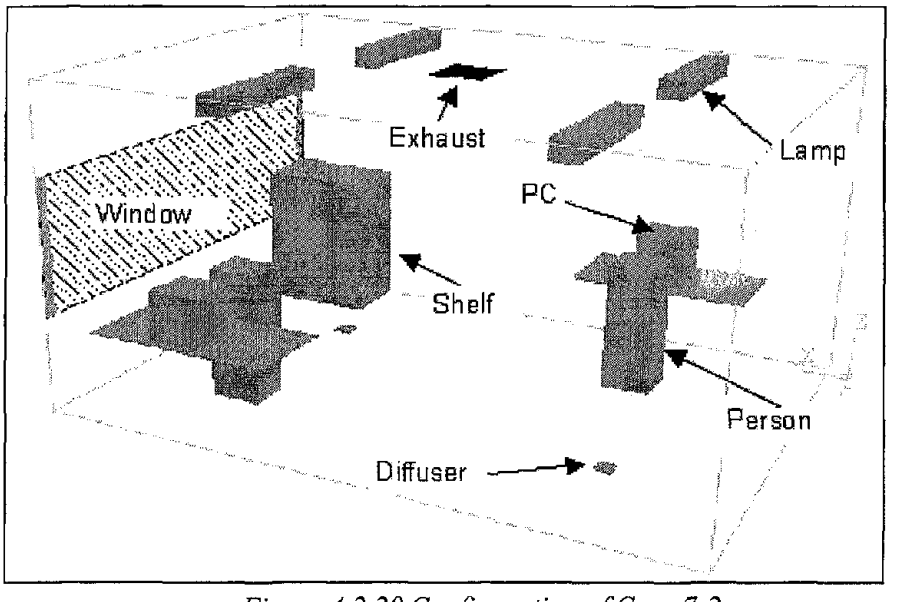

Figure 4.2.20 Configuration of Case 7-2

The temperature distributions are almost the same in all the three cases. Similar to the temperature distributions, PD and PPD distributions are almost same in three cases. This is because the distance between two diffusers and the nearest wall in Case 7-1 is 1 m, which is larger than the area where the air velocity is higher than 0.1 m/s. Therefore, there is little interference between the two diffusers and the wall and the diffuser. If the distance is smaller, there would be some airflow interference and airflow from the diffusers would be disturbed.

In addition, indoor air quality parameters, such as CO_2 concentration, mean age of air, and ventilation effectiveness, also have almost the same vertical distributions and averaged values in three cases and no difference can be seen among these cases.

Change of cooling load (Cases 11and 12)

This research focuses on high cooling load cases for U.S. buildings. From the previous studies, we found that the air change rate, airflow rate from one diffuser, and supply air temperature have a large impact on the indoor environment. Therefore, in this study, high cooling load cases are investigated with those parameters.

Table 4.2.8 shows the thermo-fluid conditions used. All the cases use the office configuration, and each case has four different air change rate variations. The parameters of each case are marked as bold letters.

Table 4.2.8 Conditions for the high cooling load studies

Conditions

Room Size:	5.16m x 3.65m x 2.7m(H)		
Heat source:	Occupant :	75W(total)	(Convection 60W/80%)
	PC :	173.4W(total)	(Convection 97W/56%)
	Printer:	205W(total)	(Convection 115W/56%)
	Ceiling Light x 4:	68W(total) x 4	(Convection 41W/60%)

Study Case

	cooling load (w/m2)	ach	supply air temperature	# of diffusers	# of occupants	# of PCs	# of printers
Case-11-1	**80**	**8**	**17**	4	4	**5**	**1**
Case-11-2	**80**	**10**	**18**	4	4	**5**	**1**
Case-11-3	**80**	**12**	**20**	4	4	**5**	**1**
Case-11-4	**80**	**16**	**22**	4	4	**5**	**1**
Case-12-1	**100**	**8**	**16**	4	4	**6**	**2**
Case-12-2	**100**	**10**	**17**	4	4	**6**	**2**
Case-12-3	**100**	**12**	**19**	4	4	**6**	**2**
Case-12-4	**100**	**16**	**21**	4	4	**6**	**2**

In a typical high-tech office building, the cooling load could be up to 100W/m^2. This study assumes that the cooling load for Case 11 to be 80W/m^2 and that for Case 12 100W/m^2. Each case has four different air change rates. The supply air temperature in each case is determined in order to make the room air temperature around 25 °C. All cases have four diffusers and four occupants in the room, the differences are number of PCs and printers. The configuration of Case 11 is almost the same as that of Case R.

In Table 4.2.9 shows the averaged temperature, PD and PPD at the height of 0.1m (ankle level), 1.1m (head level at sitting), and 1.7m (head level at standing), and the temperature differences between 0.1m and 1.7m (DT1), between 0.1m and 1.1m (DT2)

Table 4.2.9 Averaged temperature, PD, and PPD at 0.1m, 1.1m, and 1.7m high

	Height (m)	TEM (°C)	DT1 (1.7m-0.1m)	DT2 (1.1m-0.1m)	PD (%)	PPD (%)
Case 11-1	**0.1**	22.5	5.1	3.0	9.2	6.2
	1.1	25.5			0.3	9.0
	1.7	27.6			0.4	12.1
Case 11-2	**0.1**	24.4	3.2	1.2	9.9	6.2
	1.1	25.6			4.1	6.7
	1.7	27.5			0.7	10.4
Case 11-3	**0.1**	24.9	1.4	0.3	8.6	6.5
	1.1	25.2			8.3	6.4
	1.7	26.3			4.1	8.0
Case 11-4	**0.1**	25.4	0.7	0.2	9.4	7.1
	1.1	25.6			9.2	6.6
	1.7	26.1			6.7	7.0

It is obvious that a higher air change rate has a smaller temperature gradient in the occupied zone. The temperature difference between the foot and the head level (DT1) is the smallest in Case 11-4. In Case 11-2, DT1 is about 3.0 °C, which is almost the maximum of the acceptable range, and in Case 11-1, DT1 is about 5 °C, which is beyond the acceptable range. Therefore, for the temperature gradients, higher air change rates are better and 8ach (Case 11-1) is not acceptable in this case.

The PD distributions at section of Y=2.635m in four cases are shown in Figure 4.2.21. Contrary to temperature gradients, a higher air change rate has a higher PD due to the high air velocity from the diffusers. In Case 11-3 and Case 11-4, averaged PD at 1.1m is near 10%, while in Case 11-1 and Case 11-2, it is less than 5%. Therefore, as for PD, too high an air change rate must be avoided.

The above results show that temperature gradients and PD are opposed to each other. In addition, higher air change rates need more energy than lower air change rates. Therefore, if both the temperature gradient and PD are acceptable, the lower air change rate would be better in terms of energy consumption. For example, Case 11-2 would be the best air change rate among four cases.

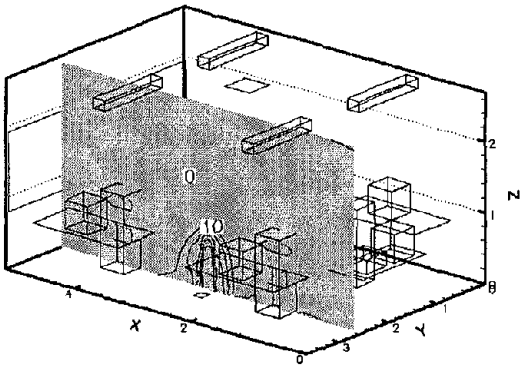

Case 11-1

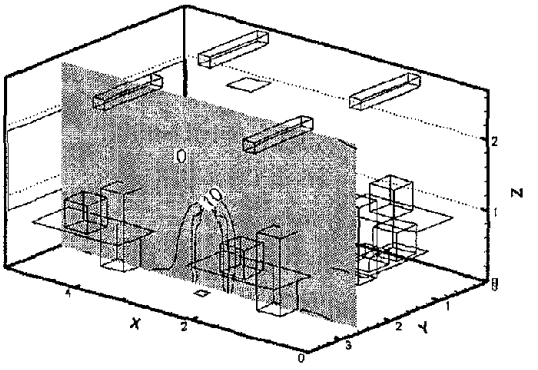

Case 11-2

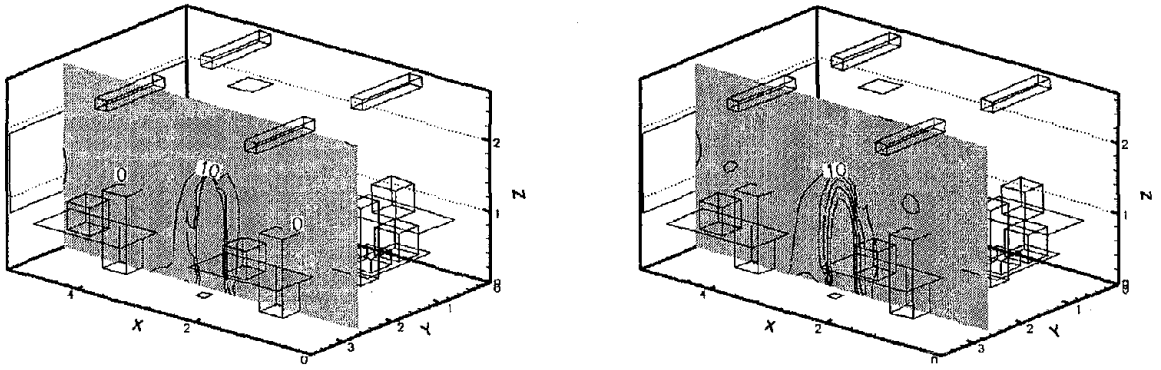

Figure 4.2.21 PD distributions at section of Y=2.635m

Figure 4.2.22 shows the averaged CO_2 concentrations and mean ages of air at the height of 1.1 m in all the four cases. It is obvious that the mean age of air corresponds to the air change rate. A higher air change rate has a lower CO_2 concentration and a younger age of air. As for relationship between the air change rates and ages of air, for example, Case 11-3 has 20% higher ach than Case 11-2 and the averaged age of air at 1.1 m in Case 11-3 is about 20% lower than that in Case 11-2, which seems like a reasonable relationship. Therefore, higher air change rates can obtain a younger age of air, if consume more energy.

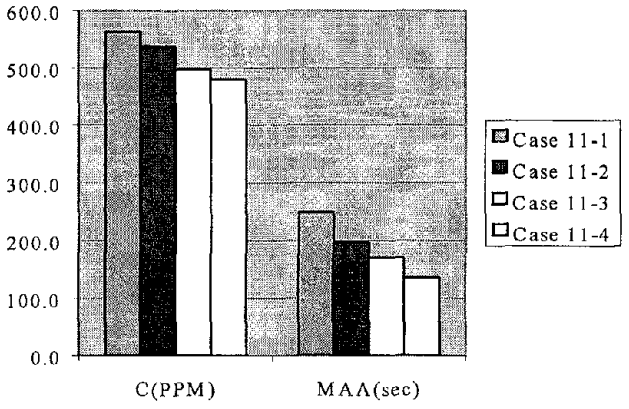

Figure 4.2.22 Averaged CO_2 concentrations (C) and mean ages of air (MAA) at 1.1m

Figure 4.2.23 shows the configuration of Case 12 in which the cooling load is 100W/m^2 and the room has a PC and printer cluster. In this case, the temperature, PD, and PPD distributions have almost same tendency as those in Case 11. However, because of the higher cooling loads, the averaged values are different. Table 4.2.10 shows the averaged temperature, PD, and PPD at the height of 0.1m (ankle level), 1.1m (sitting head level), and 1.7m (standing head level), and the temperature differences between 0.1m and 1.7m (DT1) and between 0.1m and 1.1m (DT2).

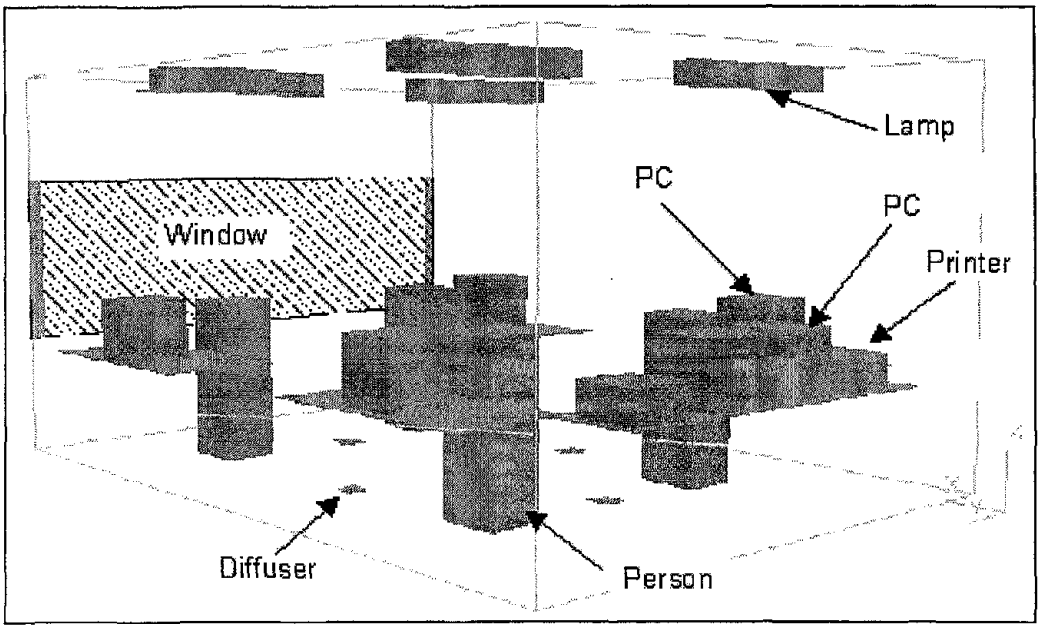

Figure 4.2.23 Configuration of Case 12

Table 4.2.10 Averaged temperature, PD, and PPD at 0.1m, 1.1m, and 1.7m high

	Height (m)	TEM (C)	DT1 (1.7m-0.1m)	DT2 (1.1m-0.1m)	PD (%)	PPD (%)
Case 9-1	**0.1**	22.2	6.0	3.8	10.5	6.6
	1.1	26.0			0.5	9.9
	1.7	28.2			0.5	13.0
Case 9-2	**0.1**	23.6	4.3	2.1	12.6	6.4
	1.1	25.8			2.9	7.0
	1.7	28.0			0.7	11.2
Case 9-3	**0.1**	24.6	2.1	0.6	9.7	6.4
	1.1	25.2			8.6	6.5
	1.7	26.7			3.2	8.6
Case 9-4	**0.1**	25.1	1.1	0.2	9.9	6.9
	1.1	25.2			10.3	6.4
	1.7	26.2			5.6	7.4

The temperature differences between the foot level and the head level (DT1) are larger than those in Case 11 because of the higher cooling load. In Cases 12-1 and 12-2, DT1 is larger than 3.0 °C, which is beyond the acceptable range. Therefore, for acceptable temperature gradients, the air exchange rate should be higher than 12ach (Case 11-3) for such a high cooling load ($100W/m^2$). The PD distributions are almost same as those in Case 11. A higher air change rate has a higher PD.

The indoor air quality aspects are almost same as those in Case 11. A higher ach has a lower CO_2 concentration and a younger age of air.

4.3 Floor Displacement Ventilation for Workshops

This section focuses on the impacts of several parameters on thermal comfort and indoor air quality for a workshop with floor-supply displacement ventilation systems. With the validated CFD program, we have studied the following parameters:

- Exhaust location and number
- Supply airflow rate and supply air temperature
- Partition arrangement
- Number of diffusers
- Diffuser location
- Distance between the workers
- Furniture arrangement

Table 4.3.1 summarized the conditions used in the study. Seven different cases were made from the reference case (Case LW-R), and each case has two variations. The different parameters of each case were marked as bold letters.

Table 4.3.1 Conditions for Case LW-R Parameter studies

Conditions

Room Size:	13.1m x 10.2m x 4.5m		
Heat source:	Occupant	28 (75% convective)	Total heat: 200W x 28
	Machine	28 (55% convective)	Total heat: 100W x 28
	Ceiling Light	18 (60% convective)	Total heat: 62W x 18

Case Studied

	Ach	supply air temperature (oC)	# of diffusers	partition	Exhaust Location	Diffuser location (# of diffusers per	Occupant arrangement	Furniture
Case LW-R	**5**	**16.8**	**16**	**0**	**2 sides (on East and West)**	**regular (4,8,4)**	**4 rows**	**2 big tables**
Case LW-1-1	5	16.8	16	0	**2 sides (on North and South)**	regular (4,8,4)	4 rows	2 big tables
Case LW-1-2	5	16.8	16	0	**4 sides**	regular (4,8,4)	4 rows	2 big tables
Case LW-2-1	**4**	**14.5**	16	0	2 sides (on East and West)	regular (4,8,4)	4 rows	2 big tables
Case LW-2-2	**6**	**18.3**	16	0	2 sides (on East and West)	regular (4,8,4)	4 rows	2 big tables
Case LW-3-1	5	16.8	16	**2**	2 sides (on East and West)	regular (4,8,4)	4 rows	2 big tables
Case LW-3-2	5	16.8	16	**4**	2 sides (on East and West)	regular (4,8,4)	4 rows	2 big tables
Case LW-4-1	5	16.8	**12**	0	2 sides (on East and West)	regular (4,8,4)	4 rows	2 big tables
Case LW-4-2	5	16.8	**24**	0	2 sides (on East and West)	regular (4,8,4)	4 rows	2 big tables
Case LW-5-1	5	16.8	16	0	2 sides (on East and West)	**regular (6,4,6)**	4 rows	2 big tables
Case LW-5-2	5	16.8	16	0	2 sides (on East and West)	**far (6,4,6)**	4 rows	2 big tables
Case LW-6-1	5	16.8	16	0	4 sides	regular (4,8,4)	**22 on the surrounding and 6 in middle**	2 big tables
Case LW-6-2	5	16.8	16	0	4 sides	regular (4,8,4)	**18 on the surrounding and 8 in middle**	2 big tables
Case LW-7-1	5	16.8	16	0	2 sides (on East and West)	regular (4,8,4)	4 rows	**add 4 boxes**
Case LW-7-2	5	16.8	16	0	2 sides (on East and West)	regular (4,8,4)	4 rows	**add 4 boxes + 2 side benches**

Reference Case for large workshop (Case LW-R)

Our preliminary studies found that swirl diffusers are better than the perforated panels and carpet. Therefore, swirl diffusers are used as air supply diffusers in the floor-supply displacement ventilation system. Figure 4.3.12 shows the configuration for the reference case (Case LW-R).

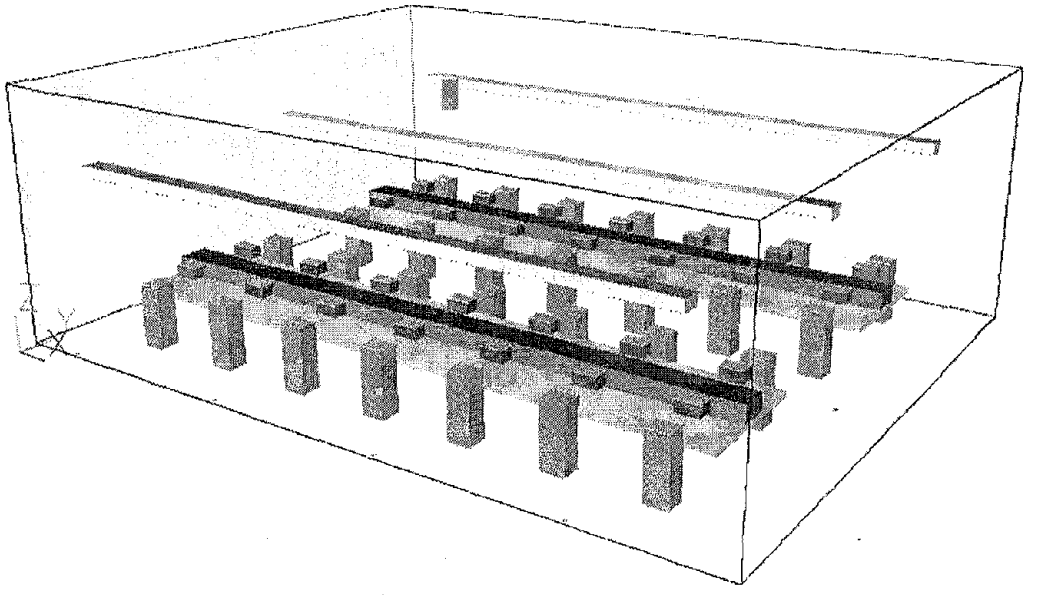

Figure 4.3.1 Configuration of the reference case (Case LW-R)

The computational results are illustrated in three sections: X=3.5m, X=9.75m and Y=5m. Section at Y=5 m was a plane at the center in Y-direction while for X=3.5m and x=9.75 were sections which cut through the heat source inside the room such as equipments and occupants.

Temperature

The temperature distributions at section of X=3.5m, X=9.75m and Y=5m are shown in Figure 4.3.2. There is temperature stratification in vertical direction, which indicates that the floor-supply system provides displacement ventilation. In general, the vertical temperature gradient depends on the airflow from the floor diffusers and the distribution of the heat sources in the room. The gradient in the occupied zone is larger than that above the occupied zone because it is where most of the heat sources are located. Therefore, the system should be carefully designed so that the temperature difference between the ankle level and the head level can be maintained to be less than 3 °C, which is the ASHRAE standard's criterion.

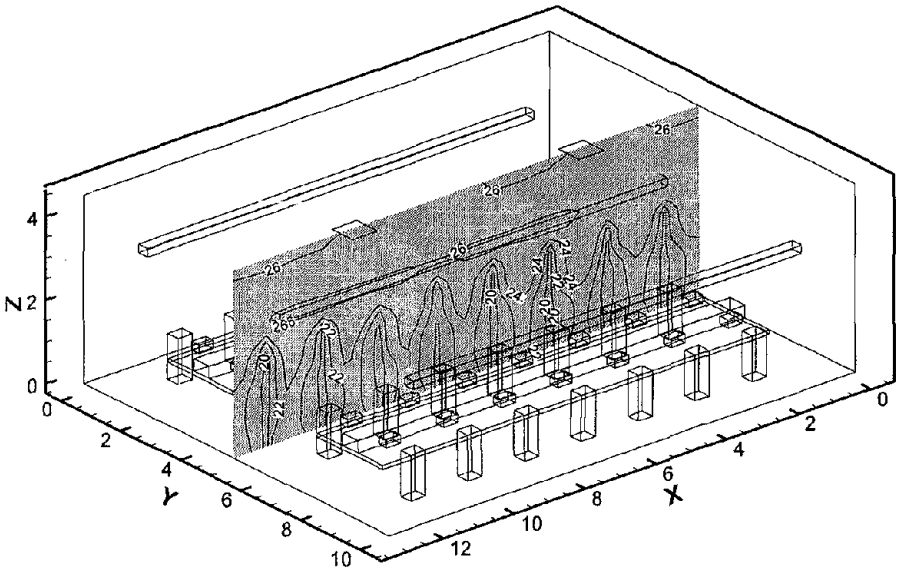

(a) Y=5m

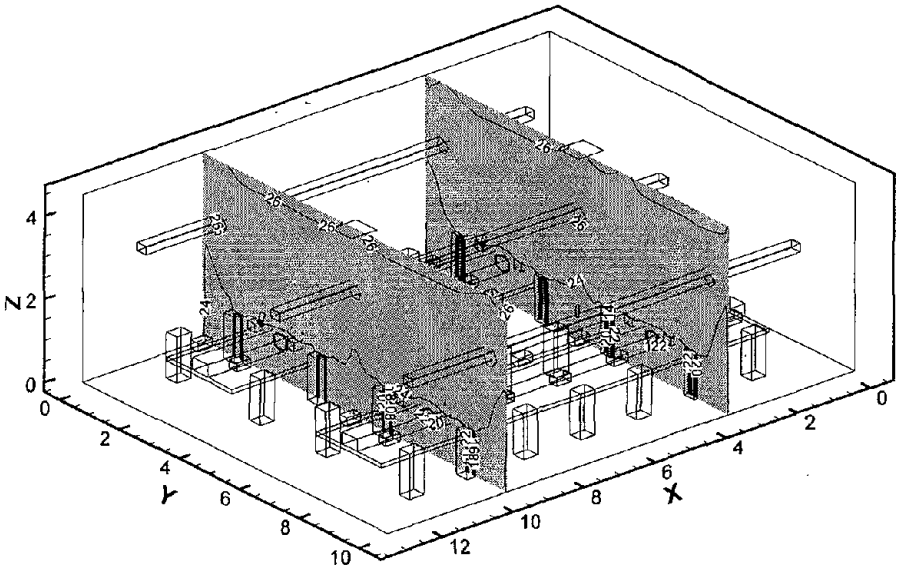

(b) X=3.5m and X=9.75m

Figure 4.3.2 Temperature distributions at X=3.5m, X=9.75m and Y=5m for Case LW-R

Velocity

Figure 4.3.3 shows the velocity distributions at section of X=3.5m, X=9.75m and Y=5m, respectively. The supply air velocity from a diffuser is about 2 m/s in this condition. It can be seen that supply air velocity is quickly reduced around the diffuser. Section in X direction which cut through the occupant indicated that the air velocity is lower than 0.1m/s in the occupant sitting region. Therefore, the risk of draft due to the high air velocity is considered to be small.

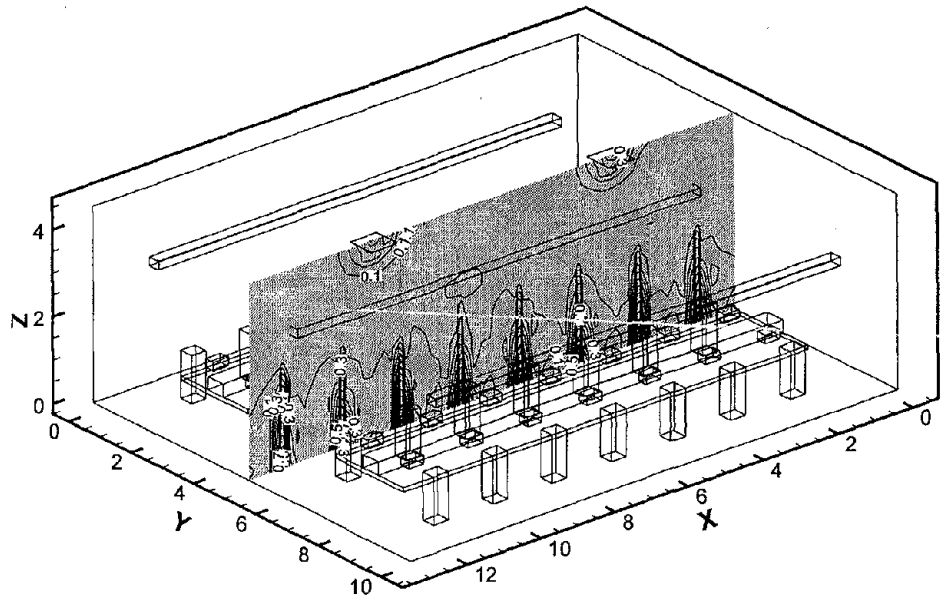

(a) Y=5m

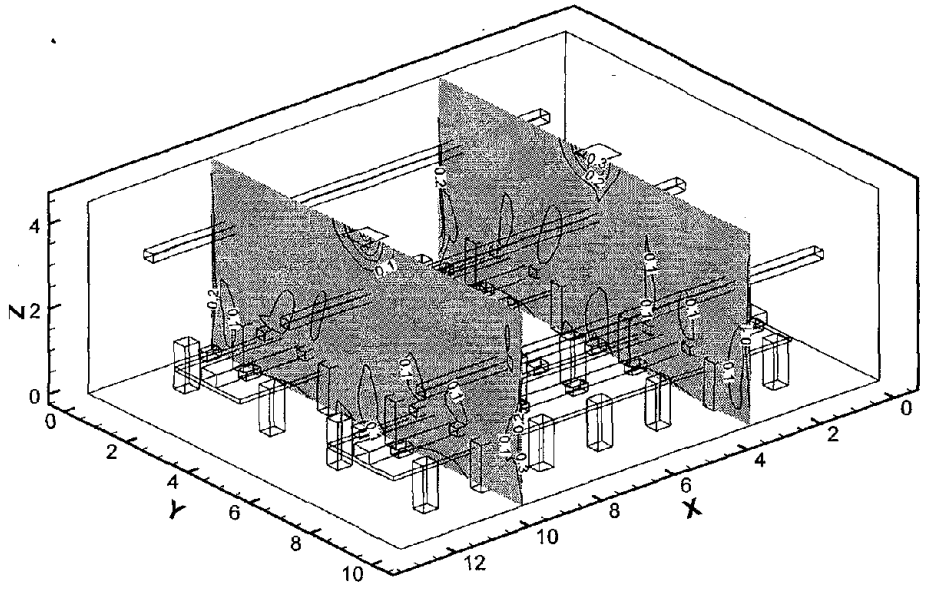

(b) X=3.5m and X=9.75m

Figure 4.3.3 Velocity distributions at X=3.5m, X=9.75m and Y=5m for Case LW-R

PD

The PD distributions at the three selected sections are shown in Figure 4.3.4. PD is generally less than 10% in the room. Only around diffuser is PD more than 10% due to the supply air velocity from the diffusers. The area where PD is more than 10% is similar to the area where air velocity is more than 0.1 m/s.

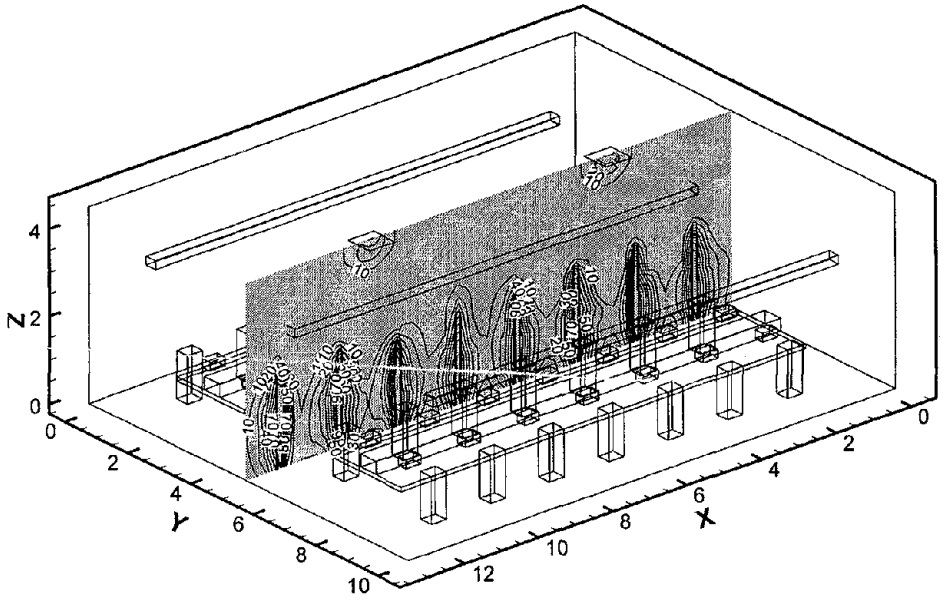

(a) Y=5m

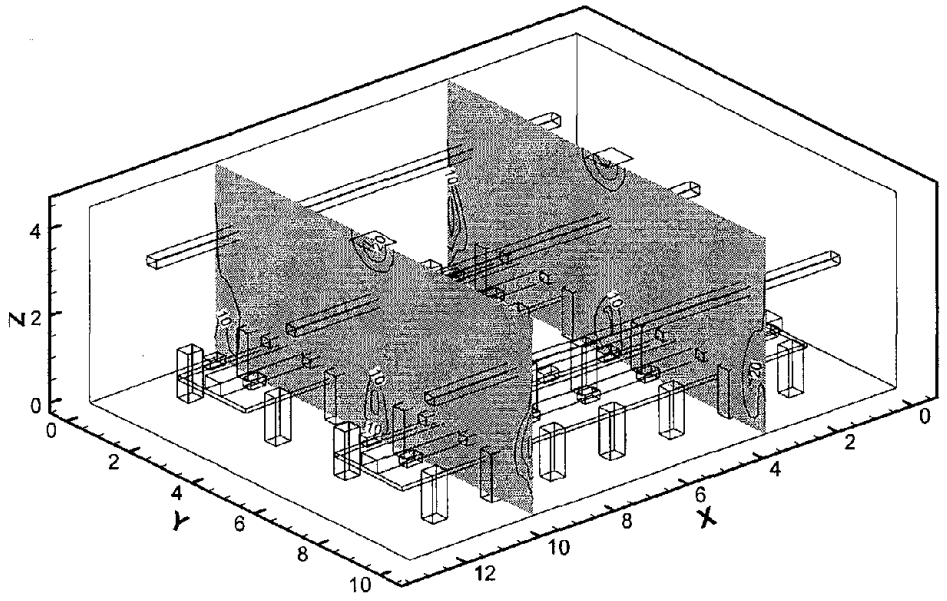

(b) X=3.5m and X=9.75m

Figure 4.3.4 PD distributions at X=3.5m, X=9.75 and Y=5m for Case LW-R

PPD

The PPD distributions at the three selected sections are shown in Figure 4.3.5. The PPD has a vertical stratification similar to the temperature due to the fact that PPD is a temperature related value. The PPD is generally less than 12% in the room, which can be considered to be acceptable comfort level.

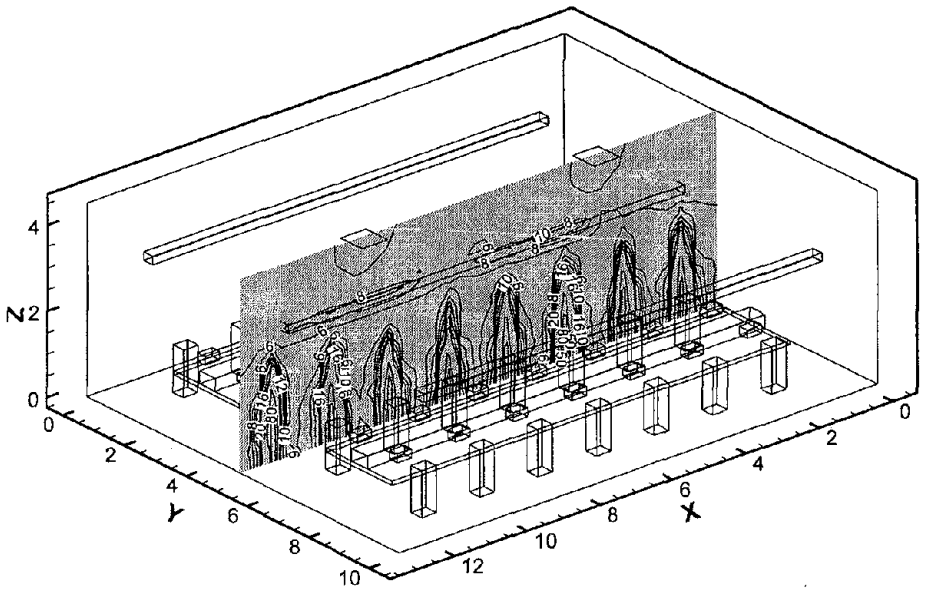

(a) Y=5m

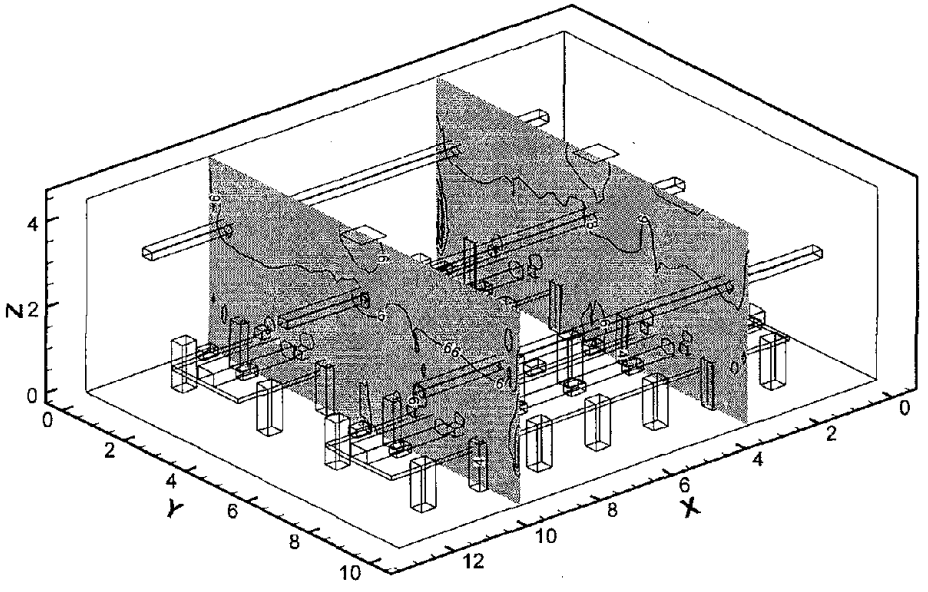

(b) X=3.5m and X=9.75m

Figure 4.3.5 PPD distributions at X=3.5m, X=9.75m and Y=5m for Case LW-R

CO_2 Concentration

The CO_2 distributions at the three selected sections are shown in Figure 4.3.6. In this study, CO_2 is used as an indicator for contaminant concentrations. The CO_2 distributions also have a vertical stratification in that the CO_2 concentration in the lower zone is lower than that in the upper zone. The stratification occurs because the fresh air is supplied directly to the occupied zone from the

diffusers on the floor and because the heat from the heat sources generates thermal plumes which can bring the CO_2 to the upper zone.

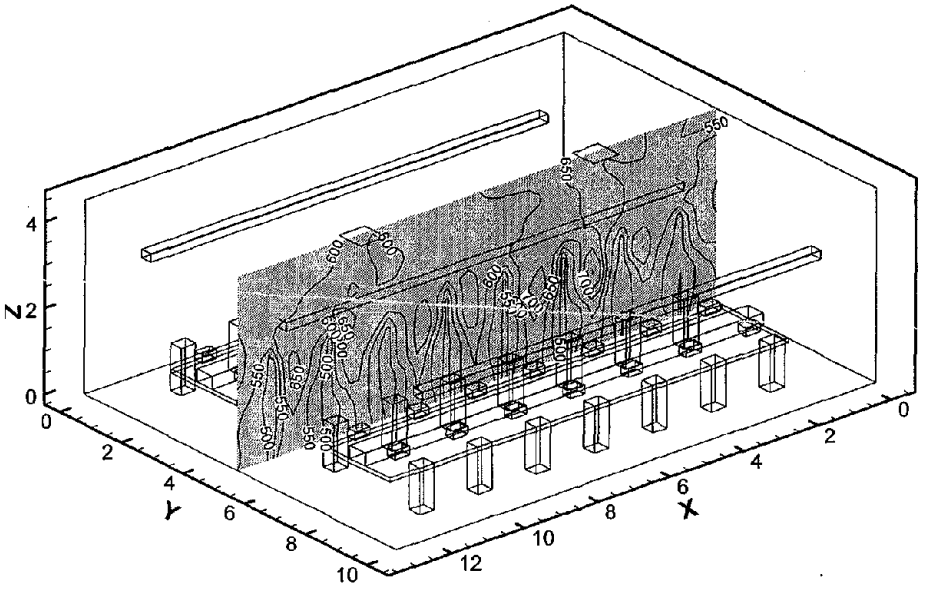

(a) Y=5m

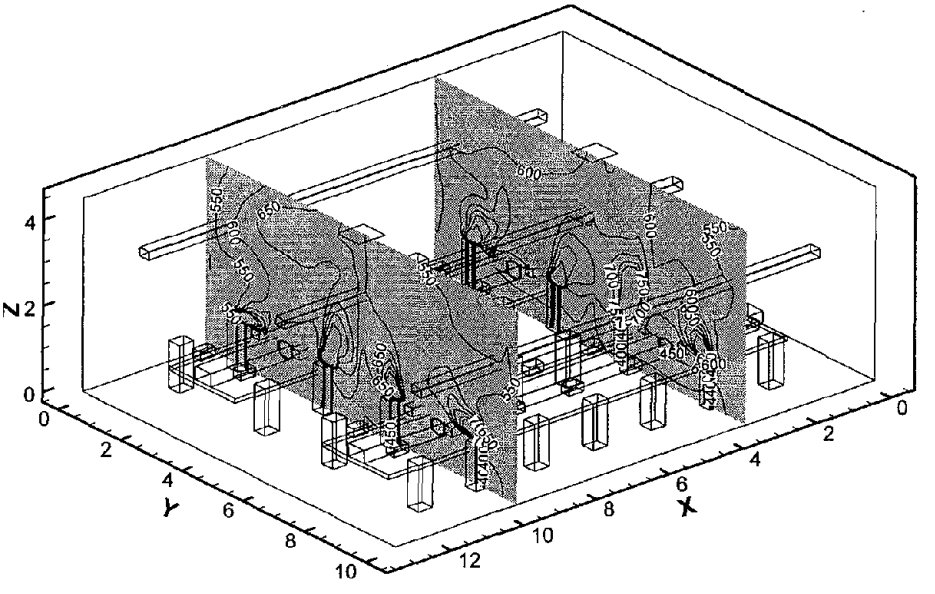

(b) X=3.5m and X=9.75m

Figure 4.3.6 CO_2 distributions at X=3.5m, X=9.75m and Y=5m for Case LW-R

Mean age of air

The mean age of air distributions at the three selected sections are shown in Figure 4.3.7. The mean age of the air in the lower part of the room is much younger than that in the upper part of

the room. The averaged mean age of air at the height of 0.1 m, 1.1 m, and 1.7 m are approximately 443 s, 486 s, and 509 s, respectively. For complete mixing ventilation, the mean age of air in the room is about 700-800 s. The floor-supply ventilation systems thus provide better indoor air quality to the occupied zone than mixing ventilation systems.

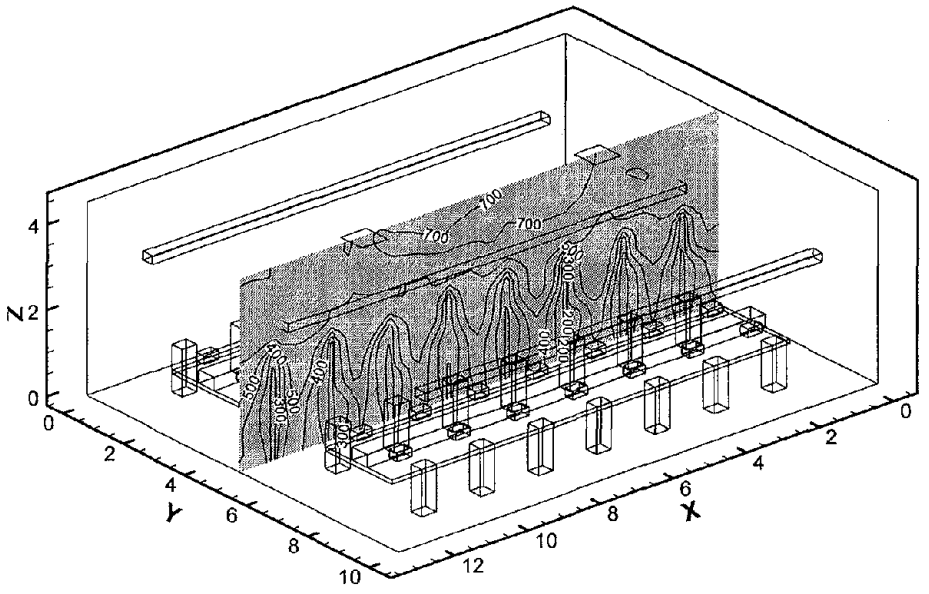

(a) Y=5m

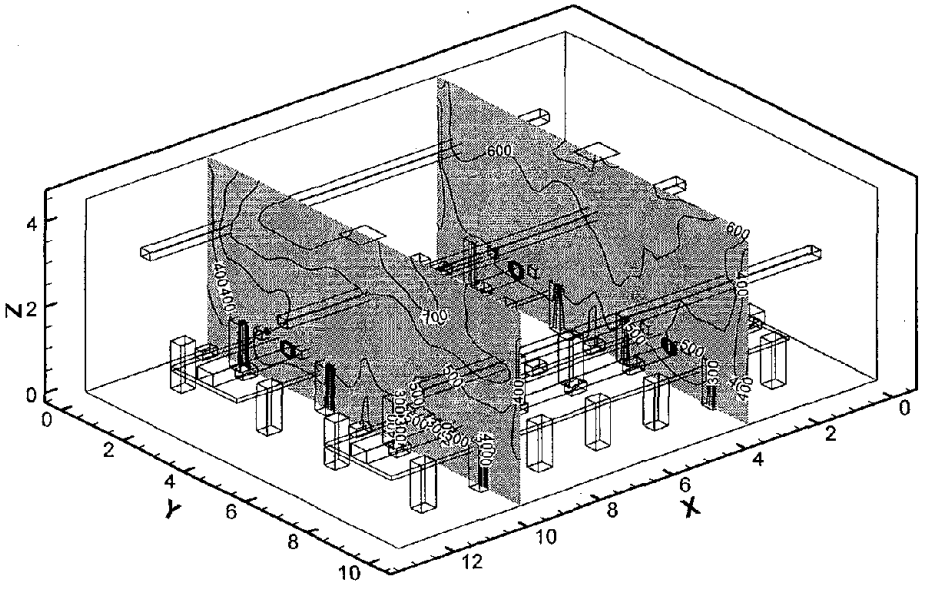

(b) X=3.5m and X=9.75m

Figure 4.3.7 Mean age of air distributions at X=3.5m, X=9.75m and Y=5m

Ventilation effectiveness

The ventilation effectiveness distributions at the three selected sections are shown in Figure 4.3.8. The occupied zone in the room has higher ventilation effectiveness than that of the complete mixing system, which has a value of 1.0.

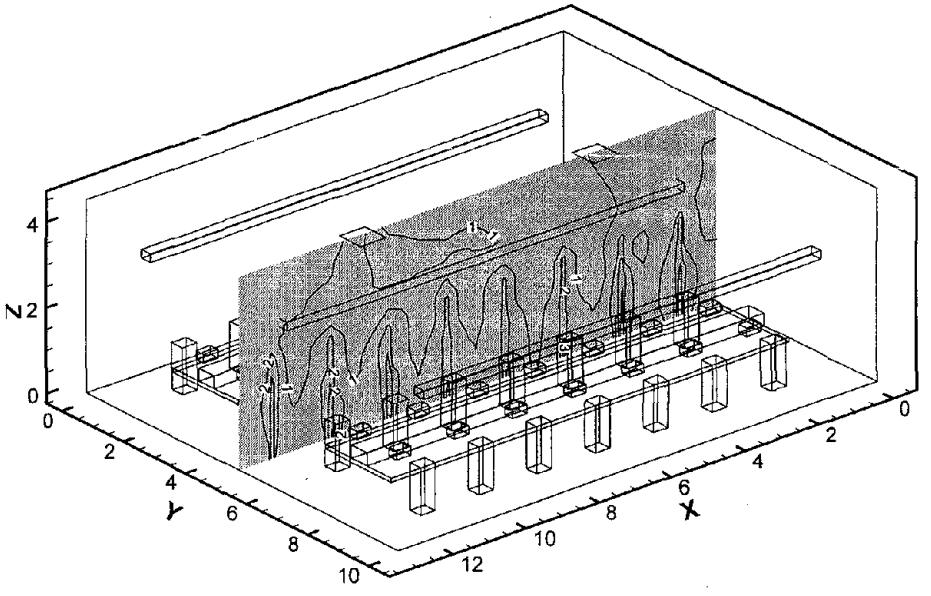

(a) Y=5m

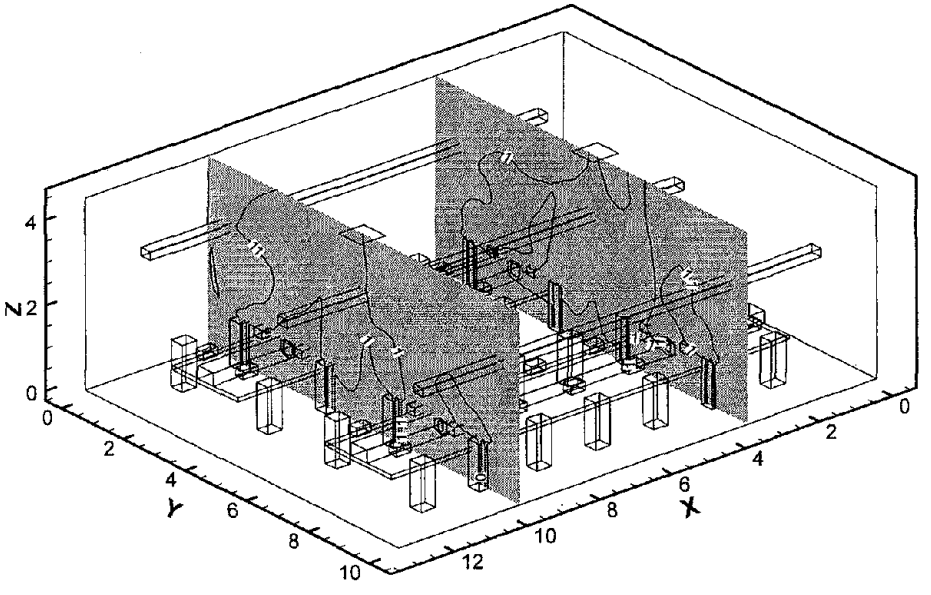

(b) X=3.5m and X=9.75m

Figure 4.3.8 Ventilation effectiveness distributions at section of X=3.5m, X=9.75m and Y=5m

The above results show that the floor-supply ventilation system provides a better indoor air quality and at the same time achieve the thermal comfort which is acceptable according to

ASHREA Standard 55. With these advantages, it is beneficial to study the impacts of different design parameters on indoor air quality and thermal comfort.

Change of exhaust location and number (Case LW-1)

The vertical temperature distributions were almost the same in the three cases and no large influence of the different exhaust location can be seen. This is similar to the observation for the office cases. Unlike the cases in the office, the impact of the exhaust location on air quality is not significant in the large workshops. It was because the contaminant sources were quite evenly distributed in the room. Therefore, changing the exhaust location will not affect the ventilation effectiveness.

Change of air change rate and supply air temperature (Case LW-2)

Table 4.3.2 summarized the temperature, PD and PPD at different heights. The higher the supply air flow rate, the less stratified it was. Even for the reduced flow rate in Case LW-2-1, the indoor space was still maintained at the standard of thermal comfort. Therefore, with a careful design, the energy could be saved by using lower flow rate and at the same time, the thermal comfort was still achieved.

Table 4.3.2 Temperature, PD, and PPD at Z= 0.1, 1.1 and 1.7meter

	Height	TEM	DT1	DT2	PD	PPD
	(m)	°C	(1.7m-0.1m)	(1.1m-0.1m)	(%)	(%)
	0.1	23			8.9	6.6
	1.1	23.7			7.3	6.1
Case LW-R	1.7	24.5	1.5	0.7	5.7	5.9
	0.1	22.5			9	7
	1.1	23.5			4.7	6
Case LW-2-1	1.7	24.6	2.1	1	2.7	5.7
	0.1	23.6			10.2	6.7
	1.1	24.1			8.8	6.4
Case LW-2-2	1.7	24.5	0.9	0.5	9	6.1

Table 4.3.3 presented the ages of air and CO_2 concentration at different height. As explained in the office cases, the ages of air corresponds to the air change rate. The higher air change rate, the younger the age of air. For the height with younger age of air, the CO_2 concentration would also be lower.

Table 4.3.3 Age of air and CO_2 concentration at Z= 0.1, 1.1 and 1.7 meter

	Height	AGE	CO2
	(m)	(sec)	(ppm)
	0.1	443	567
	1.1	486	597
Case LW-R	1.7	509	603
	0.1	439	583
	1.1	516	642
Case LW-2-1	1.7	567	647
	0.1	431	551
	1.1	467	591
Case LW-2-2	1.7	477	571

Change of partition arrangement (Case LW-3)

Table 4.3.3 summarized the temperature, PD and PPD at different heights due to partition arrangement. The influence of the partitions is not significant in these workshop cases. It is because the partition was arranged in parallel to the air flow direction of the room of the large workshop cases. In these cases, the arrangement of the swirl diffusers reduced the airflow in the x-direction, therefore, the partition parallel to x-direction will not block the air flow much.

Table 4.3.3 Temperature, PD, and PPD at Z= 0.1, 1.1 and 1.7 m

	Height	TEM	DT1	DT2	PD	PPD
	(m)	°C	(1.7m-0.1m)	(1.1m-0.1m)	(%)	(%)
	0.1	23			8.9	6.6
	1.1	23.7			7.3	6.1
Case LW-R	1.7	24.5	1.5	0.7	5.7	5.9
	0.1	22.9			9.3	6.7
	1.1	23.3			7.4	6.2
Case LW-3-1	1.7	24	1.1	0.4	6.1	5.8
	0.1	22.9			10.1	6.9
	1.1	23.2			7.6	6.3
Case LW-3-2	1.7	23.9	1	0.3	6.1	5.8

Table 4.3.4 presented the ages of air and CO_2 concentration at different height. The average value of the mean age of air and CO_2 concentration in the room is similar for these three cases. The partition arrangement does not have a significant impact on indoor air quality.

Table 4.3.4 The mean age of air (MAA) and CO_2 concentration at Z= 0.1, 1.1 and 1.7 m

	Height	MAA	CO_2
	(m)	(sec)	(ppm)
	0.1	443	567
	1.1	486	597
Case LW-R	1.7	509	603
	0.1	448	576
	1.1	486	606
Case LW-3-1	1.7	514	619
	0.1	434	571
	1.1	471	605
Case LW-3-2	1.7	491	615

Change of diffuser number (Case LW-4)

In this study, the total air change rate of the room is maintained the same for these cases; however, the individual flow characteristics of the diffusers were changed when the number of diffusers in the room were changed.

Table 4.3.5 summarized the temperature, PD and PPD at different heights. For case LW-4-1, the number of diffusers is less than that of the reference case. The air velocity at the diffusers was larger, which induce a higher turbulence and mixing effect. The temperature stratification was reduced. Comparatively, for case LW-4-2, the air velocity at the diffusers was reduced. It was result in less mixing effect and more stratified.

Table 4.3.5 Temperature, PD, and PPD at Z= 0.1, 1.1 and 1.7 m

	Height	TEM	DT1	DT2	PD	PPD
	(m)	°C	(1.7m-0.1m)	(1.1m-0.1m)	(%)	(%)
	0.1	23			8.9	6.6
	1.1	23.7			7.3	6.1
Case LW-R	1.7	24.5	1.5	0.7	5.7	5.9
	0.1	23.5			10	6.5
	1.1	24.1			8.9	6.4
Case LW-4-1	1.7	24.7	1.2	0.6	8.2	6.3
	0.1	23			8.9	6.4
	1.1	24.1			4.3	5.8
Case LW-4-2	1.7	25.4	2.4	1.1	2.2	6.2

Table 4.3.6 presented the mean ages of air and CO_2 concentration at different heights. The higher supply air velocity, the stronger mixing effect. The mean age of air and CO_2 at the height 1.7m are significantly higher.

Table 4.3.6 The mean age of air (MAA) and CO_2 concentration at Z= 0.1, 1.1 and 1.7 m

	Height	MAA	CO_2
	(m)	(sec)	(ppm)
Case LW-R	0.1	443	567
	1.1	486	597
	1.7	509	603
Case LW-4-1	0.1	608	591
	1.1	656	630
	1.7	681	622
Case LW-4-2	0.1	583	544
	1.1	705	597
	1.7	937	653

Change of diffuser location and distance (Case LW-5)

Table 4.3.7 summarized the temperature, PD and PPD at different heights with different diffuser location and distance. The average value of the temperature does not vary much. The height of the stratification layer was very close among the three cases. Therefore, the distance of the diffusers would not affect the global temperature distribution but it would affect locally. The occupant should keep sitting at the distance of 0.5 m from the diffusers to avoid local draft.

Table 4.3.7 Temperature, PD, and PPD at Z= 0.1, 1.1 and 1.7 m

	Height	TEM	DT1	DT2	PD	PPD
	(m)	°C	(1.7m-0.1m)	(1.1m-0.1m)	(%)	(%)
Case LW-R	0.1	23	1.5	0.7	8.9	6.6
	1.1	23.7			7.3	6.1
	1.7	24.5			5.7	5.9
Case LW-5-1	0.1	23.3	1.3	0.6	7.8	6.4
	1.1	23.9			6.5	6
	1.7	24.6			4.9	5.9
Case LW-5-2	0.1	23.4	1	0.4	7	6.3
	1.1	23.8			5.6	6
	1.7	24.4			4.7	5.8

Table 4.3.8 presents the mean age of air and CO_2 concentration at different height. Very similar to those in the office cases, the impact of the distance of the diffusers on indoor air quality is not very significant.

Table 4.3.8 The mean age of air (MAA) and CO_2 concentration at Z= 0.1, 1.1 and 1.7meter

	Height	MAA	CO_2
	(m)	(sec)	(ppm)
Case LW-R	0.1	443	567
	1.1	486	597
	1.7	509	603
Case LW-5-1	0.1	464	569
	1.1	490	600
	1.7	517	616
Case LW-5-2	0.1	483	533
	1.1	512	572
	1.7	533	607

Change of occupant arrangement (Case LW-6)

In this study, a different occupant sitting arrangements from the reference case was used as shown in Figure 4.3.9.

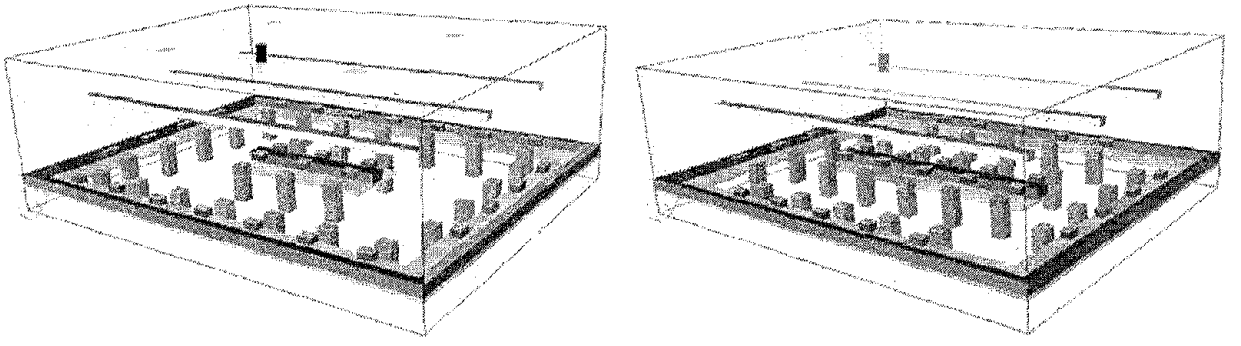

Configuration for Case LW-6-1 Configuration for Case LW-6-2

Figure 4.3.9 Different arrangements for occupants

Tables 4.3.9 and 4.3.10 summarize the temperature, PD and PPD, and the mean age of air and CO_2 concentration at different heights. The new arrangement of the occupants did not change the temperature and contaminant stratifications. The vertical distributions of the parameters are similar for the three cases.

Table 4.3.9 Temperature, PD, and PPD at Z= 0.1, 1.1 and 1.7 m

	Height	TEM	DT1	DT2	PD	PPD
	(m)	°C	(1.7m-0.1m)	(1.1m-0.1m)	(%)	(%)
Case LW-6-1	0.1	22.4	1	0.3	10.1	7.3
	1.1	22.7			9.8	6.7
	1.7	23.4			6.3	5.7
Case LW-6-2	0.1	22.4	1	0.2	10	7.3
	1.1	22.6			9.3	6.7
	1.7	23.4			5.3	5.7

Table 4.3.10 The mean age of air (MAA) and CO_2 concentration at Z= 0.1, 1.1 and 1.7 m

	Height	MAA	CO2
	(m)	(sec)	(ppm)
Case LW-6-1	0.1	386	544
	1.1	426	581
	1.7	473	611
Case LW-6-2	0.1	399	548
	1.1	438	586
	1.7	486	548

Change of furniture arrangement (Case LW-7)

Eight boxes were added in Case LW-7-1 and two more benches were added in Case LW-7-2 as shown in Figure 4.3.10.

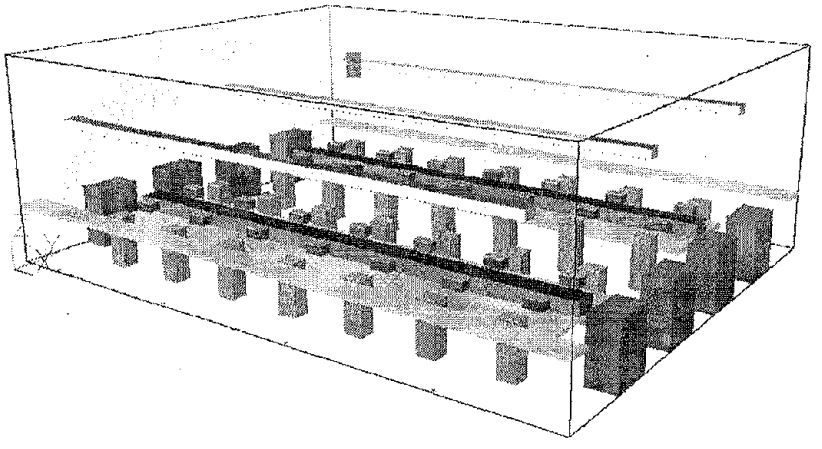

Figure 4.3.10 Furniture arrangement of the Case LW-7-2

Table 4.3.11 summarizes the temperature, PD and PPD at different heights. The temperature distribution of Case LW-R is similar to that of Case LW-7-1. It was because the boxes on two side were not heat sources and they did not obstruct the airflow in the room. However, in Case LW-7-2, the benches obstructed the flow from the diffusers and had a higher PD at 1.1m because the high velocity of the air was reflected at the height of occupant zone.

Table 4.3.12 presented the mean afe of air and CO_2 concentration at different heights. For Case LW-7-2, the supply air provided by the diffusers was reflected by the benches above them. Therefore, the average age at the height was only 431 s and it was the lowest among these three cases.

Table 4.3.11 Temperature, PD, and PPD at Z= 0.1, 1.1 and 1.7 m

	Height	TEM	DT1	DT2	PD	PPD
	(m)	°C	(1.7m-0.1m)	(1.1m-0.1m)	(%)	(%)
	0.1	23			8.9	6.6
	1.1	23.7			7.3	6.1
Case LW-R	1.7	24.5	1.5	0.7	5.7	5.9
	0.1	22.9			9	6.7
	1.1	23.5			7.2	6.2
Case LW-7-1	1.7	24.3	1.4	0.6	5.5	5.8
	0.1	22.5			11.2	7.3
	1.1	22.5			16.2	8.5
Case LW-7-2	1.7	23.5	1	0	5.4	5.4

Table 4.3.12 The mean age of air (MAA) and CO_2 concentration at Z= 0.1, 1.1 and 1.7 m

	Height	MAA	CO_2
	(m)	(sec)	(ppm)
	0.1	443	567
	1.1	486	597
Case LW-R	1.7	509	603
	0.1	459	577
	1.1	511	620
Case LW-7-1	1.7	530	624
	0.1	360	578
	1.1	356	611
Case LW-7-2	1.7	431	618

4.4 Conclusions

The performance of the floor-supply ventilation system was evaluated by using a validated CFD program for the indoor environment study. The parameters calculated and used to evaluate the indoor environment were the distributions of air temperature distribution, air velocity, percentage of dissatisfied people due to draft (PD), predicted percentage dissatisfied people for thermal comfort (PPD), contaminant concentration, mean age of air, and ventilation effectiveness.

For the office cases, which has a moderate cooling load (approximately 40W/m^2), the impact of different parameters was investigated. The indoor environment has a temperature gradient in the occupied zone, which can create comfort problems due to the temperature difference between the ankle level and the head level. Higher air velocity and higher PD around diffusers could also be a problem, especially with high air change rates. As for indoor air quality aspects, the floor-supply ventilation system provides better indoor air quality to the occupied zone than mixing ventilation systems. Then, the impacts of the load parameters, which are cases with 100 W/m^2, were also studied.

For the large workshop cases, the impact of different parameters was investigated. The parameters were supply airflow rate and air temperature, number of diffusers, partition arrangement, occupant arrangement, furniture arrangement, location and number of exhaust and location of diffuser.

Generally, the impacts of a changed parameter are similar between the offices and workshops. Higher air change rates are better for reducing the temperature gradient. However, higher air change rates are worse for the draft related aspects because of the higher supply air velocity. Higher air change rate has better indoor air quality. In addition to the quality of the indoor environment, energy consumption should be considered because higher air change rate would consume more energy. In high cooling load cases, temperature gradients are large and attention should be paid in order to make gradients less than 3 °C between the head and ankle levels. In principle, higher cooling loads need higher air change rates in order to make the temperature gradient acceptable. This is because the temperature gradient largely depends on both the heat sources in the occupied zone and the air change rate with the floor-supply system. Therefore, neither too low nor too high an air change rate is appropriate because of the temperature gradient and comfort distribution. Appropriate air change rates should have both acceptable temperature gradients and comfort distributions.

The number of diffusers and the supply air velocity are related to each other, since the total air flow rate is determined from the cooling load or heating load and the required amount of fresh air. Therefore, if more diffusers are used, the air flow rate per diffuser and supply air velocity would be smaller. Neither a low supply air velocity nor a small number of diffusers can obtain good indoor environment because the large vertical temperature gradient or the old mean age of air distribution is not acceptable. The important thing to obtain better indoor environment is to find a good balance between the supply air velocity and the number of diffusers in the room.

Partitions affect the indoor air quality in the floor-supply system when they become obstacles of the airflow. If the floor diffusers are installed appropriately inside the partition area, where the heat and contaminant sources are located, the room environment would be better than that without partitions. However, if the floor diffusers are not installed appropriately, the room environment might be worse. If the partitions were installed parallel to the air flow, the impact on the thermal comfort and indoor air quality is minimal.

Exhaust locations have influence on the indoor air quality in the office cases. It is because the contaminant source in the room is located at several specific spots. If the exhausts are installed near the contaminant sources, contaminant is removed faster and the indoor air quality would be better. For the workshop cases, the contaminant sources are quite evenly distributed, therefore, the influence of the exhaust location on indoor air quality is small.

Diffuser locations do not affect indoor environment so much, so long as the distance between diffusers or between the diffuser and the other object is not less than about 1.0 m to avoid interference.

Occupant locations would not have a significant impact on indoor environment if the heat source density is not more than the capacity of the diffusers near that area. If heat source density is

much higher in a certain area in a room and the capacity of diffusers near that area is not enough to remove the heat, the temperature and contaminant concentration would be higher than other areas in the room.

Furniture itself does not affect the indoor environment of the room unless it disturbs the airflow from floor diffusers. If any furniture, such as a table, is installed above the floor diffusers, thermal comfort in the room would be bad.

From these results of the non-load parameter study, the impact of the parameters can be ranked as follows:

Large impact	: air change rate, supply air velocity, supply air temperature, number of diffusers,
Medium impact	: partition location, exhaust location
Small impact	: diffuser location, occupant location, furniture arrangement

The diffuser location, occupant location, and furniture arrangement were investigated for typical cases. In some extreme cases, the impact of those parameters could be larger.

When the ventilation effectiveness of a space is higher, the indoor air quality is better and therefore, the risk of cross contamination would be reduced by the increased ventilation effectiveness. Therefore, the floor-supply ventilation system is a suitable ventilation system to be used in offices and workshops.

5. ENERGY ANALYSIS

The previous chapters show that floor-supply displacement ventilation system can provide a better indoor air quality with an acceptable thermal comfort level. However, proper design of displacement ventilation system should consider the energy consumption associated with the system. This chapter presents the fundamentals of energy analysis and the corresponding results of energy use for buildings with floor-supply displacement ventilation. The investigation uses a mixing system for comparison.

Energy simulation methods range from manual methods to detailed computer simulation methods. The manual methods, such as the degree-day and bin methods (ASHARE 1997), are still widely used in practical designs, although they are not accurate. The degree-day method uses only one value of temperature, while the bin method calculates the energy over several intervals (bins) of temperature. However, the detailed methods often calculate the energy on an hour-by-hour basis. Although the manual methods are simple, they could not, for example, be used for the comparison of energy consumption by displacement ventilation with that by mixing ventilation. The detailed computer simulation can consider the differences between displacement ventilation and mixing ventilation, such as the differences in the control strategies for the air handling processes of the two ventilation systems. Therefore, the present investigation uses a detailed computer simulation method by using EnergyPlus Program.

The detailed methods calculate the cooling and heating loads hour-by-hour for an entire year for a building, using weather data, the building characteristics, and thermal conditions as the inputs. Then the energy consumption of the ventilation system components is calculated on the basis of the hourly cooling/heating loads, the hourly weather data, and the control strategies associated with the configuration of the ventilation system.

Since the room air stratification has an impact on the load calculation, it was considered by applying a room air model which account for temperature stratification in cooling load calculation. To calculate the hourly cooling/heating loads, the study needs hourly weather data such as dry-bulb temperature, relative humidity and solar radiation. Typical meteorological year weather data (TMY2) for the U.S. were used.

We studied the energy analysis for both the displacement and mixing ventilation systems in both a large office and a workshop in each of the five climatic regions in the U.S. The five regions are: Seattle, WA (maritime), Portland, ME (cold), Phoenix, AZ (hot and dry), New Orleans, LA (hot and humid) and Nashville, TN (moderate). These five regions represent different climates in the U.S. They have been used widely in different research projects by the ASHRAE. At present, the floor-supply displacement ventilation is mainly used in Scandinavia and Japan. The climates there are not the same as the most of the U.S. The energy performance in those areas might not be applicable for the building in U.S. Therefore, the performances of the floor-supply system in these representative U.S. cities were studied.

5.1 Load Calculations

EnergyPlus solves simultaneously energy consumption by all three of the major parts: building, system, and plant, must be solved. In programs with sequential simulation, such as BLAST or DOE-2, the building zones, air handling systems, and central plant equipment are simulated sequentially with no feedback from one to the other. The sequential solution begins with a zone heat balance that updates the zone conditions and determines the heating/cooling loads at all time steps. This information is fed to the air handling simulation to determine the system response; but that response does not affect zone conditions. Similarly, the system information is passed to the plant simulation without feedback. This simulation technique works well when the system response is a well-defined function of the air temperature of the conditioned space. Basic equations used in EnergyPlus were shown in the following for further analysis and explanations. A more comprehensive study was presented in EnergyPlus User Manuel.

5.2 Room Air Model

The fully mixed room air approximation that is currently used in most whole building analysis tools is extended to a three node approach, with the purpose of obtaining a first order precision model for vertical temperature profiles in displacement ventilation systems. The use of three nodes allows for greatly improved prediction of thermal comfort and overall building energy performance in low energy cooling strategies that make use of unmixed stratified ventilation flows.

Several types of models have been proposed for inclusion in building energy simulation programs. These models must be simple enough not to impose an undue computational burden on a building energy simulation program, yet provide enough predictive capability to produce useful comparisons between conventional and stratified zone operation strategies. ASHRAE RP-1222 (Chen & Griffith 2002) divides the candidate models into two categories: nodal and zonal. Nodal models describe the zone air as a network of nodes connected by flow paths; each node couples convectively to one or more surfaces. Zonal models are coarse–grained finite volume models. The model for displacement ventilation is closer to a nodal model than to a zonal model. However, it is best to classify it in a separate category: plume equation based multi-layer models (Linden et al. (1990), Morton et al. (1956)). These models assume that the dominant mechanism is plume-driven flow from discrete internal sources and that other effects (such as buoyancy driven flow at walls or windows) may be neglected. Alternatively, these heat sources also produce plumes that can be included in the model. The result is a zone divided vertically into two or more well separated regions – each region characterized by a single temperature or temperature profile.

The model is used for the present study that predicts three temperatures in the room (Figure 5.1.1):

- A foot level temperature (T_{FLOOR}). The floor region is 0.2 meters deep and T_{FLOOR} represents the temperature at the mid-point of the region.
- An occupied sub-zone temperature (T_{OC}), representing the temperature in the region between the floor layer and the upper, mixed layer.

- An upper node representing the mixed-layer/outflow temperature (T_{MX}) essential for overall energy budget calculations and for modeling comfort effects of the upper layer temperature.

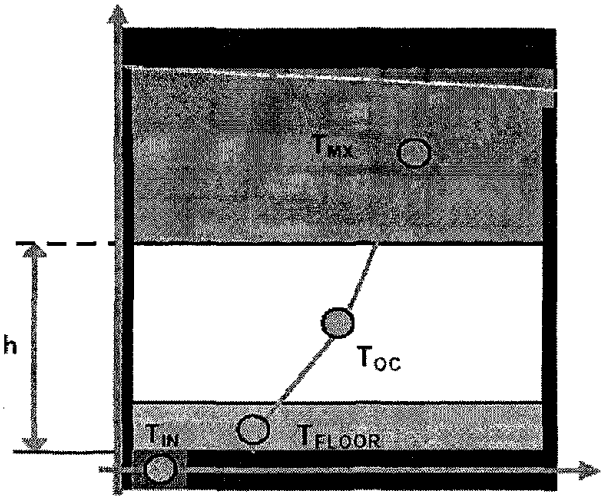

Figure 5.1.1 Schematic representation of the three temperature points and temperature gradients

5.3 Building Characteristics and Air Handling Systems

The building characteristics and thermal conditions

In order to calculate the hourly cooling/heating loads, the building characteristics and thermal conditions need to be specified. Table 5.3.1 shows the conditions of for the offices and industrial workshops discussed in Chapter 4. Hour-by-hour cooling/heating loads are calculated for these two types of buildings for the five climatic regions: Seattle, WA (maritime), Portland, ME (cold), Phoenix, AZ (hot and dry), New Orleans, LA (hot and humid) and Nashville, TN (moderate). The industrial workshop is a large space with a lot of equipment and workers inside, as can be seen in Table 5.3.1.

In addition, the investigation uses the following assumptions/ conditions:

- A fixed coefficient of performance for chiller of 2.9 for mixing ventilation and 3.1 for displacement ventilation
- A fixed boiler efficiency of 0.8
- Fan total efficiency of 0.68
- Occupancy schedule of 9.00am – 6.00pm
- Minimum outdoor air of 10L/s/ person

Table 5.3.1 Building characteristics and thermal conditions

Space Type			Small Office	Workshop
Space Size		Length (m)	4.8	26.2
		Width (m)	4.2	21.0
		Height (m)	2.5	4.5
Exterior Envelope	Wall U-Value (W/m^2-K)	Seattle & Portland	0.72	
		Phoenix, New Orleans, & Nashville	0.96	
	Glazing	Double Glazing: U = 4.6 W/m^2-K		
		50% of Exterior Wall Area is Glazed		
Internal Load (W)	Sensible	Equipment	200	3362
		Lights	384	5502
		People	2(75)=150	112(105)=11760
Room Temperature Set Point (°C)		Cooling	25	
		Heating	23	
Supply Air Temperature (°C)	DV	Cooling	19	
		Heating	32	
	Mixed	Cooling	13	
		Heating	32	
Supply Air Humidity Ratio ($g_{moist\ air}$ / $kg_{dry\ air}$)	DV	Cooling	6.5 (@18°C)	
		Heating	9.5 (@24°C)	
	Mixed	Cooling	6.5 (@18°C)	
		Heating	9.5 (@24°C)	

Air handling systems

In order to evaluation the energy performance of the floor-supply displacement ventilation system, a complete mixing ventilation system is used as reference. Figures 5.3.1 and 5.3.2 show the layouts of the displacement and mixing ventilation systems, respectively. Both systems use a heat exchanger to recover the energy from the exhaust air to heat the outdoor air in the cooling and heating season. The systems use steam for humidification, and use the cooling coil for dehumidification. Free cooling is used for both the ventilation systems in the shoulder seasons.

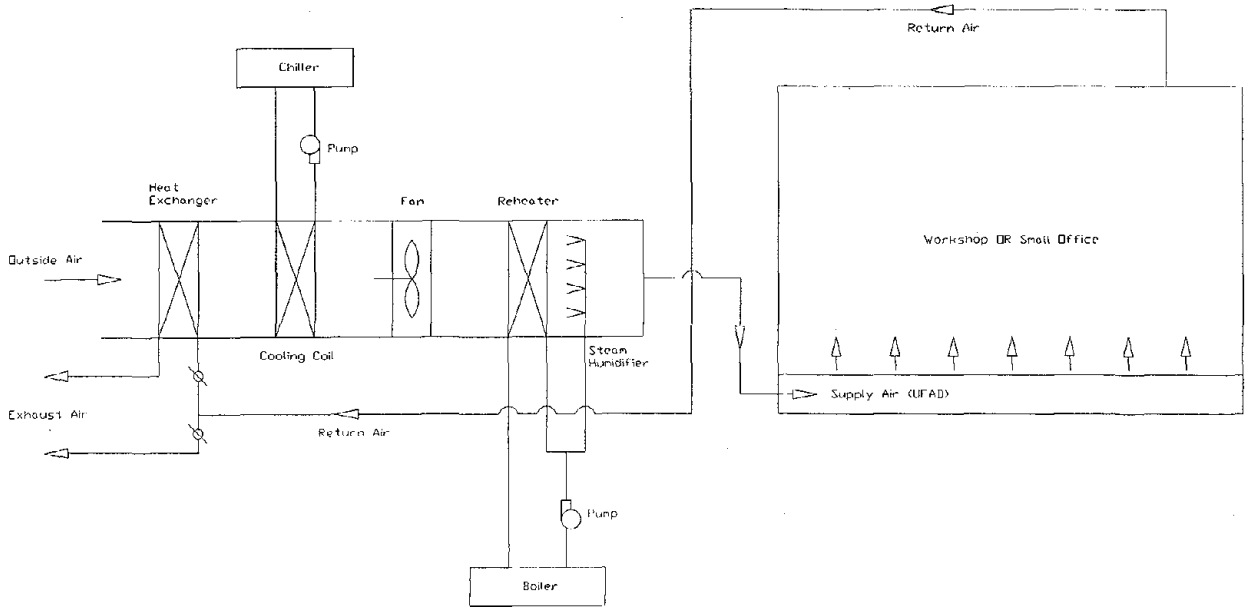

Figure 5.3.1 Air handling system for mixing ventilation

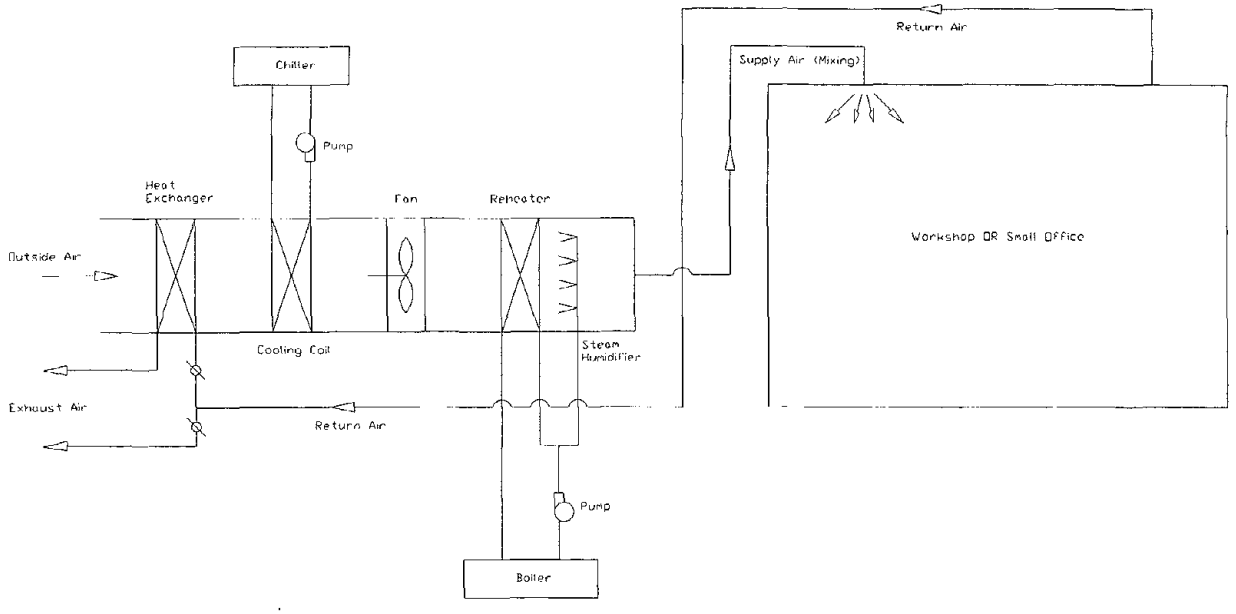

Figure 5.3.2 Air handling system for mixing ventilation

5.4 Comparison of Energy Uses

In this section, the energy use by the under-floor displacement ventilation is compared with that by mixing ventilation for the office building and the workshop building.

Office building

Figure 5.4.1 shows the monthly energy consumption of an office in Nashville, TN. The displacement ventilation system uses more fan energy than the mixing ventilation system. Although the exhaust air temperature with the displacement ventilation system is higher than that with the mixing ventilation system, the temperature difference between the exhaust and supply air is smaller. Typically, the exhaust air temperature for the displacement system is 29°C in summer and 27°C in winter. Therefore, the temperature difference between the exhaust and supply air is typically 9°C for both summer and winter. The temperature difference between the exhaust and supply air with the mixing system is higher both in summer 12°C and in winter 17°C. To offset the same amount of cooling load, a larger amount of supply air is needed with displacement ventilation. The difference is especially large during summer, when the cooling load is high.

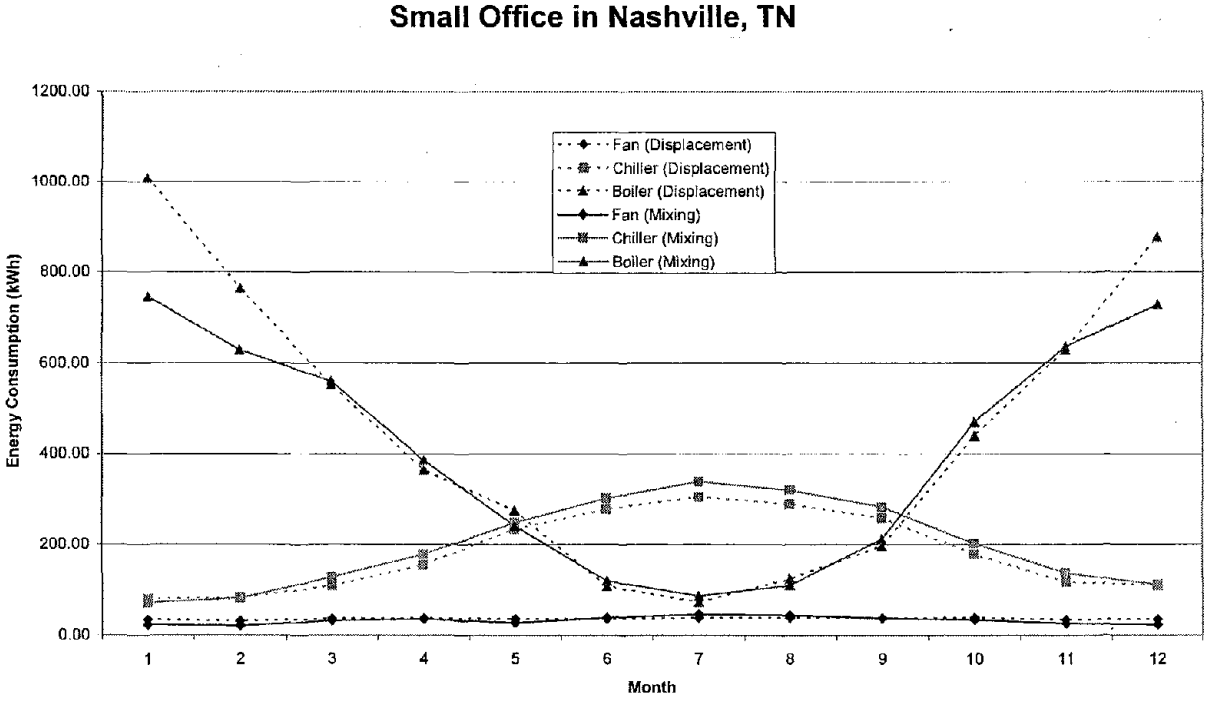

Figure 5.4.1 The monthly energy consumption of an office in Nashville, TN

In the winter, the floor-supply displacement system is used to supply heated air from the floor level. The heating demand of the displacement ventilation is increased due to the temperature stratification in the room air. Therefore, higher flow rate of supply air is demanded to maintain

the room temperature set point. The fan energy consumed by the two ventilation systems during winter is similar.

Figure 5.4.2 also indicates that the energy consumed by the chiller in the displacement ventilation system is much less. Since the supply temperature is higher in the displacement ventilation system than that in the mixing ventilation system, the chiller in the displacement system does not need to cool the air as much as in the mixing system. On the other hand, a higher supply air temperature would allow the displacement system to use more free cooling during the shoulder seasons. Also, the COP value is slightly higher with displacement ventilation (3.0) than with mixing ventilation (2.9). Another way to understand why the displacement system uses less chiller energy is to view the room and the ventilation system as a whole. The exhaust air temperature in the displacement system could be 2°C higher than that in the mixing system, which means more heat is discharged to the outdoors by the displacement ventilation system.

The energy consumed by the boiler with displacement ventilation is higher than that consumed with mixing ventilation. The room temperature stratification will consume more heat to heat up the occupied zone of the room. (Figure 5.4.2)

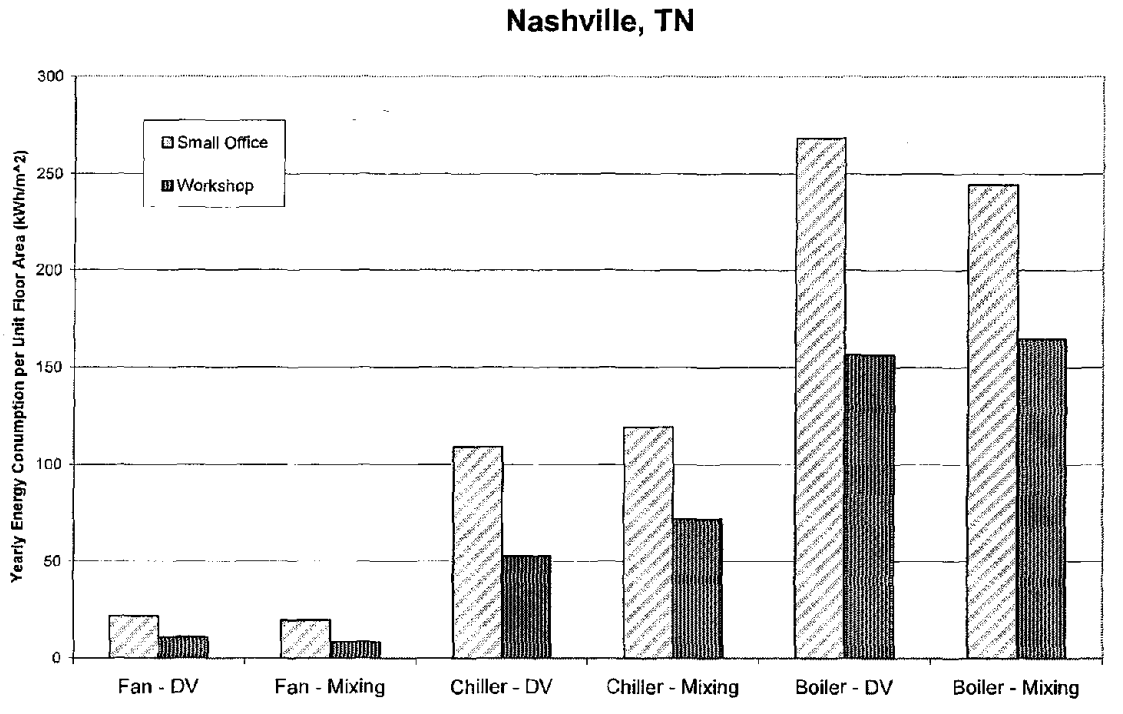

Figure 5.4.2 Yearly Energy Consumption per unit floor area of an office and a workshop in Nashville, TN

The energy consumption profiles were similar for the cases in different places. Due to the weather difference in different locations, the magnitudes of the energy consumption were different but the trends still kept the same. The results of the cases for other locations were presented in Appendix B. However, for the office case in Phoenix, the chiller energy

consumption of displacement ventilation was even higher than that of mixing ventilation. The cause of this phenomenon was not clear yet and further study should be carried out.

Workshop

The investigation also compared the annual energy consumption by the displacement and mixing ventilation systems for a workshop in the five climate regions. Figure 5.4.2 in above section had already shown the results for Nashville, TN. The energy consumption is normalized by the floor area. As can be seen from the figure, the same trend holds for workshop as for the individual office, i.e., the displacement ventilation system uses more fan energy and boiler energy, but much less chiller energy, than the mixing ventilation system.

In most cases, the sum of the energy consumed by displacement ventilation is slightly smaller than that consumed by mixing ventilation. The fan uses more energy in displacement ventilation, because of the high cooling load found in U.S. buildings.

Not surprisingly, the energy consumption for the office building in different cities is different, since the weather data is different. However, as for the comparison of energy consumption between the displacement and mixing ventilation systems, the results in other cities are similar to those in Nashville, TN. The figures in appendix B further shows the study for the five climate regions.

5.5 Conclusions

The present investigation studied the energy consumption of the displacement and mixing ventilation systems in an individual office and a large industrial workshop for five U.S. climate regions. The investigation accounted for the most important characteristics of the displacement ventilation system, such as air temperature stratification and high ventilation effectiveness. Both factors have significant impact on the energy consumption by the air handling system using displacement ventilation.

The study showed that the displacement ventilation system may use more fan and boiler energy but less chiller energy, than the mixing ventilation system. The total energy used is slightly less with displacement ventilation, although the ventilation rate is increased to handle the high cooling loads found in U.S. buildings. Therefore, displacement ventilation system is effectively saving energy during cooling mode but is not saving energy during winter mode.

6. CONCLUSIONS

Displacement ventilation has received considerable attention recently since it improves indoor air quality. The system provides fresh air directly to the occupied zone and the airflow in the occupied zone is one-dimensionally upwards, so the air quality is better. Although U.S. buildings have large interiors and most offices in the U.S. are partitioned into cubicles, the general conclusions obtained in Europe and Japan are similar to those found in this study, which is for U.S. buildings.

This investigation conducted experimental measurements of thermal comfort and indoor air quality parameters in a full-scale environmental chamber, obtaining reliable data on the floor-supply ventilation system. With the reliable data, a computational-fluid-dynamics (CFD) program used in this research was validated. The CFD program can reasonably predict the distributions of air velocity and temperature for a simulated office and a simulated workshop with floor-supply displacement ventilation. However, it seemed more difficult to simulate the distribution of gaseous contaminant concentration with the SF_6 tracer-gas used in the experiment.

This study has successfully simulated a complex air supply device, such as a swirl diffuser, a perforated panel, and a perforated carpet. The experimental data, such as air velocity and flow direction, are crucial for a correct simulation by CFD.

The results from both the experimental measurements and CFD simulations demonstrate that an office and a workshop with floor-supply displacement ventilation can greatly improve indoor air quality in terms of the distributions of CO_2 concentration, the mean age of air, and ventilation effectiveness. However, the indoor spaces with floor-supply displacement ventilation could have a high risk of discomfort, because of the high temperature stratification between the ankle and head levels. The swirl diffuser can provide a better comfort level than perforated panels or carpets due to the mixing around the diffuser. Nevertheless, the draft risk is high in an area within 1 m around the diffuser.

The results also show that the risk of cross contamination in an indoor space with floor-supply displacement ventilation is much smaller than that with a traditional side-wall supply displacement ventilation.

This research used the CFD program as a tool to study the impacts of several parameters, such as the air change rate and supply air temperature, number of diffusers, furniture and occupant arrangement, and cooling loads, on the indoor environment, based on the thermal comfort and indoor air quality levels. The total supply air flow rate and number of diffusers affected most critically the thermal comfort and indoor air quality. In addition, the partition and exhaust location will also have significant impacts on indoor air quality.

The present investigation also studied the energy consumption of the displacement and mixing ventilation systems in an office and an industrial workshop for five U.S. climate regions. The investigation accounted for the most important characteristics of the displacement ventilation system, such as air temperature stratification and high ventilation effectiveness. The results show

that a displacement ventilation system may use more fan and boiler energy but less chiller energy than a mixing ventilation system. The total energy used is slightly less with displacement ventilation.

The above conclusions suggest that the floor-supply ventilation system is a suitable ventilation system for offices and workshops, as well as other similar indoor spaces in the United States. When the displacement ventilation systems are widely used in U.S. buildings, the indoor environment would be improved.

REFERENCES

Akimoto T: [1998] Research on Floor-Supply Displacement Air-Conditioning System, Ph.D. Thesis, Waseda University, Japan

ASHRAE: [1997] 1997 ASHRAE Handbook – Fundamentals, ASHRAE, Atlanta

ASHRAE: [2001] ASHRAE standard 62-2001: Ventilation for Acceptable Indoor Air Quality. Atlanta, ASHRAE

ASHRAE: [2004] ASHREA Standard 55-2004: Thermal Environmental Conditions for Human Occupancy. Atlanta, ASHRAE

Chen Q: [1995] Comparison of different k-e models for indoor airflow computations. Numerical Heat Transfer, Part B: Fundamentals, Vol. 28, 353-369.

Chen Q, Griffith B: [2002] Incorporating Nodal Room Air Models into Building Energy Calculation Procedures. ASHRAE RP-1222 Final Report

Hu S, Chen Q, and Glicksman LR: [1999] Comparison of Energy Consumption Between Displacement and Mixing Ventilation Systems for Different U.S. Buildings and Climates. ASHRAE Transactions, 105(2)

Linden PF, Lane-Serff GF, Smeed DA: [1990] Emptying Filling Boxes: The Fluid Mechanics of Natural Ventilation. Journal of Fluid Mechanics, Vol. 212, pp. 309-335

Liu Y, Hiraoka K: [1997] Ventilation Rate requirement for Raised Floor HVAC System. Shase Journal, 67 October, 75-84

Matsunawa K et al: [1995] Development and Application of an Underfloor Air-Conditioning System with Improved Outlets for a 'Smart' Building in Tokyo. ASHRAE Transactions, 101(2): 887-901

Mattson M: [1998] Displacement Ventilation in a Classroom-Influence of Contaminant Position and Physical Activity. Proceeding of AIVC Conference, Oslo, Norway

McCarry B: [1995] Underfloor Air Distribution Systems: Benefits and When to Use the System in Building Design. ASHRAE Transactions, 101(2): 902-911

Morton BR, GI Taylor, Turner JS: [1956] Turbulent Gravitational Convection from Maintained and Instantaneous Sources. Proceedings of the Royal Society of London, Vol. A234, pp. 1-23

Sodec F, Craig R: [1990] Underfloor Air Supply System - The European Experience. ASHRAE Transactions, 96(2): 690-695

Spoormaker H: [1990] Low-Pressure Underfloor HVAC System. ASHRAE Transactions, 96(2): 670-677

Tanabe S et al: [1994] Evaluating Thermal Environments by Using a Thermal Manikin with Controlled Skin Surface Temperture. ASHRAE Transactions, 100(1): 39-48

Tanigawa M et al: [1993] Measurement of Environment with Under-Floor Air-Conditioning System for Smart Building. Nippon Kenchikugakkai Transactions, 1555-1556

APPENDIX-A MORE VALIDATION OF THE CFD PROGRAM

This appendix shows further validation of the CFD program by four sets of additional data obtained from the environmental chamber at Purdue University. The four cases simulate a workshop and an office with different thermo-fluid conditions: Workshop-2, Office-2, Office-3 and Office-4. Table A1 summaries the configuration used in the experiment.

Table A1 Summary of the experimental configuration

Case	***Diffuser Type***	***Occupancy***	***Chamber***	***Internal furniture***
Workshop-2	Perforated Panel	4	Purdue	2 Tables with 4 equipments
Office-2	Perforated Panel	2	Purdue	2 Tables with 2 equipments
Office-3	Swirl diffuser	2	Purdue	2 Tables with 2 equipments and partition
Office-4	Perforated Panel	2	Purdue	2 Tables with 2 equipments and partition

Table A2 Values used for the diffuser simulation

	Vertical angle	range of air velocity range (m/s)
Workshop-2	N/A	0.16-0.43
Office-2	N/A	0.11-0.14
Office-3	75	0.88-1.51
Office-4	N/A	0.05-0.14

Figures A1 to A4 present, respectively, the measured and computed temperature, velocity, and SF_6 concentration for the four cases. The measurements were done at nine different pole locations. Each pole has sensors at different heights to measure temperature, velocity, and SF_6 concentration. Table A3 summarized the figure number and the corresponding results shown in the figures.

Table A3 Figure number and the corresponding cases

Case	Figure number	Remark
Workshop-2	A1	(a) – Temperature
Office-2	A2	(b) – Velocity
Office-3	A3	(c) – SF_6 concentration
Office-4	A4	

Figures A1 (a) to A4 (a) clearly shows that the floor-supply system created temperature stratification in these 4 cases. By comparing the Figure A3(a) with figure A4(a), the impact of

the diffusers and the perforated panels on the indoor environment could be studied. The temperature gradient in the lower part of the room was larger when the perforated panels were used. This is because the supply velocity from the perforated panels was smaller then that from swirl diffusers. The cold supply air tended to spread over the room and stayed at the lower level while swirl diffusers induced a stronger turbulence and mixing effect. The computed temperature and measured results were generally in reasonable agreement except the region near the swirl diffusers.

Figures A1 (b) to A4 (b) present velocity distributions for these four cases. The velocities in the room were generally low for the all cases. The velocities in the room with perforated panels were even lower (less than 0.2 m/s) except around the diffusers and exhaust. The agreements between the computed velocity and measured data are acceptable in both cases, although the velocity is low in the most part of the room.

Figures A1 (c) to A4 (c) present tracer gas distributions. In most of the cases, the agreement between the computed tracer-gas concentration and measured data is not as good as that for the air temperature and velocity. Since the tracer-gas is a point source and the concentration is very sensitive to the position, it is difficult to get good agreement between the computed tracer-gas concentration and measured data at every point. Nevertheless, the accuracy of the computed concentration is still usable.

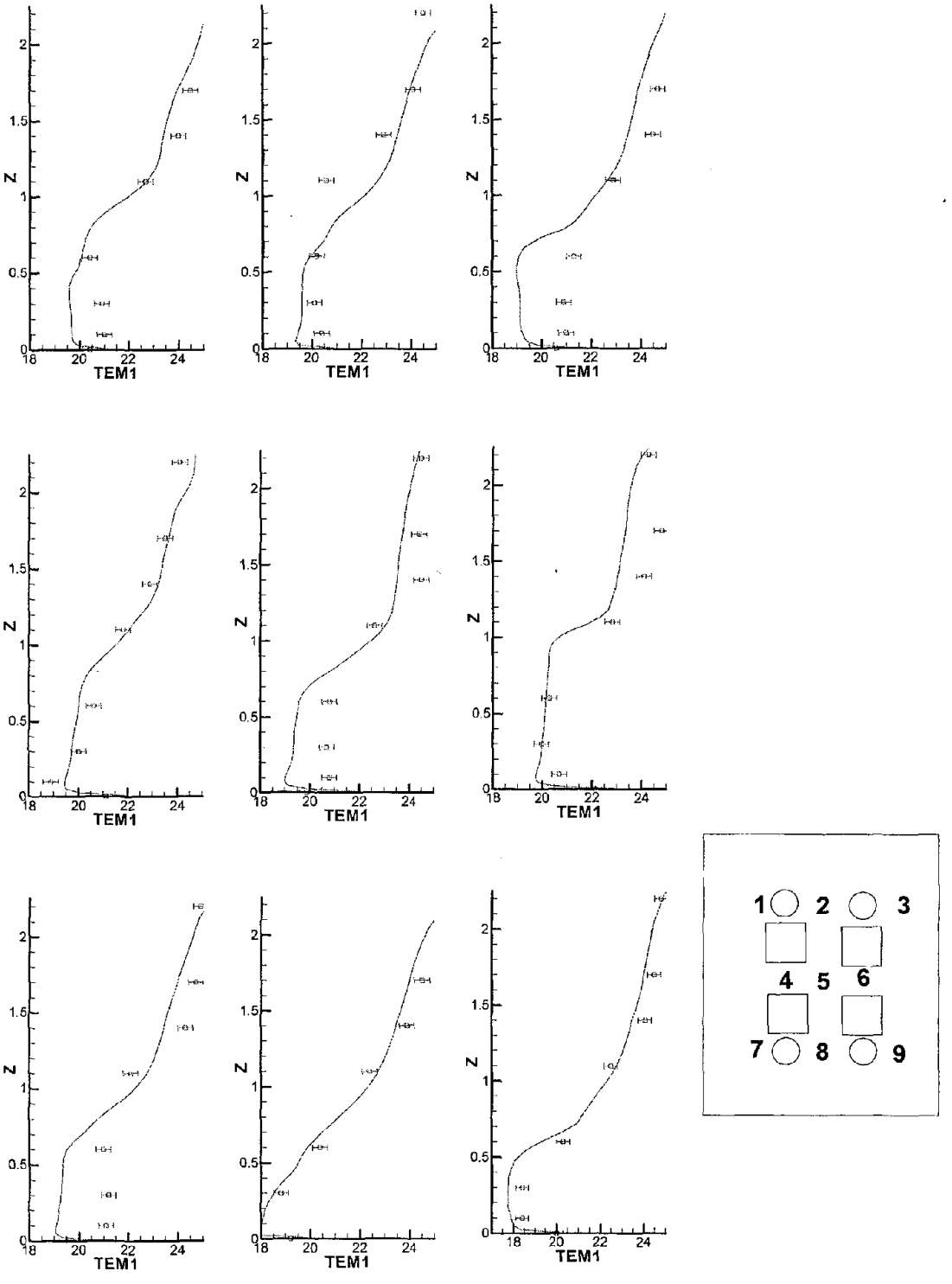

Figure A1(a) Comparison of the vertical temperature profiles of Workshop-2 units: (^{O}C), Symbols: measurement, Lines: computation

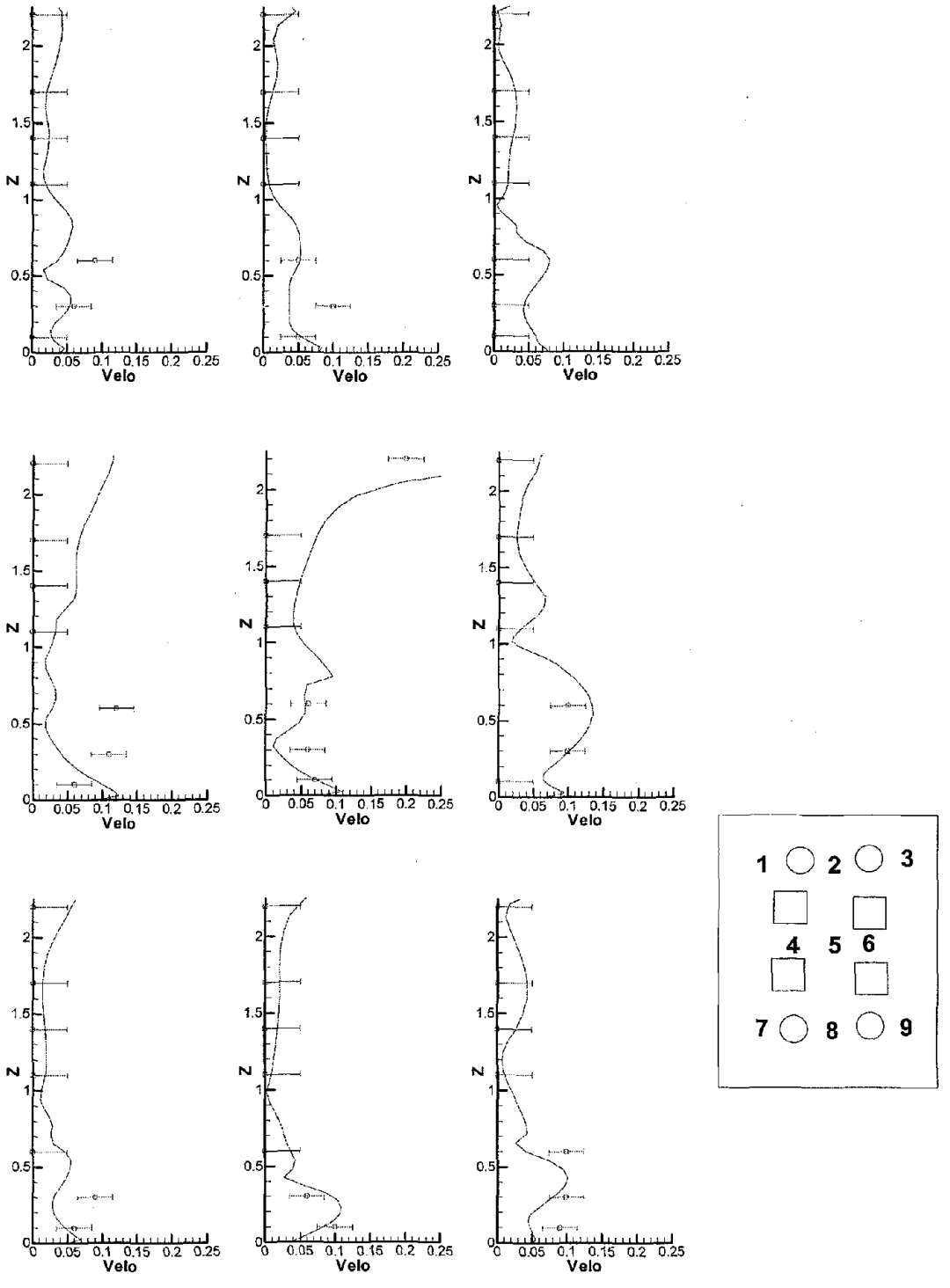

Figure A1(b) Comparison of the vertical velocity profiles of Workshop-2 units: (m/s), Symbols: measurement, Lines: computation

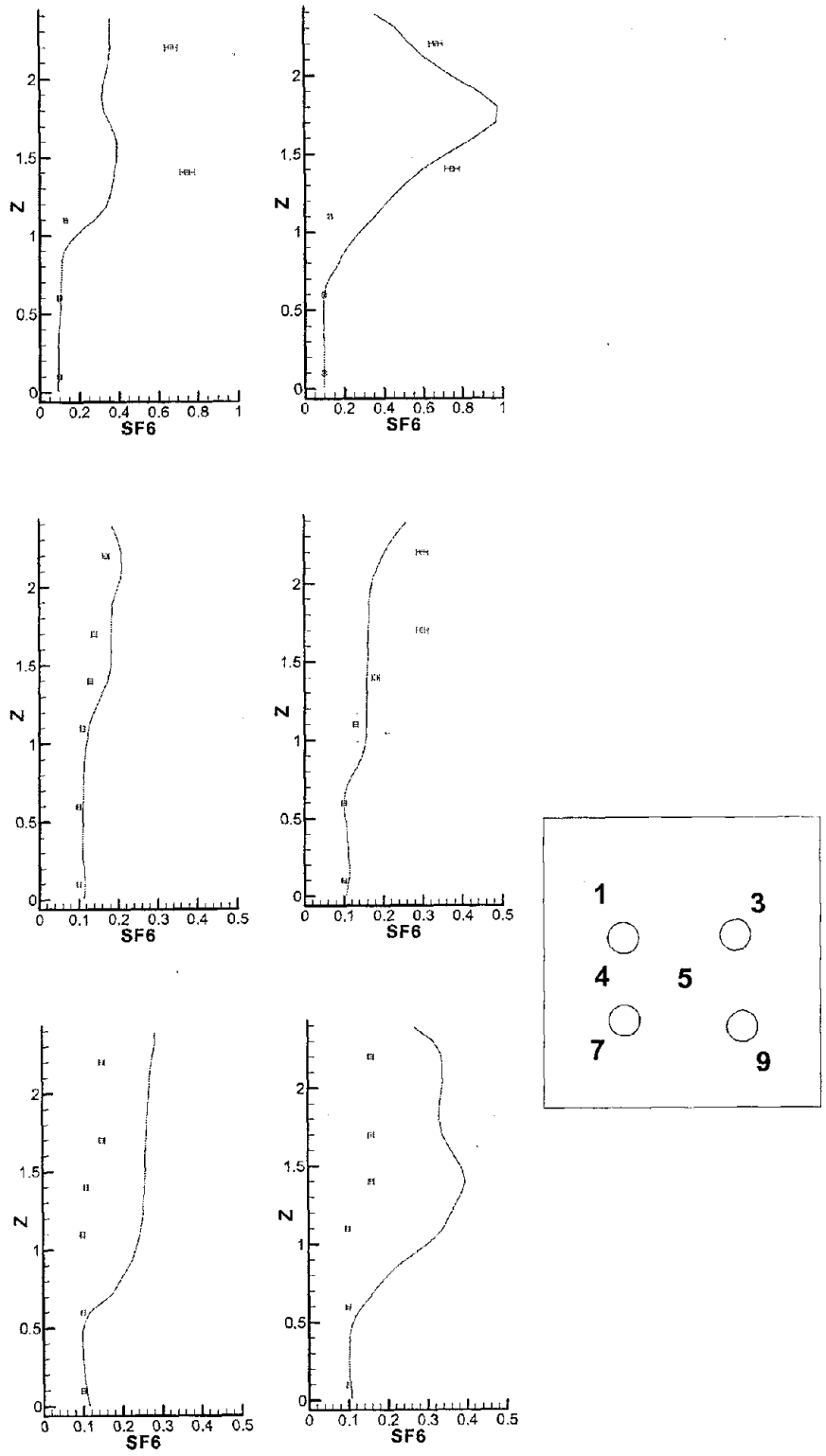

Figure A1(c) Comparison of the vertical SF_6 concentration profiles of Workshop-2 units: (ppm), Symbols: measurement, Lines: computation

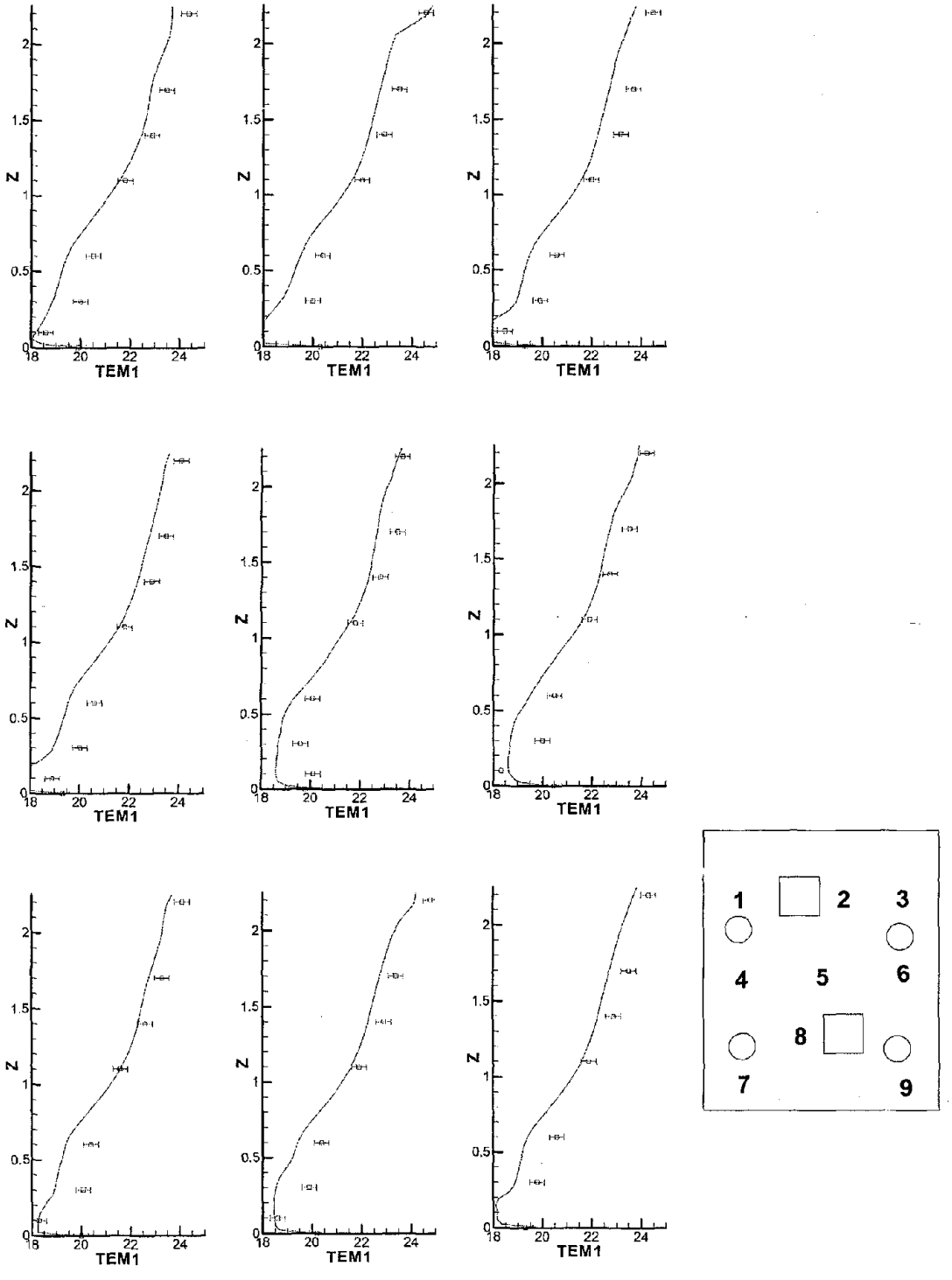

Figure A2(a) Comparison of the vertical temperature profiles of Office-2 units: (^{O}C), Symbols: measurement, Lines: computation

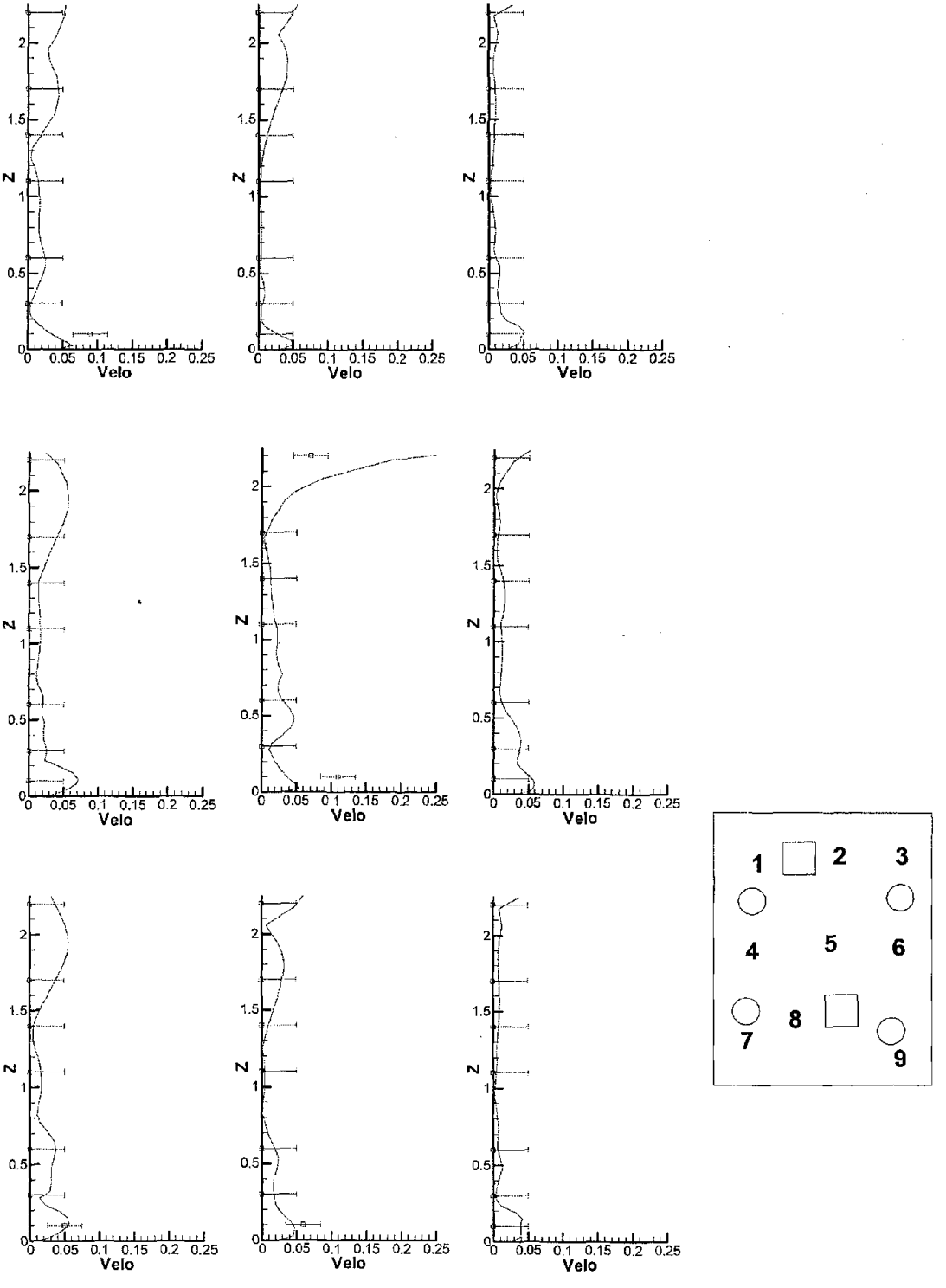

Figure A2(b) Comparison of the vertical velocity profiles of Office-2 units: (m/s), Symbols: measurement, Lines: computation

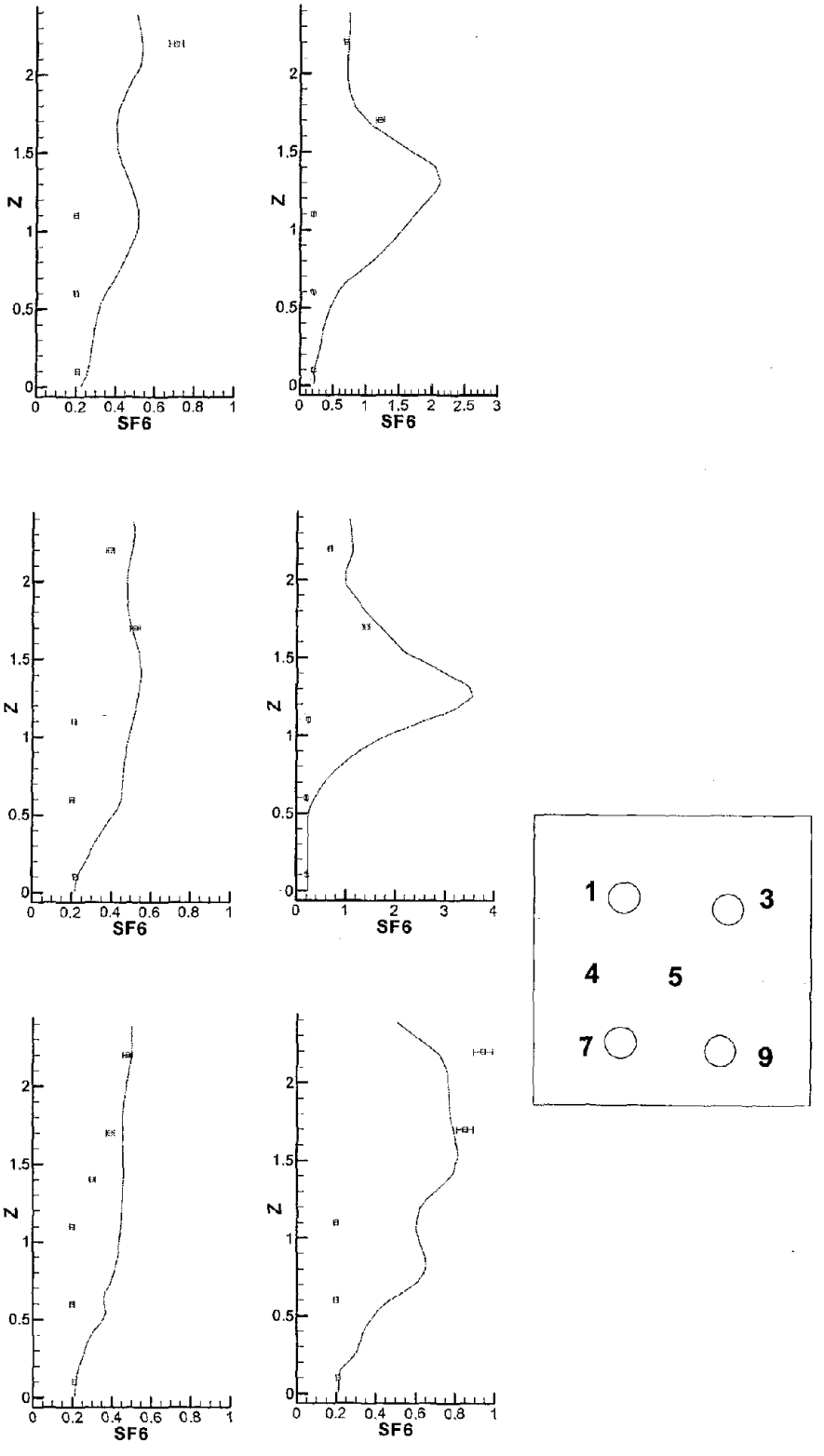

Figure A2(c) Comparison of the vertical SF_6 concentration profiles of Office-2 units: (ppm), Symbols: measurement, Lines: computation

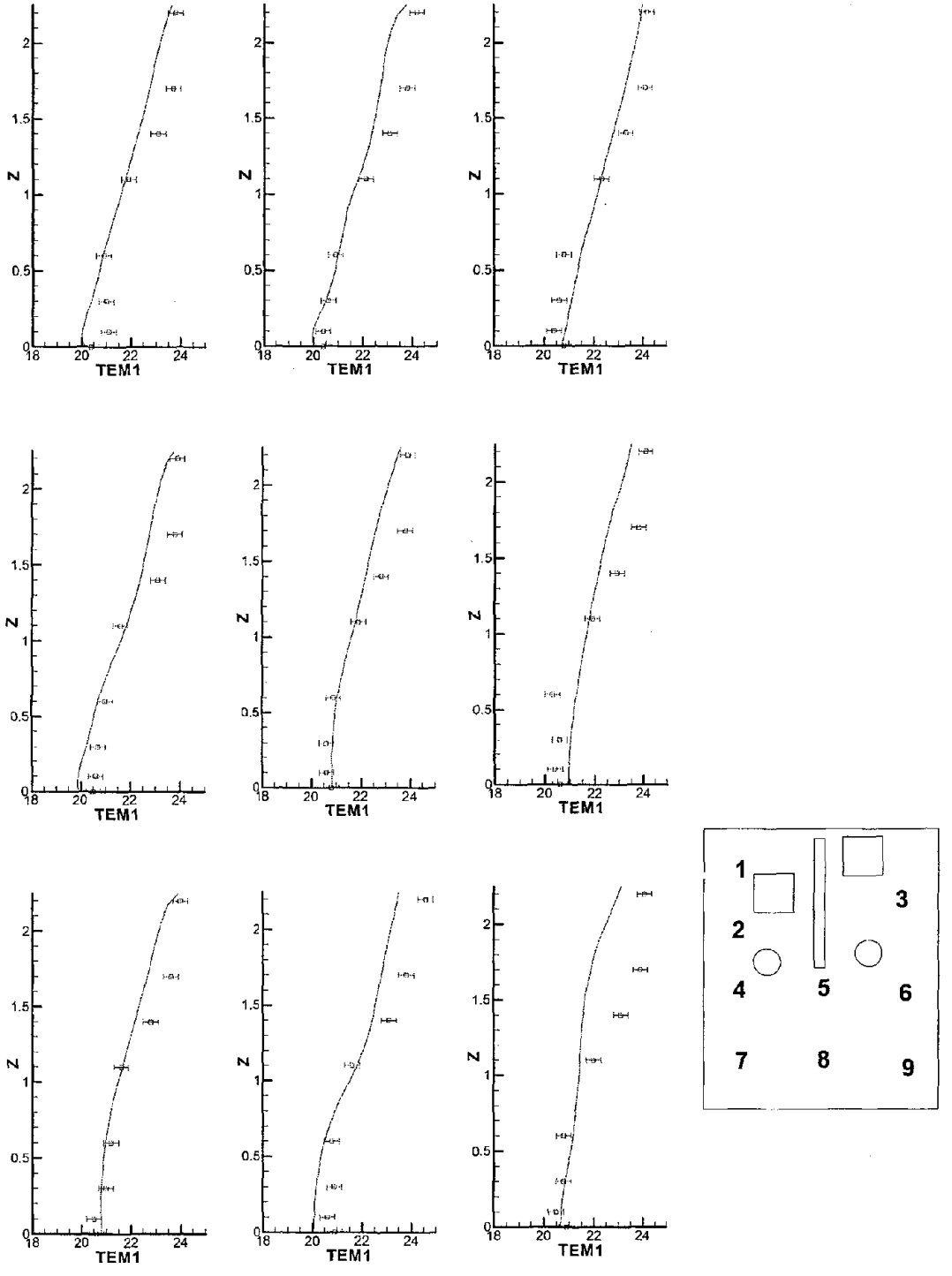

Figure A3(a) Comparison of the vertical temperature profiles of Office-3 units: (^{O}C), Symbols: measurement, Lines: computation

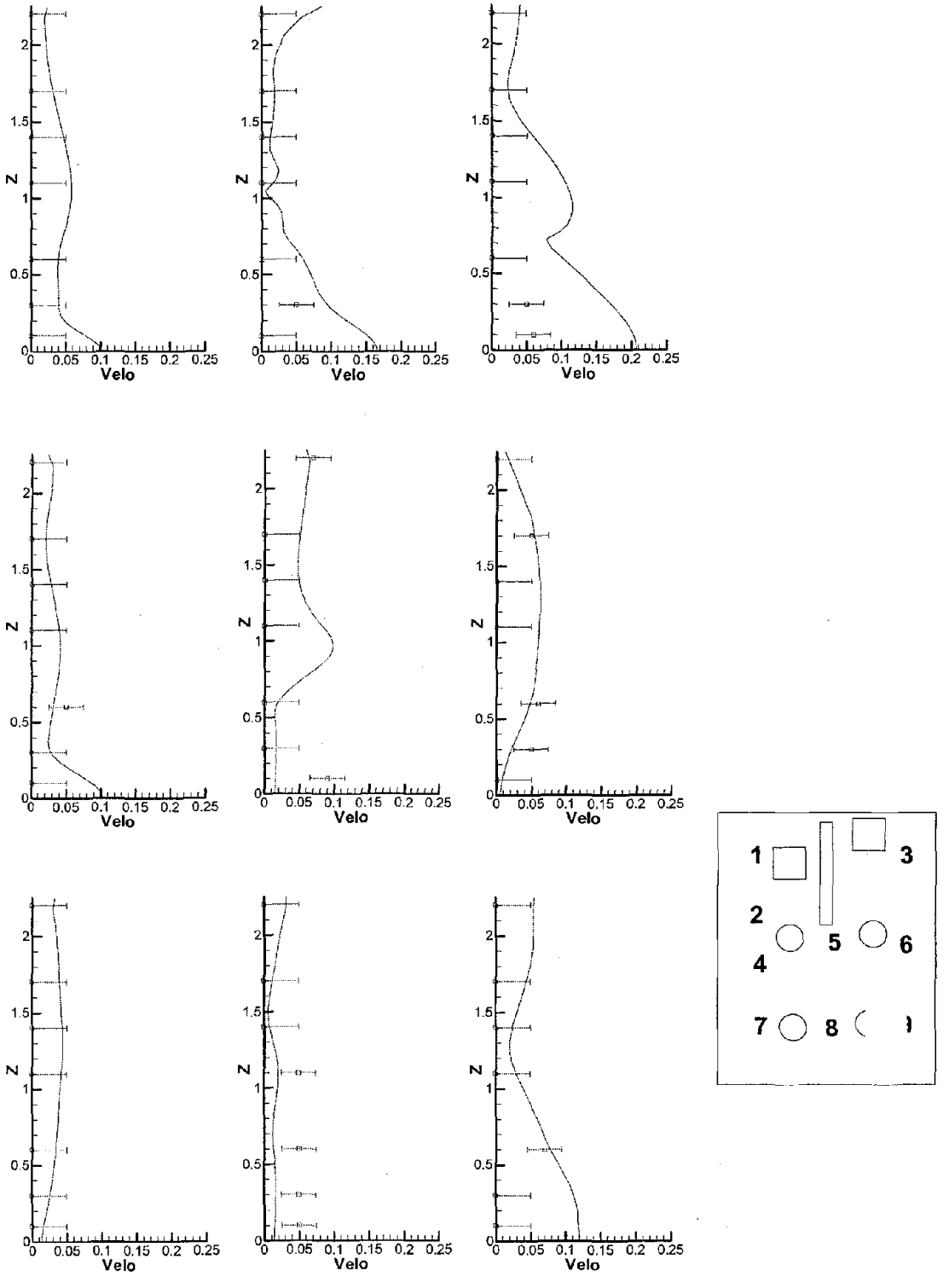

Figure A3(b) Comparison of the vertical velocity profiles of Office-3 units: (m/s), Symbols: measurement, Lines: computation

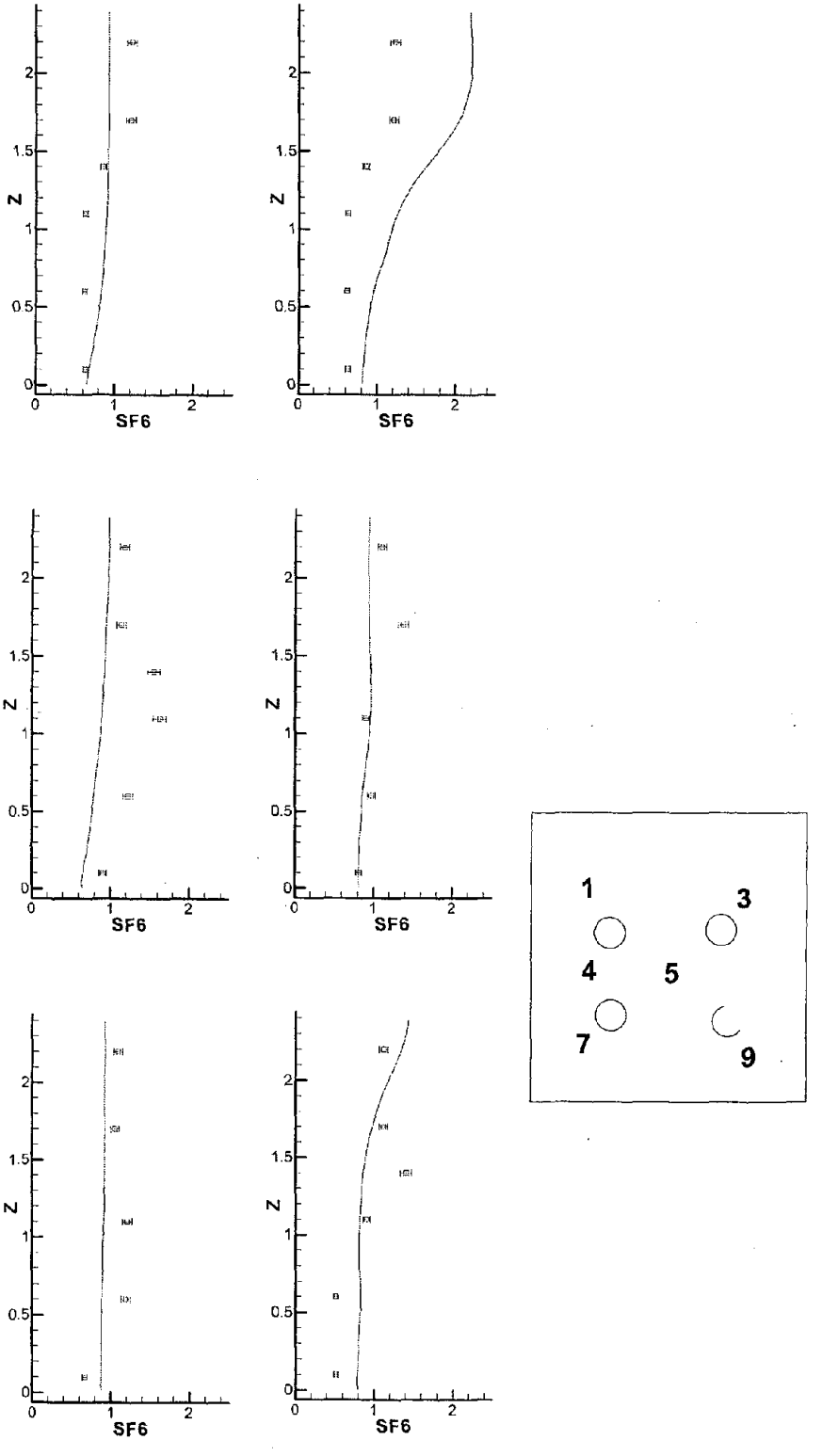

Figure A3(c) Comparison of the vertical SF_6 concentration profiles of Office-3 units: (ppm), Symbols: measurement, Lines: computation

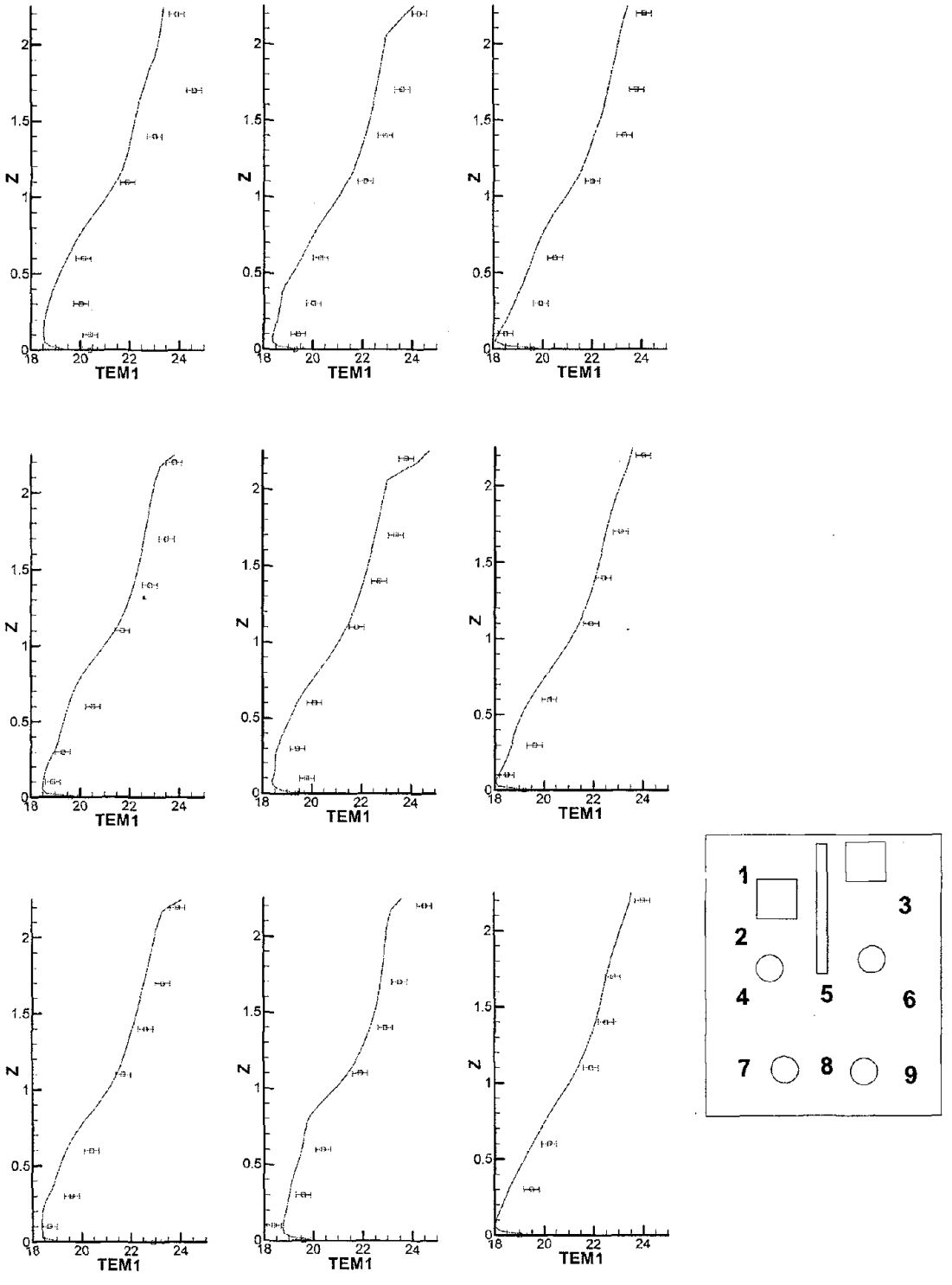

Figure A4(a) Comparison of the vertical temperature profiles of Office-4 units: (^{O}C), Symbols: measurement, Lines: computation

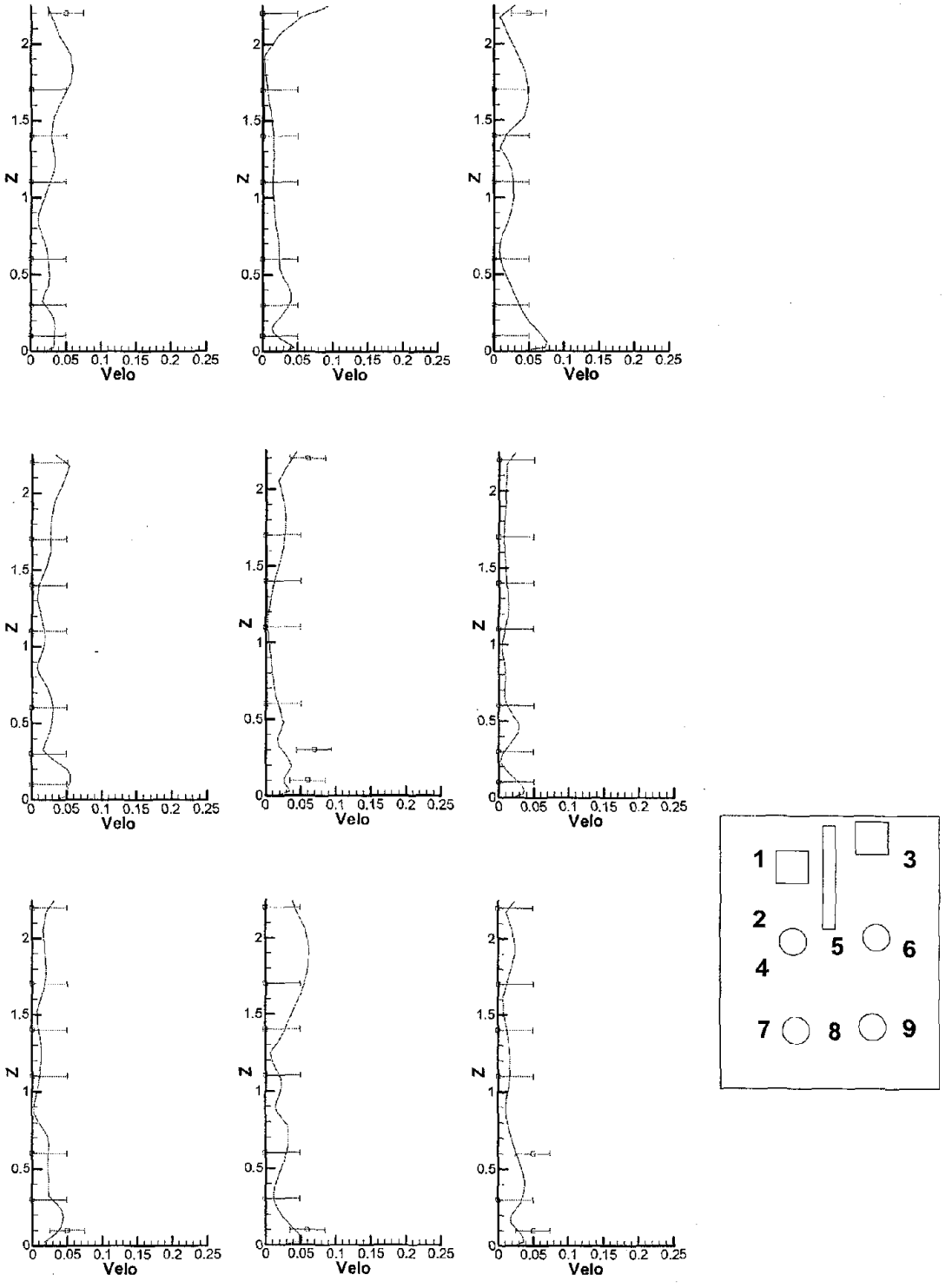

Figure A4(b) Comparison of the vertical velocity profiles of Office-4 units: (m/s), Symbols: measurement, Lines: computation

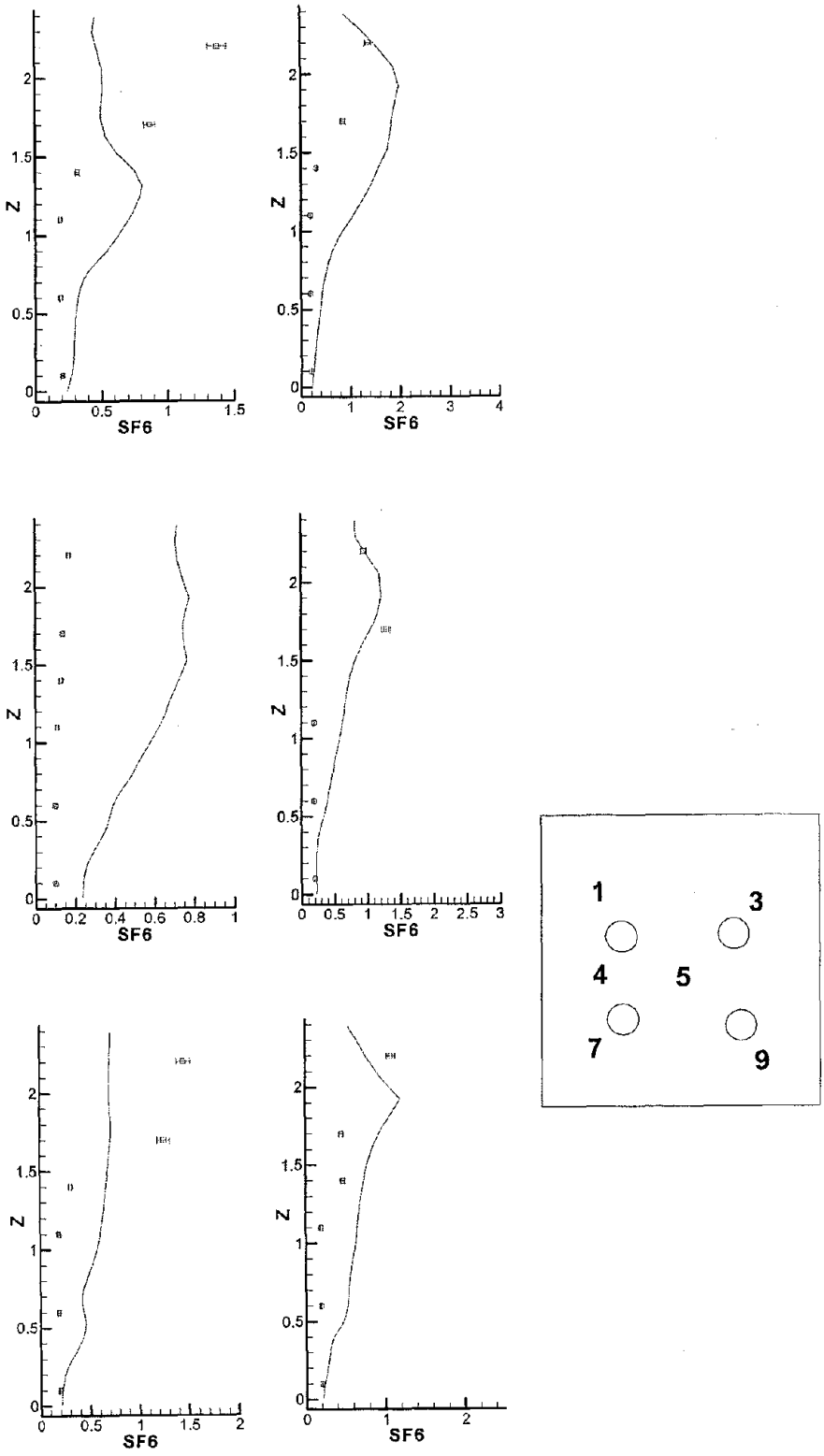

Figure A4(c) Comparison of the vertical SF_6 concentration profiles of Office-4 units: (ppm), Symbols: measurement, Lines: computation

APPENDIX-D
ENERGY ANALYSIS FOR FIVE CLIMATE REGIONS

This appendix shows the energy simulation results for the office and the workshop for the five U.S. climate regions. The top figure is for the annual energy consumption by different air-handling components. The middle figure is the energy consumption per month for the office and the bottom figure is that for the workshop. Each page represents the results for one climate region.

Nashville, TN

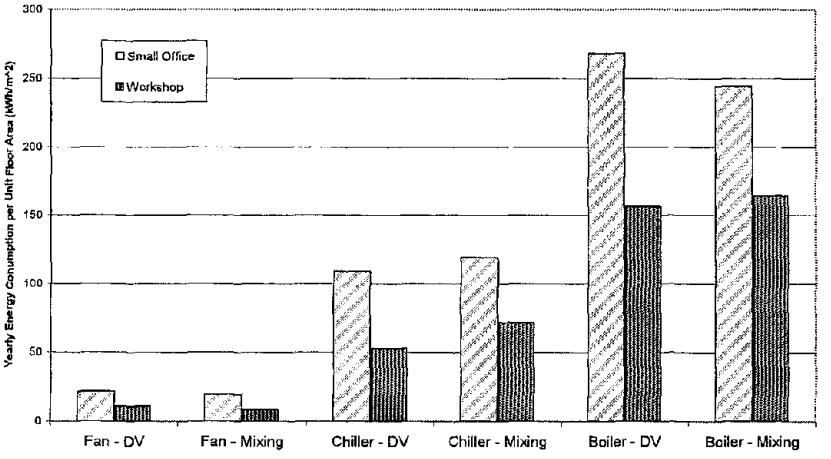

Small Office in Nashville, TN

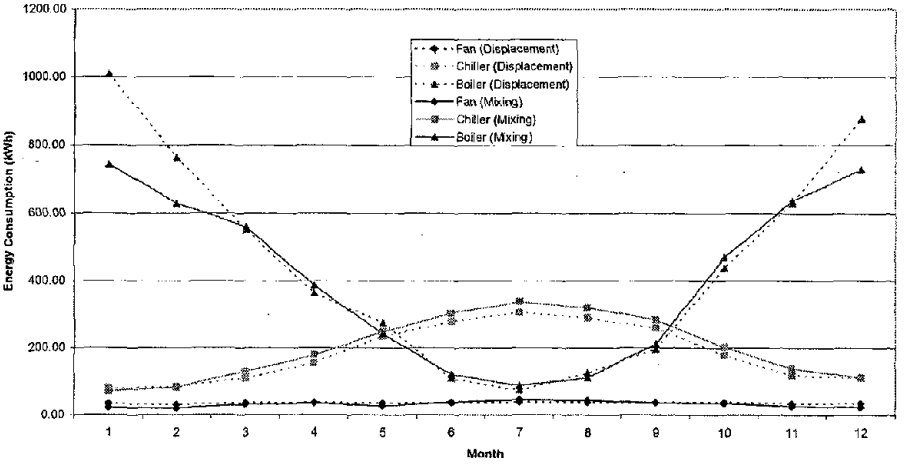

Workshop in Nashville, TN

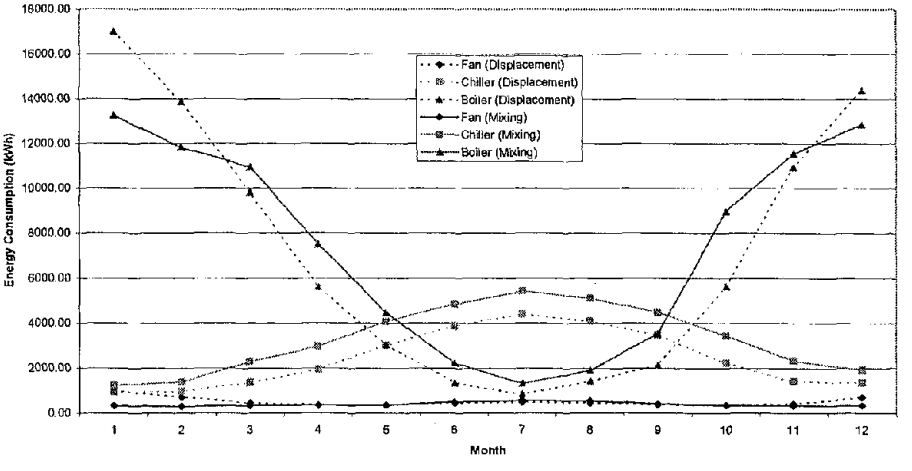

New Orleans, LA

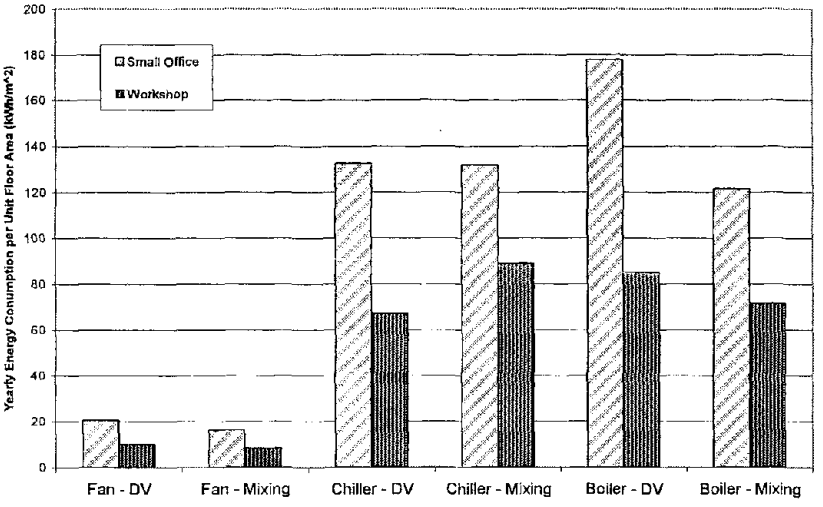

Small Office in New Orleans, LA

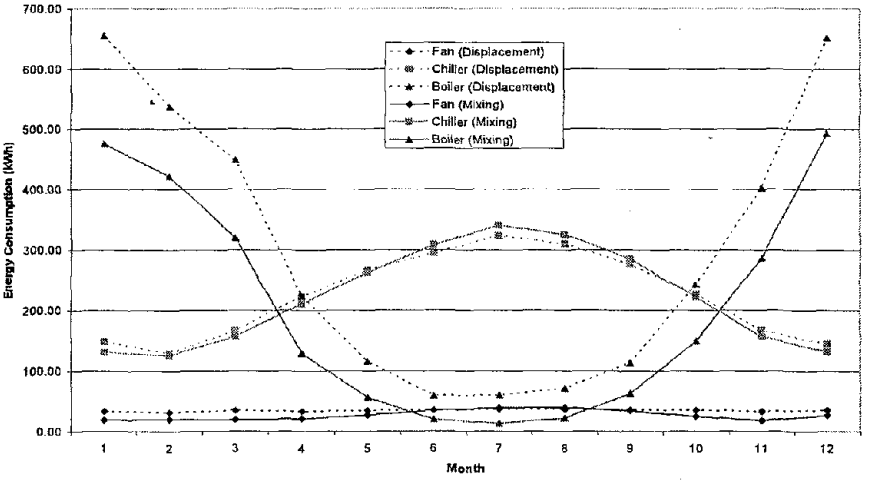

Workshop in New Orleans, LA

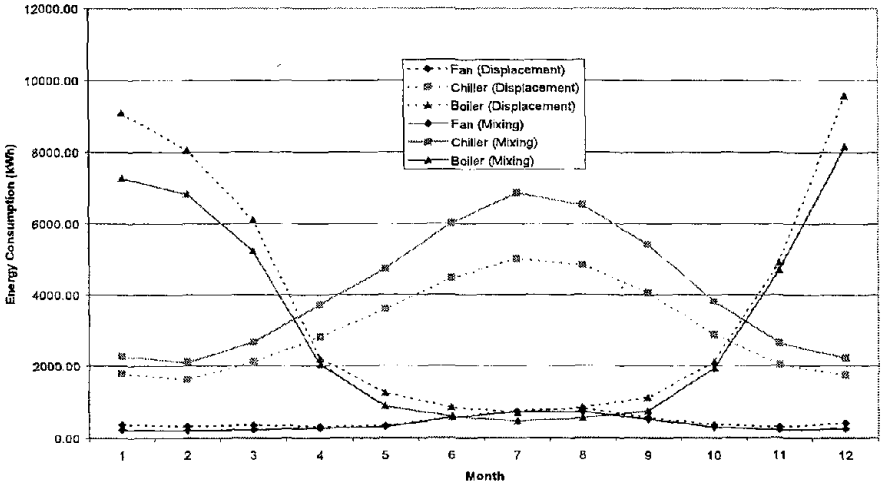

Portland, ME

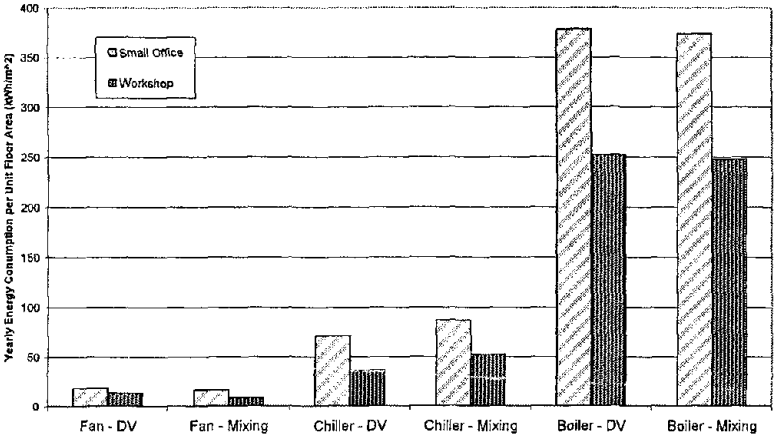

Small Office in Portland, ME

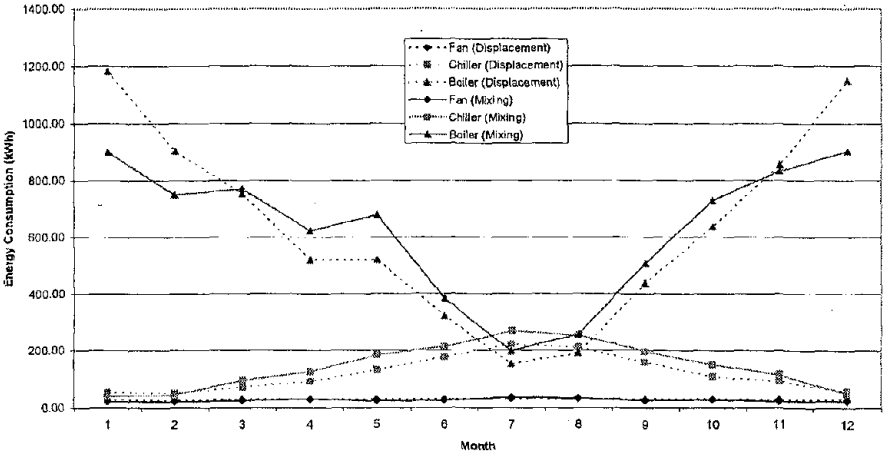

Workshop in Portland, ME

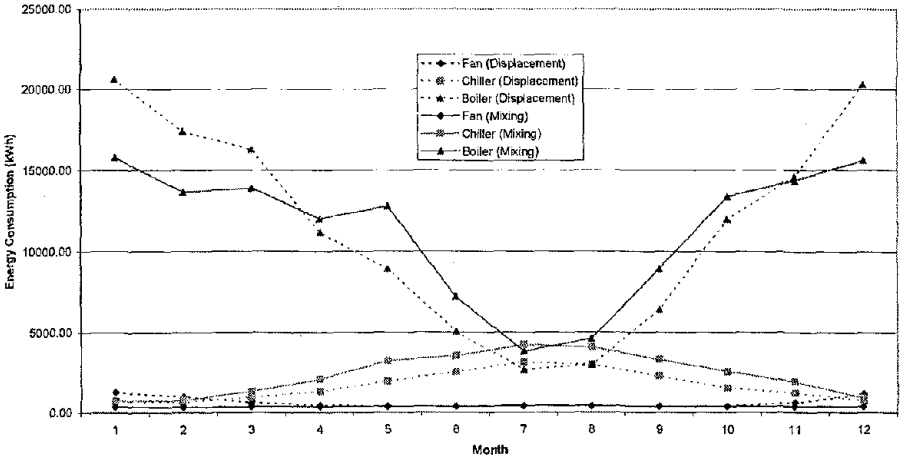

Seattle, WA

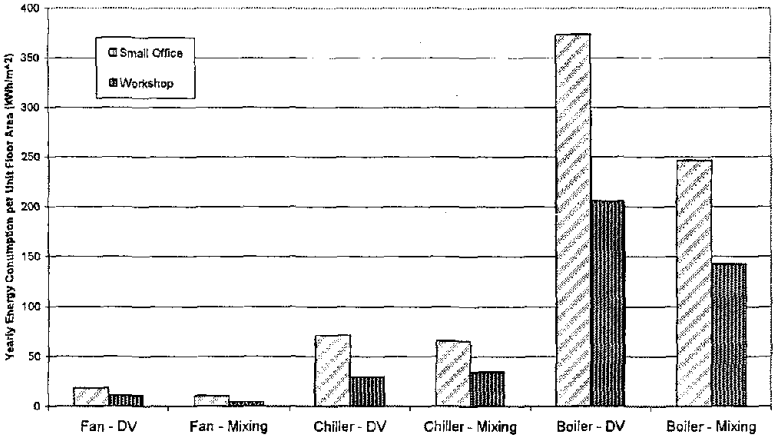

Small Office in Seattle, WA

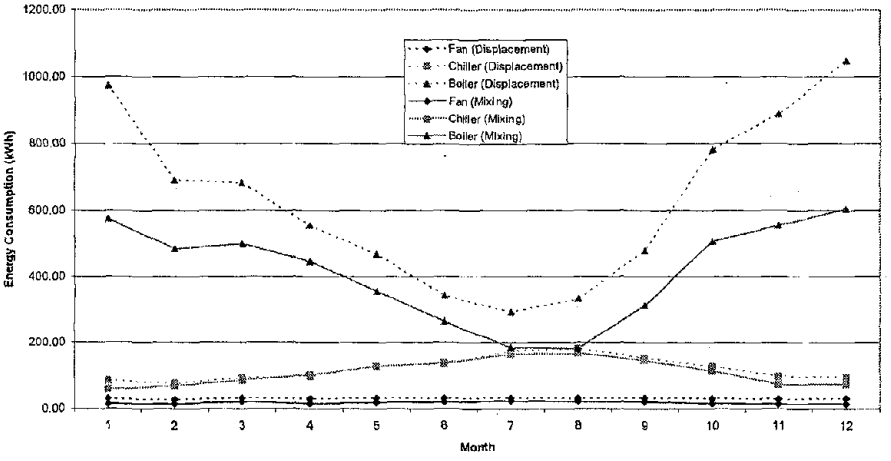

Workshop in Seattle, WA

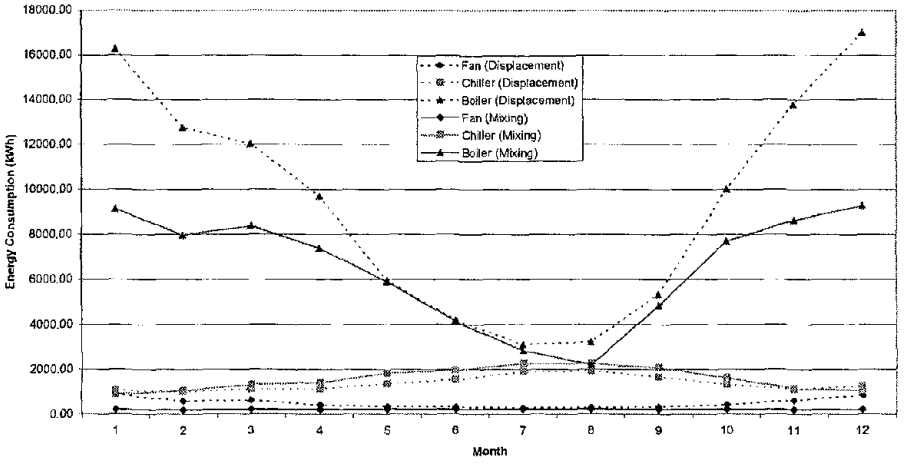

Phoenix, AZ

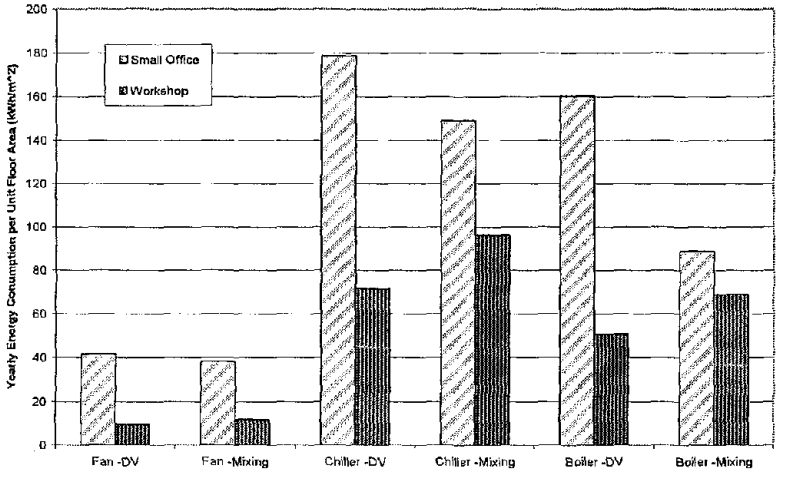

Small Office in Phoenix, AZ

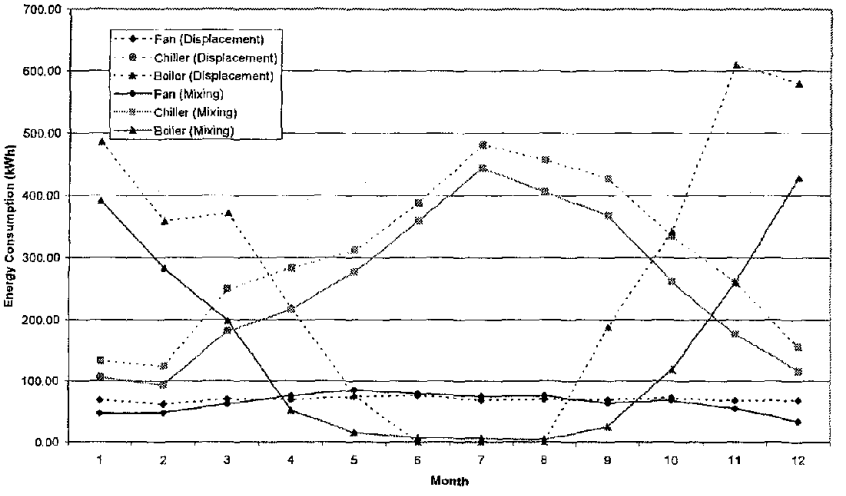

Workshop in Phoenix, AZ